R-10-44

Characterization of a backfill candidate material, IBECO-RWC-BF

Baclo Project – Phase 3

Laboratory tests

Lars-Erik Johannesson, Torbjörn Sandén,
Ann Dueck, Lars Ohlsson
Clay Technology AB

January 2010

Svensk Kärnbränslehantering AB
Swedish Nuclear Fuel
and Waste Management Co

Box 250, SE-101 24 Stockholm
Phone +46 8 459 84 00

ISSN 1402-3091
SKB R-10-44

Characterization of a backfill candidate material, IBECO-RWC-BF

Baclo Project – Phase 3

Laboratory tests

Lars-Erik Johannesson, Torbjörn Sandén,
Ann Dueck, Lars Ohlsson
Clay Technology AB

January 2010

Keywords: Bentonite, backfill, geotechnical properties, hydraulic conductivity.

Abstract

A backfill candidate material, IBECO-RWC-BF, which origin from Milos, Greece, has been investigated. The material was delivered both as granules and as pellets. The investigation described in this report aimed to characterize the material and evaluate if it can be used in a future repository. Some of the methods used for the investigation are not standard methods as no standards exist. The following investigations have been done and are presented in this report:

1. **Standard laboratory tests**. Water content, liquid limit and swelling potential are examples on standard tests that have been performed.
2. **Block manufacturing**. The block compaction properties of the material have been determined. A first test was performed in laboratory but also tests in large scale have been performed. After finishing the test phase, 60 tons of blocks were manufactured at Höganäs Bjuf AB. The blocks will be used in large scale laboratory tests at Äspö HRL.
3. **Mechanical parameters**. The compressibility of the material was investigated with oedometer tests (four tests) where the load was applied in steps after saturation. The evaluated oedometer modulus varied between 34–50 MPa.

   Tests were made to evaluate the elastic parameters of the material (E, υ). Altogether three tests were made on specimens with dry densities of about 1,710 kg/m^3. The evaluated E-modulus and Poisson´s ratio varied between 231–263 MPa and 0.16–0.19 respectively.

   The strength of the material, both the compressive strength and the tensile strength were measured on specimens compacted to different dry densities. The test results yielded a relation between density and the two types of strength.

   Furthermore, tests have been made in order to determine the compressibility of the unsaturated filling of pellets. Two tests were made where the pellets were loosely filled in a Proctor cylinder and then compressed at a constant rate of strain during continuously measurement of the applied load.
4. **Swelling pressure and hydraulic conductivity**. There is, as expected, a very clear influence of the dry density on the hydraulic conductivity and swelling pressure for this kind of material. The influence of granule size of the material was investigated and also the influence of the salt content of the water was investigated.
5. **Erosion properties**. Erosion tests have been performed both with the compacted blocks and pellets material. The results from the tests are well inside the limits of the earlier suggested erosion model with the block properties at the upper limit and the pellets properties in the middle.
6. **Self healing ability**. The self healing ability has been tested for both blocks and pellets. The tests were performed using water with 1% and 3.5% salinity. The self healing ability was tested by drilling holes in saturated specimens and then let them have access to water again for three weeks. The hydraulic conductivity was measured before drilling of the central hole and then again after three weeks of healing. The results from the tests are consistent and the ability of the material to self-heal can be summarized as follows:
   - **Compacted blocks**. The specimens had largely healed but there were still visual traces of the drilled hole that could be seen after finishing the tests. The two specimens with the lower density had however a distinct increase in hydraulic conductivity measured after the healing time when compared to the value determined before drilling.
   - **Pellets**. During termination it was observed that the former drilled holes were filled with gel. There was, however, an evident increase of hydraulic conductivity when comparing the values achieved after the healing period with the ones achieved before drilling.

7. **Homogenization of backfill blocks and pellets**. Three tests investigating the homogenization process of high density backfill blocks and pellets have been performed. Compacted specimens with a diameter of 50 mm and a height of 40 mm were placed in an oedometer. At the top of each specimen, pellets (somewhat crushed) were placed to a thickness of 4.8 and 12 mm respectively. The specimens had access to water only from the pellets side i.e. the simulated rock wall. Similar tests have been performed earlier using the same test equipment and with the same test layout but with different materials /Johannesson et.al 2008/. With the experience from the old tests it was possible to focus on the important parameter i.e. the slot width. The new tests with the IBECO-RWC-BF material showed that the homogenization of the specimens after two months testing had gone far even if there was a very clear difference between the specimens depending on the initial slot width. One example of the homogenization rate is that the differences in dry density at test start (block = 1,600 kg/m^3, pellets = 885 kg /m^3) has evened out to a density gradient from 1,250–1,400 kg/m^3 (12 mm initial width of pellets slot) after two months. The degree of saturation was for all three specimens between 92 and 100% at termination.
8. **Water uptake tests**. This type of test was made in order to study how the backfill material will take up water and which parameters affect this process. From the performed tests the following conclusions have been made:
   - The water uptake rate of a material is depending on the initial dry density. As expected, the samples with lower density take up water faster compared to the samples with higher density.
   - The water uptake tests can be used as "bench mark" tests for evaluating different models for simulating the water uptake.
9. **Relative humidity induced swelling**. Tests where compacted backfill blocks (in small scale) were exposed for high relative humidity for three months were also performed. During the test the water uptake from the air humidity was measured.
10. **Water retention curve.** The specific water retention curve has been determined for the material.

Sammanfattning

I denna rapport beskrivs de undersökningar som har gjorts på ett tänkbart backfillmaterial, IBECO-RWC-BF. Materialet kommer från Milos i Grekland och har levererats dels som ett granulat men också som pellets. Undersökningarna som är beskrivna i denna rapport syftar till att karakterisera materialet och utvärdera om det kan användas i ett framtida förvar. En del av metoderna som använts för att karakterisera materialet är inte standardmetoder eftersom det inte finns några standardiserade metoder för denna typ av undersökningar. Följande undersökningar har gjorts och är presenterade i denna rapport:

1. **Standard tester**. Vatteninnehåll, flytgräns och svällningspotential är exempel på standard tester som har gjorts.
2. **Blocktillverkning**. Egenskaperna hos materialet vid kompaktering av block har fastställts. Undersökningar har gjorts både i laboratorieskala men också i stor skala. Efter avslutning av försöken tillverkades ca 60 ton block på Höganäs Bjuf AB. Blocken skall användas vid storskaliga laboratorieförsök på Äspö HRL.
3. **Mekaniska parametrar**:
   - Kompressibiliteten hos materialet har undersökts med ödometerförsök (4 st.) där lasten applicerades i steg efter vattenmättnaden. Den utvärderade ödometermodulen varierade mellan 34 och 50 MPa.
   - Tester har också gjorts för att utvärdera de elastiska parametrarna hos materialet (E, υ). Totalt tre försök har gjorts på prov med en torrdensitet på ca 1,710 kg/m^3. Den utvärderade E-modulen varierade mellan 231 och 263 MPa och Poisson´s tal mellan 0.16–0.19.
   - Tryckhållfastheten och draghållfastheten bestämdes på prov som hade kompakterats till olika torrdensiteter. Resultaten visade att det finns ett samband mellan densitet och de två typerna av hållfasthet.
   - Tester har också gjorts för att bestämma kompressibiliteten hos den omättade pelletsfyllningen. Två försök gjordes där pelletsen hälldes i ett s.k. Proctorkärl som sedan pressades med konstant hastighet under det att lasten mättes.
4. **Svälltryck och hydraulisk konduktivitet**. Som väntat finns det en stark koppling mellan torrdensitet och hydraulisk konduktivitet samt svälltryck för denna typ av material. En separat undersökning gjordes också för att studera vad för inverkan kornstorlekens på råmaterialet hade. Även inverkan från saltinnehållet i vattnet undersöktes.
5. **Erosion**. Erosionsförsök har gjorts både med kompakterade block och pellets. Resultaten från försöken visar att de uppmätta erosionshastigheterna är väl inom gränserna för den föreslagna modellen.
6. **Självläkningsförmåga**. Självläkningsförmågan har testats både vad gäller block och pellets. Testerna har gjorts med vatten innehållande 1% och 3.5% salt. Efter vattenmättnad borrades genomgående hål genom proven och sedan fick de åter tillgång till vatten. Den hydrauliska konduktiviteten mättes dels före borrningen och sedan igen efter tre veckors läkning. Resultaten är logiska och materialets förmåga att självläka kan sammanfattas enligt följande:
   - Kompakterade block. Alla prov visade upp en stor förmåga att läka men det fanns fortfarande visuella spår av det borrade hålet som kunde ses vid brytningen. På de två prov med lägst densitet kunde en tydlig ökning av hydraulisk konduktivitet mätas efter läkning jämfört med mätningen innan borrningen.
   - Pellets. Vid brytningen av försöket kunde det noteras att de tidigare hålen var fyllda med gel. Emellertid kunde en tydlig ökning av hydraulisk konduktivitet mätas efter läkningsperioden jämfört med mätningen som gjordes innan borrningen.

7. **Homogenisering av block och pellets**. Tre tester har gjorts för att undersöka hur homogenisering av block med hög densitet och pellets kommer att ske. Kompakterade prov med diametern 50 mm och höjden 40 mm placerades i en ödometer. På toppen av varje prov placerades pellets (något krossad) i ett lager med tjockleken 4, 8 eller 12 mm. Proven hade tillgång till vatten enbart från pelletssidan dvs. den simulerade bergväggen. Liknande försök har gjorts tidigare med andra material /Johannesson et al. 2008/. Med erfarenheten av dessa försök var det möjligt att fokusera på den viktiga parametern dvs. spaltvidden. De nya försöken med IBECO-RWC-BF visade att efter två månaders test hade homogeniseringen av proven gått långt. Där var dock som väntat en tydlig inverkan av spaltvidden. Ett exempel på homogeniseringen är att torrdensiteterna vid start (block = 1,600 kg/m^3, pellets = 885 kg/m^3) hade jämnats ut till en densitetsgradient mellan 1,250 och 1,400 kg/m^3 (provet med 12 mm spalt) efter två månader. Vattenmättnadsgraden var för alla proven mellan 92 och 100% vid brytningen.
8. **Vattenupptag**. Denna typ av försök gjordes för att studera hur backfill materialet tar upp vatten och vilka parametrar som påverkar denna process. Från försöken kan följande slutsatser dras:
   - Vattenupptagningshastigheten hos ett material beror på startdensiteten. Som väntat tar prov med låg densitet upp vatten snabbare jämfört med prov med hög densitet.
   - Vattenupptagstesterna kan användas som en "bench-mark test" för att utvärdera olika modeller som simulerar vattenupptaget.
9. **Relativ fuktighets inducerad svällning**. Försök har gjorts där kompakterade block (i liten skala) har exponerats för hög relativ fuktighet under tre månader. Under försöket mättes vattenupptaget från luftfuktigheten.
10. **Vattenhållningskurvan.** Specifika vattenhållningskurvan har bestämts för materialet.

Contents

1 Introduction

The investigations described in this report belong to the third phase of the joint SKB-Posiva project "*Backfilling and Closure of the Deep Repository, BACLO*". The overall objective of the BACLO project is to develop a backfilling concept for the deep repository that can be configured to meet SKB's and Posiva's requirements in the chosen repository sites. The project is divided into four phases, of which two have already been finished. The second phase of the BACLO project consisted of laboratory tests and deepened analyses of the investigated backfill materials and methods and resulted in recommendation to focus on the development and testing of the block placement concept with three alternative backfill materials. The investigations in the third phase comprise laboratory and large-scale experiments aiming at testing the engineering feasibility of the concept. In addition, how site-specific constraints, backfilling method & materials affect the long-term functions of the barriers are described and analyzed in order to set design specifications for the backfill.

The work described in this report belongs to the group of laboratory investigations performed in third phase of the BACLO project, this work has however only been a SKB activity. The results from the investigations are aimed to characterize a backfill candidate material named IBECO-RWC-BF.

2 Material and test description

2.1 General

The IBECO-RWC-BF is a backfill candidate material for the Swedish KBS-3 concept. Other materials have been tested and characterized earlier with the same methods.

IBECO-RWC_BF is a material that origins from Milos in Greece. IBECO is the name of the company delivering the material, RWC stands for Radioactive Waste Clay and BF stands for BackFill. It is a natural calcium bentonite with medium montmorillonite content.

2.2 Test types

The test methods are chosen for studying the behavior of the backfill material during emplacement and during the early saturation phase. In addition different modeling parameters are measured and evaluated in order to model the wetting and homogenization processes. The following investigations have been done and are presented in this report:

- **Standard laboratory tests.** Standard investigations such as measuring of initial water ratio at delivery and the liquid limit have been made. For the pellets also the bulk density has been measured.
- **Block compaction.** The density after compacting blocks with different pressures and water content has been investigated in the laboratory. In order to find the optimal water ratio samples with different water ratios have been compacted with the same pressure. The influence of different compaction pressure has also been investigated.
- **Geotechnical parameters.** The compressibility of a water saturated bentonite has been investigated with oedometer tests. The elastic properties of the block material are also determined (Young`s modulus (E) and Poisson ratio (υ)). Furthermore the strength of the unsaturated blocks have been tested.
- **Swelling pressure and hydraulic conductivity.** The swelling pressure and hydraulic conductivity have been determined at different densities using water with different salinity.
- **Erosion.** The erosion properties of both compacted blocks and of pellets fillings have been measured. Both the applied water flow rate and the salinity of the water have been varied.
- **Self healing ability.** The self healing ability after a piping scenario has also been investigated with some laboratory tests. The hydraulic conductivity was measured on saturated specimens. Then holes (d = 5 mm) were drilled in the middle of the specimen and after 3 weeks of healing time with full access to additional water, the hydraulic conductivity measurement was repeated.
- **Homogenization of backfill blocks and pellets.** Tests have been performed in standard oedometers with a diameter of 50 mm. Compacted block with a height of 40 mm were placed in the oedometers and a pellet filling of different thickness (4, 8 and 12 mm) was placed above. The samples had access to water only from the pellet side. After three months of homogenization the tests were terminated and the water content and density distribution in the specimens were determined.
- **Water uptake.** Tests samples were compacted in a cylinder with a diameter of about 100 mm and a height of 100 mm. The samples had access to water from one end during specified time periods. After this time the distribution of water content and density of the samples were determined. The tests were made with two different salt contents in the water.
- **Relative humidity induced swelling.** The backfill blocks will absorb water from the air humidity after emplacement. This may cause swelling and cracking of the blocks. The phenomena have been investigated in specially designed equipment, where compacted specimens were exposed to high relative humidity. The specimens were weighed and inspected at pre-selected intervals.
- **Water retention curve.** The retention curve is an important material property for modeling the behavior during the saturation phase.

The tests and results are described in chapters 3 to 12.

2.3 Materials and water used in the tests

Two materials have been used in the tests described in this report,:

- **Specimen of compacted IBECO-RWC-BF**. Granules made of material that origin from Milos compacted to different densities. The material is described by the supplier as a natural calcium bentonite with medium montmorillonite content. A data sheet from the supplier is attached in Appendix 1.
- **Pellets of IBECO-RWC-BF**. Pellets made of the same material as above. The pellets are extruded and have a diameter of 6 mm and a length of 5–20 mm.

In order to be able to use the pellets in the homogenization tests in the rather small slot widths, they were crushed to a maximum diameter of about 4 mm.

The following water types were used in the tests:

- **Water1**: tap water.
- **Water2**: water with salinity of 1% (50/50 NaCl/$CaCl_2$).
- **Water3**: water with salinity of 3.5% (50/50 NaCl/$CaCl_2$).

The water type that most likely will exist in the repository during the installation phase is type 2, but due to possible "upconing effect" in Olkiluoto /Pastina et al. 2006/ a number of tests were also made with the higher salinity of the water (3.5%) which also has been the design salinity used throughout all Baclo investigations. Some supplementary tests were made with tap water.

2.4 Uncertainties

The number of tests performed is limited and the repeatability of the results has not been investigated in this project.

3 Standard laboratory tests

3.1 Results

A number of standard geotechnical properties of the backfill material were determined:

- **Water content**. The water content of the as-delivered raw material and the pellets was determined. The water content is defined as mass of water per mass of dry substance. The dry mass is obtained by drying the wet specimen at 105°C for 24 hours.
- **Bulk density of filling**. The density of the bulk filling after pouring it into a cylinder was determined by weighing a certain volume which was measured with a graduated glass.
- **Liquid limit**. The liquid limit of a soil is the water content where the properties of the soil changes from plastic to liquid. The liquid limit was determined with the fall-cone method.
- **Swelling capacity**. One gram of the dry test material is poured down very carefully into a glass cylinder filled with de-ionized water. The volume occupied by the swelled clay is recorded after 24 hours to provide the volumetric swelling capacity. The swelling capacity depends mainly on the montmorillonite content of the material.
- **Granule size distribution**. The granule size distribution was determined by sieving the material, see Figure 3-1.

The results from the tests are presented in Table 3-1 and in Figure 3-1.

The granule size distribution of the material is shown in Figure 3-1. The figure shows that about 60% of the material has a larger granule size than 1 mm.

Table 3-1. Table showing some standard properties investigated.

Sample	Water content %	Bulk density of filling kg/m³	Liquid limit %	Swelling capacity ml
IBECO-RWC-BF, granules	18.5	1,165	122	4.4
IBECO-RWC-BF, pellets	14.8	1,015	208	9.1

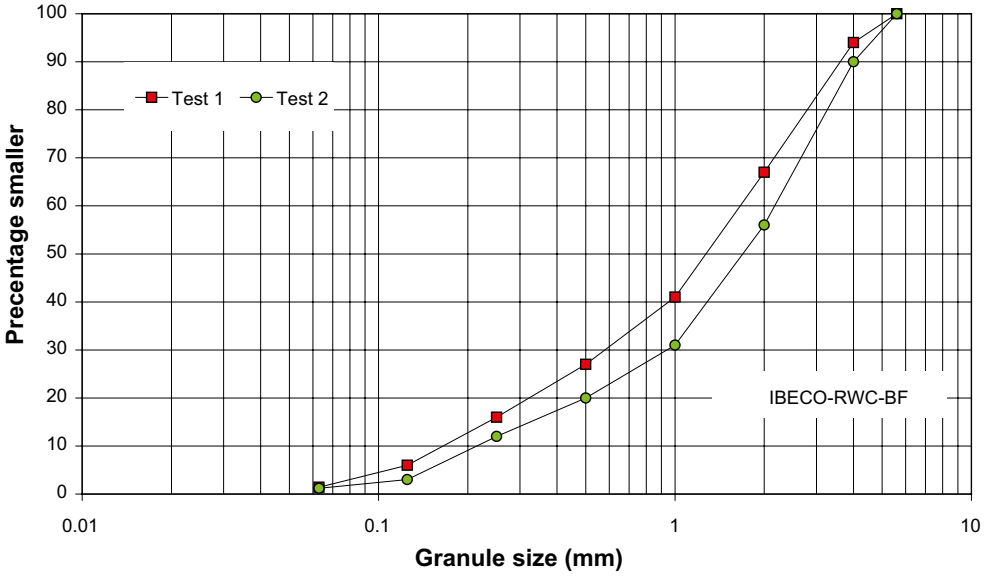

Figure 3-1. *Granule size distribution for the IBECO-RWC-BF.*

4 Block compaction

4.1 General

The reference technique for backfilling the deposition tunnels in the KBS3-V concept is to use pre-compacted blocks together with a filling of pellets close to the tunnel wall. The final density of the backfill depends on the following parameters:

- The density of the individual blocks.
- The part of the total tunnel volume that can be filled with blocks.
- The part of the remaining tunnel volume (after block emplacement) that can be filled with pellets.
- The density of the pellet filling.

The density of the individual block depends on mainly two factors, the compaction pressure and the water content of the backfill material. In the following sections these parameters are investigated for the IBECO-RWC-BF material. Tests have been made both in laboratory scale and in larger scale at Höganäs Bjuf AB.

4.2 Laboratory investigation

In order to investigate the resulting density of the blocks after uni-axial compaction, a number of small samples were compacted in the laboratory. The tests were prepared and made in the following steps:

- The material was mixed to different water contents (approximately 10 different water contents).
- The material was placed in a rigid form with an inner diameter of 50 mm.
- The material was compacted with two different compaction pressures (25 MPa and 50 MPa).
- After compaction the density and water content of the samples were determined and the dry density and the void ratio calculated.

The results from the measurements are shown in Figure 4-1. The dry density is plotted as function of the water content. The black line in the figure (marked $S_r = 100\%$) correspond to the dry density at full saturation (assuming a density of the solid particles of $\rho_s = 2{,}780$ kg/m^3). The tests were made at two occasions. The test marked as old tests were made on a previous delivery of a similar material.

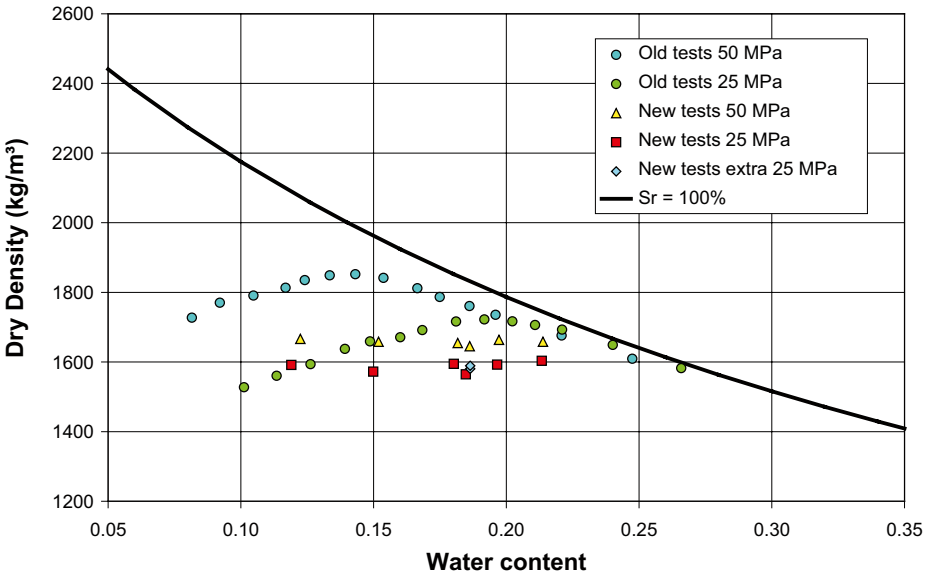

Figure 4-1. *The dry density of samples compacted with two different compaction pressures (25 and 50 MPa) as function of the water content.*

The old tests indicated that the maximum dry density at a compaction pressure of 25 MPa was reached at a water content of about 19%. The new material to be used for the presented tests was therefore ordered with a water content of about 19%. Tests were then made on the on the new material (marked as "New tests" in the plot). These tests do not show an evident maximum. The expected dry density at a water content of 19% and at a compaction pressure of 25 MPa is about ρ_d = 1,600 kg/m^3.

4.3 Block manufacturing in large scale

The material tested in the laboratory has also been used to manufacture of blocks in large scale at the Höganäs Bjuf factory. The objectives of the large scale manufacturing were both to study the achieved block quality and to get a suitable amount of blocks (about 60 tons) that could be used for large scale tests of this backfill material at Äspö HRL.

The preparations before the manufacturing could start were done according to the following:

1. A pre-test was made in the laboratory in order to study the influence of compaction pressure on the dry density of the blocks. All the tests were made with a water content of about 18.5%. The tests were used for determining the required compaction pressure. (Blue dots in Figure 4-2).
2. A pre-test was also performed at the factory in Bjuv in November 2008. Blocks, shaped as bricks, with dimensions of about 300×150×75 mm were compacted. About 1 ton of the raw material was used. (Green dots in Figure 4-2).
3. Manufacturing of 60 ton backfill blocks was made in February 2009. (Black dot in Figure 4-2).

The result from an earlier test made in Germany with the same material is also plotted in the diagram.

An investigation of the blocks compacted in Bjuv with the purpose to determine the variation of the density both within a block and between blocks have also been made. The results from this investigation are reported in Appendix 7. The investigation shows that the produced blocks are very homogeneous and that the variation in density between the blocks also is very small.

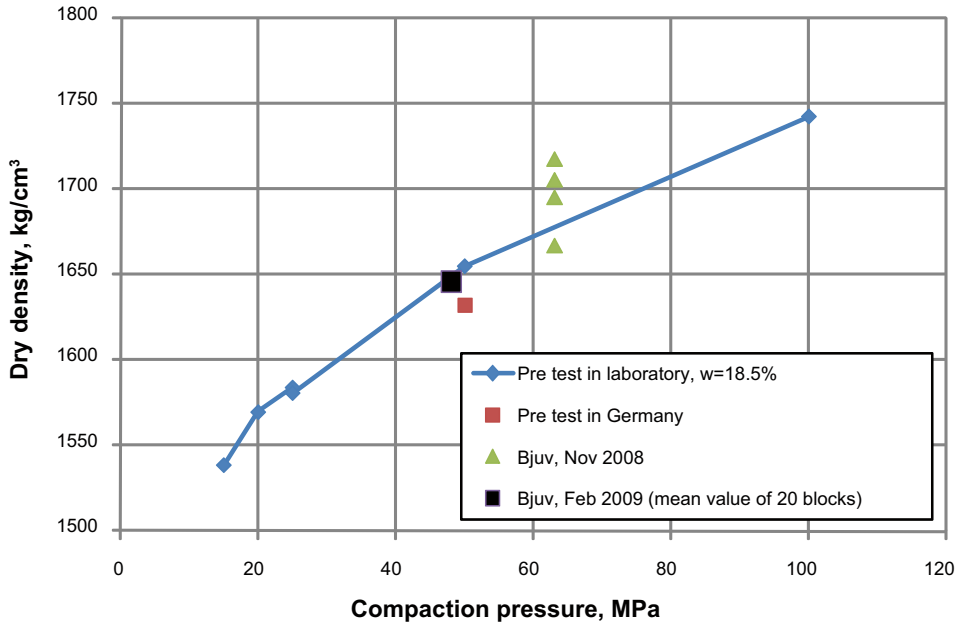

Figure 4-2. *The dry density of samples compacted at different compaction pressure. All the samples had a water content of about 18.5%.*

5 Geotechnical parameters

It is of vital importance to be able to describe the behavior of the backfill material both during and after installation and in place in the tunnel. An important parameter during installation is the strength of the compacted blocks. After installation the compressibility of the material both at unsaturated and saturated conditions must be known to be able to calculate the upwards swelling of the buffer inside a deposition hole. Furthermore the compressibility of the pellets filling, which will be used both to fill the slot between the blocks, the roof and the walls of the tunnel and as a bedding of the floor, must be known. Earlier investigations have been made regarding geotechnical properties of backfill materials /Johannesson et al. 2006/ and /Johannesson 2008/.

5.1 Compressibility of the saturated backfill

5.1.1 Introduction

The compressibility of the clay was determined in oedometer tests. The equipment used for the tests is shown in Figure 5-1. The material was compacted into the oedometer ring and the piston was placed on top of the specimen. The samples were saturated through the two filters at a constant vertical stress of about 200 kPa. The water used for the oedometer tests had a salinity of 1 and 3.5% (50/50 $NaCl/CaCl_2$). When the specimens had been completely saturated the vertical load was increased in steps during continuous measurement of the displacement of the specimen. The following approximate load steps were used; 400, 800, 1,600 and 3,200 kPa. After the final load step, the oedometer was demounted and the density and water content of the specimen determined. From these data void ratio, degree of saturation, dry density and density at saturation could be calculated. These data received from the tests are listed in Table 5-1.

Table 5-1. Basic data determined on the tested clays after the last load step.

Test No	Final stress (kPa)	Dens. solid (kg/m^3)	Bulk density (kg/m^3)	Void ratio	Water content	Dens at sat. (kg/m^3)	Dry density (kg/m^3)	Degr of sat.
Test I, 1% salt	3,405	2,780	1,894	0.985	0.353	1,897	1,400	1.00
Test 2, 3.5% salt	3,262	2,780	1,903	0.959	0.341	1,908	1,419	0.99
Test 3, 3.5% salt	3,333	2,780	1,905	0.951	0.337	1,912	1,425	0.99
Test 4, 1% salt	3,131	2,780	1,895	0.985	0.353	1,897	1,401	1.00

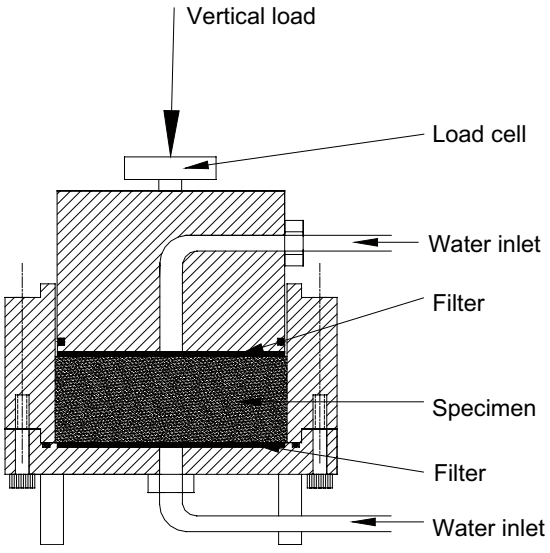

Figure 5-1. *The equipment used for the oedometer tests.*

5.1.2 Measurements

An example of measured data from the different load steps in one of the oedometer tests is shown in Figure 5-2. The void ratio as function of time is plotted for the four load steps in test 4. The corresponding curves for the other tests are shown in Appendix 8. The curves have a typical shape for this type of tests made on clays. The first part of the curve can be interpreted as a small elastic deformation of the material (instant and small). Part II of the curve represents the consolidation of the material when the increased pore water pressure caused by the increased load dissipates. The consolidation is time dependent and is normally representing a large part of the deformation of the material. The rate of consolidation is a function of the hydraulic conductivity and the bulk modulus of the material. The third part of the deformation represents the creep of the sample (creep in the particle skeleton). This deformation is also time-depending, but compared with the consolidation much smaller.

The final densities at the different load steps are plotted as function of the vertical stress for the four tests in Figure 5-3. The figure indicates that the deformation of the samples is almost proportional to the vertical stress for the vertical stress up to 3,200 kPa. Furthermore the differences in inclinations (modulus) between the samples are small, which means that the salinity of the pore water does not affect the compressibility of the material. The oedometer modulus evaluated from the test results varies between 34–50 MPa.

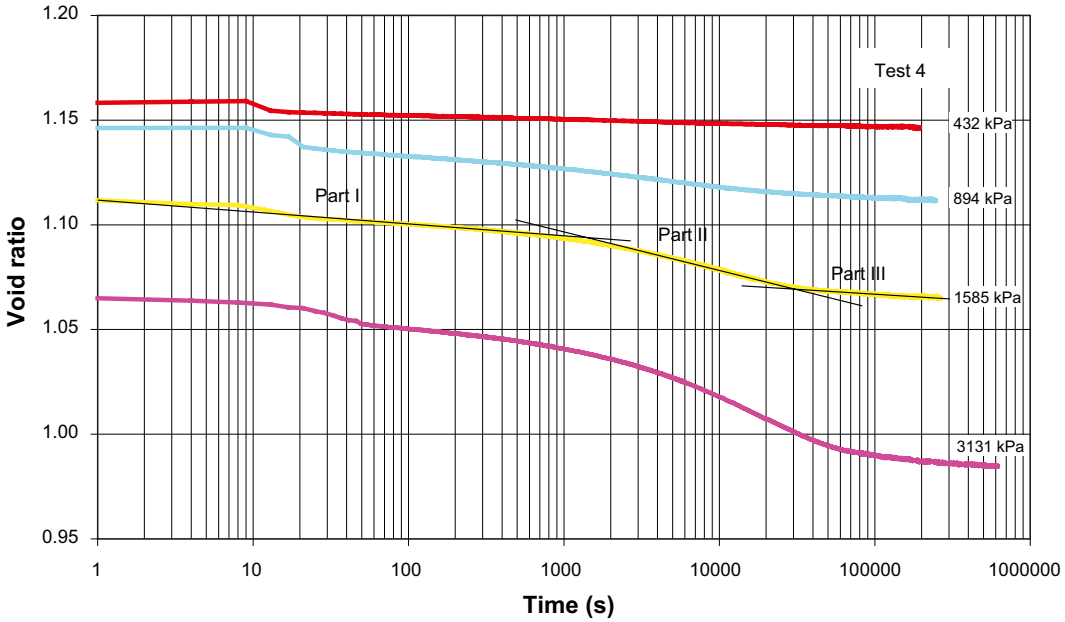

Figure 5-2. *Void ratio as function of time for the four load steps in Test 4.*

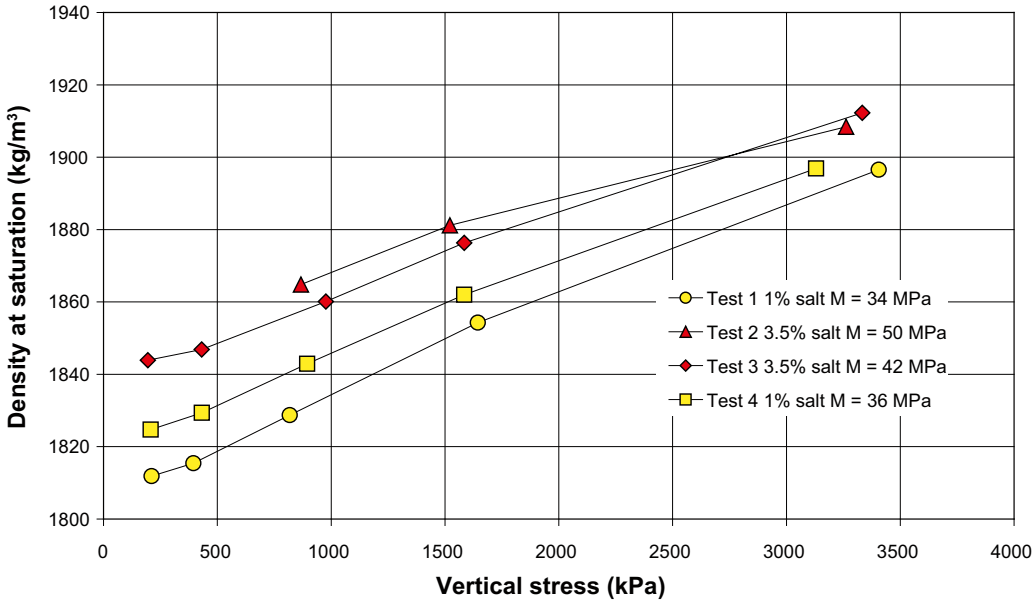

Figure 5-3. *Density at saturation plotted as function of the vertical stress for the four tests performed with two different salinity of the water.*

5.2 Evaluation of elastic parameters of unsaturated blocks

To be able to evaluate the compression of unsaturated backfill material at a stage when the buffer is saturated and a swelling pressure from the buffer acts on the backfill, the elastic parameters Young's modulus and Poisson´s ratio of the backfill blocks are required. The tests made to evaluate the parameters were as follows:

- Small specimens were made with uni-axial compaction in a mould with rigid walls with a compaction pressure of about 25 MPa (Ø 35 mm, h 60 mm). The water content was about 17%.
- The specimens were placed in a load frame and compressed in axial direction without lateral support. The deformation of the specimens (vertical and horizontal) together with the applied load (see Figure 5-4) were measured during the test.
- The evaluation of Young's modulus (E) and Poisson ratio (ν) were made with the following equations:

$$E = \frac{\Delta \sigma_v}{\Delta \varepsilon_v} = \frac{\Delta P \times L}{A \times \Delta L} \quad (5\text{-}1)$$

$$\nu = -\frac{\varepsilon_h}{\varepsilon_v} = \frac{\Delta W \times L}{W \times \Delta L} \quad (5\text{-}2)$$

where

$\Delta\sigma_v$ = Vertical stress (kPa)

$\Delta\varepsilon_v$ = Vertical strain

ΔP = Applied load (kN)

L = Sample length (m)

ΔL = Change in sample length (m)

A = Area of the sample (m^2)

ε_v = Vertical strain of the sample

ε_h = Horizontal strain of the sample

W = Sample diameter

ΔW = Change in sample diameter (m)

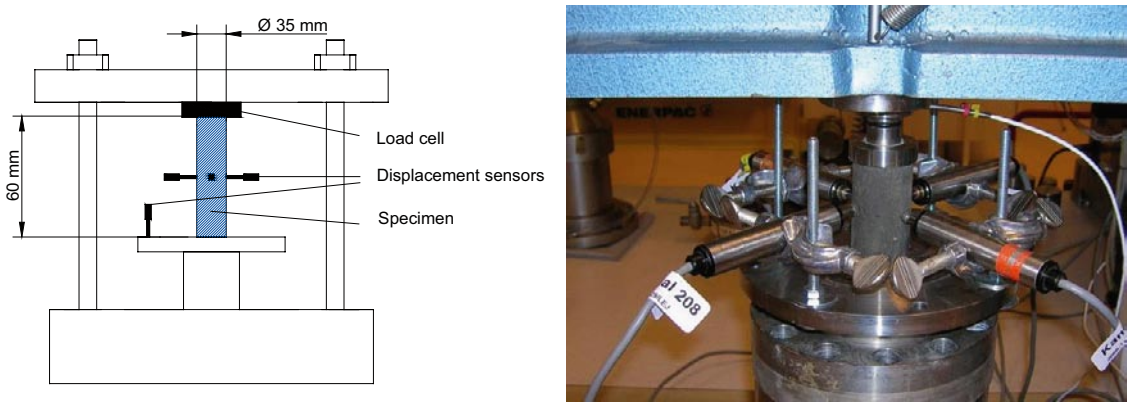

Figure 5-4. *Test arrangement for determination of Young's modulus and the Poisson´s ratio on pre-compacted backfill specimens.*

Typical results from the measurements are shown in Figure 5-5. Young's modulus was determined from a straight line applied to the test data. The interpretation of the modulus was made in the stress interval 0–2,500 kPa. Poisson ratio was determined from the measurements of the horizontal strain of the specimens, see Figure 5-5. The horizontal strain was measured in two perpendicular directions and the average of the measurements was used for the interpretation. The measurements in all the performed tests are presented in Appendix 9 and the interpreted parameters are summarized in Table 5-2.

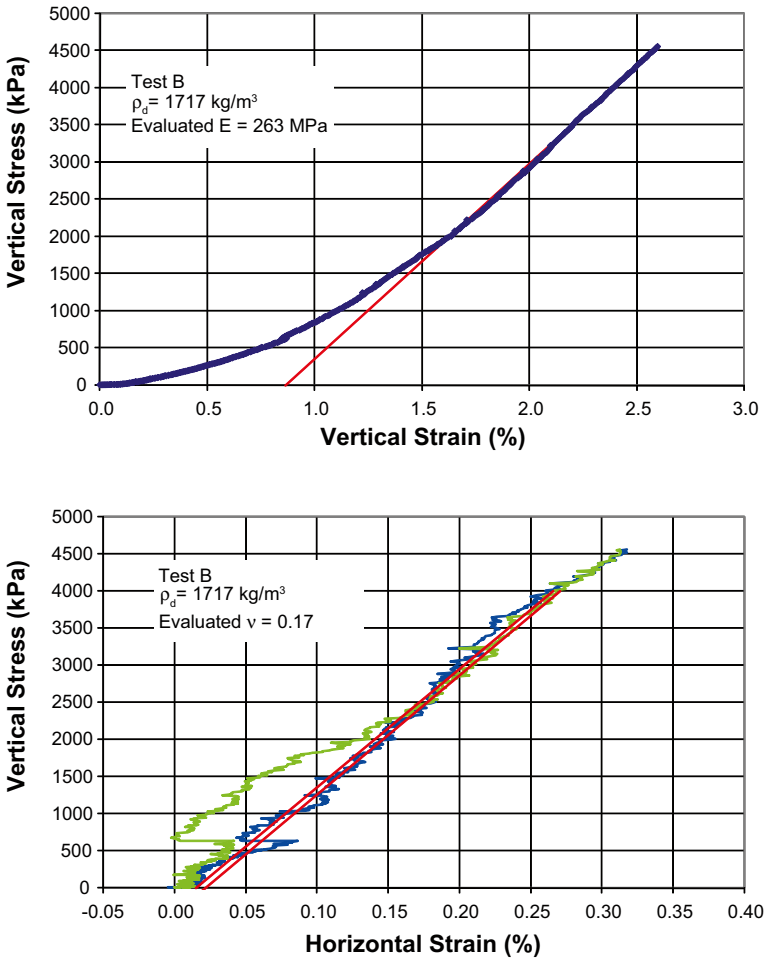

Figure 5-5. *Measurements of the vertical stress as function of the vertical and horizontal strain used for determining Young´s modulus and Poisson´s ratio on sample B.*

Table 5-2. Evaluated Young's modulus and Poisson ratio for the investigated backfill materials.

Test No	Dry density (kg/m³)	Water content	E-modulus (MPa)	v
A	1,710	0.173	245	0.19
B	1,717	0.172	263	0.17
C	1,704	0.172	231	0.16

5.3 Evaluation of the strength of the unsaturated blocks

The strength of the pre-compacted blocks needs to be measured both for the handling of the blocks (in order to avoid damages) and for interpretation of calculated stresses when high loads act on the blocks in the tunnel (for instance caused by high swelling pressure from the buffer in a deposition hole). Two types of tests have been used for determining the strength:

1. Unconfined one dimensional compression tests.
2. Beam tests.

5.3.1 Unconfined one dimensional compression tests

In the unconfined one dimensional compression tests, the samples were compressed in vertical direction until failure occurred and the compressive strength of the material was determined from the maximum applied load. The tests were made in following steps:

- Small specimens were compacted (Ø 35 mm, h 70 mm). In order to minimize the density variations a lubricated mold was used (Molycote). Furthermore the density variation within a specimen was determined after test termination and was found to be less than ± 1%.
- A specimen was placed in a load frame and compressed by applying a vertical constant deformation rate of ~0.09 mm/min with continuous measurement of the vertical load and the deformation of the specimen (see Figure 5-6).
- The strength of the specimen was evaluated according to Equation 5-3.

$$\sigma_{max} = \frac{F_{max}}{A} \qquad (5\text{-}3)$$

where

σ_{max} = Maximum Deviator stress (kPa).
A = Area of the sample determined before test start (m).
F_{max} = Maximum applied vertical load (kN).

The results from the evaluated stress at failure are shown in Figure 5-7. The results from the tests are summarized in Table 5-3. Altogether twelve tests were performed.

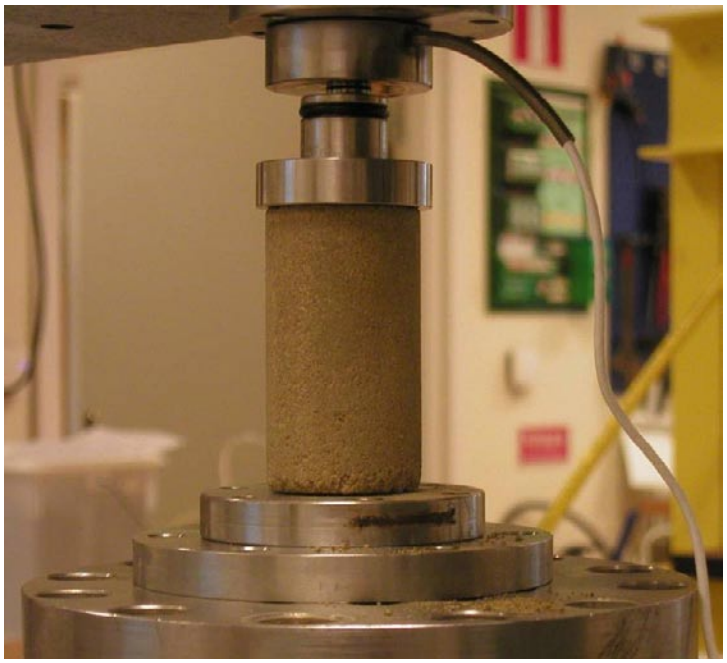

Figure 5-6. *Test arrangement for determination of the shear strength of pre-compacted samples of backfill material.*

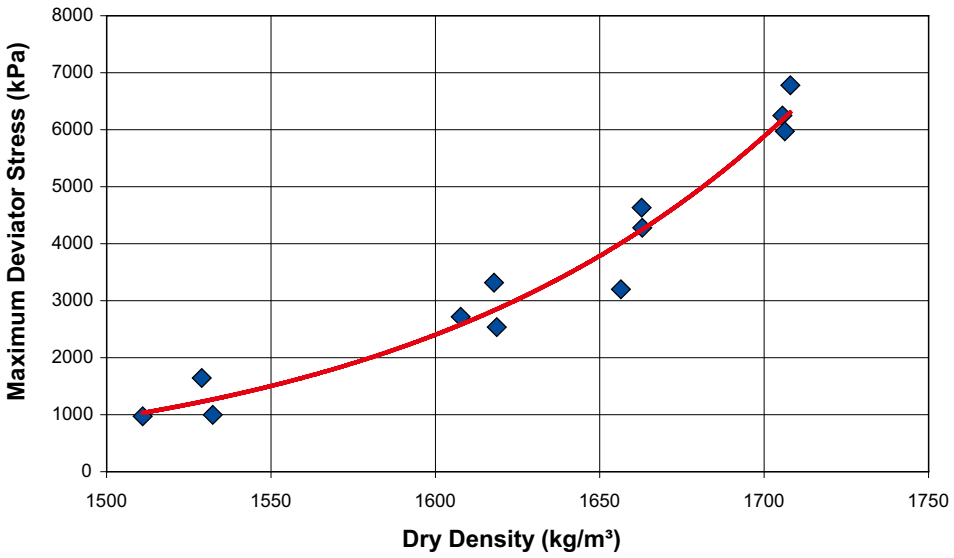

Figure 5-7. *The deviator stress at failure as function of the dry density for the unconfined compression tests made on IBECO-RWC-BF material.*

Table 5-3. The maximum deviator stress and the strain at failure evaluated from unconfined one dimensional compression tests.

Test No	Dry density (kg/m³)	Water cont.	Max Dev stress (kPa)	Strain at failure (%)
1	1,511	0.181	3,571	2.4
2	1,532	0.185	3,496	2.8
3	1,529	0.180	3,660	2.5
4	1,619	0.179	2,301	3.2
5	1,618	0.181	4,827	3.0
6	1,608	0.180	5,027	3.2
7	1,663	0.180	5,200	3.1
8	1,663	0.180	4,046	3.7
9	1,656	0.178	4,262	3.6
10	1,706	0.181	4,060	3.5
11	1,708	0.182	4,904	3.3
12	1,706	0.180	2,626	3.5

5.4 Beam tests

A second type of test was used to determine the tensile strength of specimens of backfill material. The tests were performed as follows:

- Small specimens were compacted with a pressure of ~25 MPa (Ø 50 mm, h 20 mm).
- Beams were sawn from the samples (a×b×c ~10×20×35 mm³).
- The beam was bended by applying a constant deformation rate of about 0.10 mm/min at the middle of the beam. The load and the displacement were measured continuously.
- The tensile stress (σ_t) and the strain (ε_t) were evaluated with the following equations (see Figure 5-8).

$$\sigma_t = \frac{6Qc}{4ba^2} \tag{5-4}$$

$$\varepsilon_t = \frac{a\omega 6}{c^2} \tag{5-5}$$

where

Q = vertical force
a = sample height
b = sample width
c = the length between the support points
ω = the vertical displacement at the middle of the beam

Altogether nine tests were made. The results from the tests are shown in Figure 5-9 and the maximum tensile stress and the strain at failure together with the dry density of the samples are summarized in Table 5-4 and Figure 5-10.

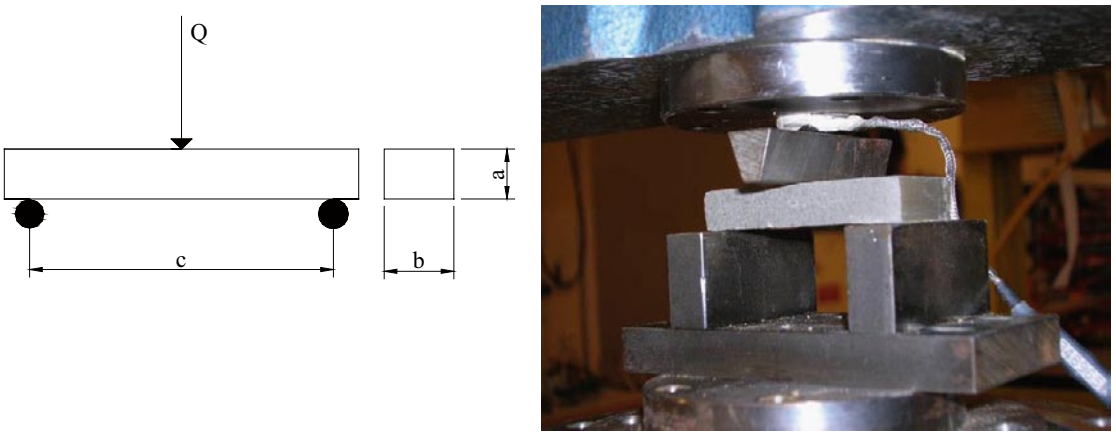

Figure 5-8. Test arrangement for determination of the tensile strength.

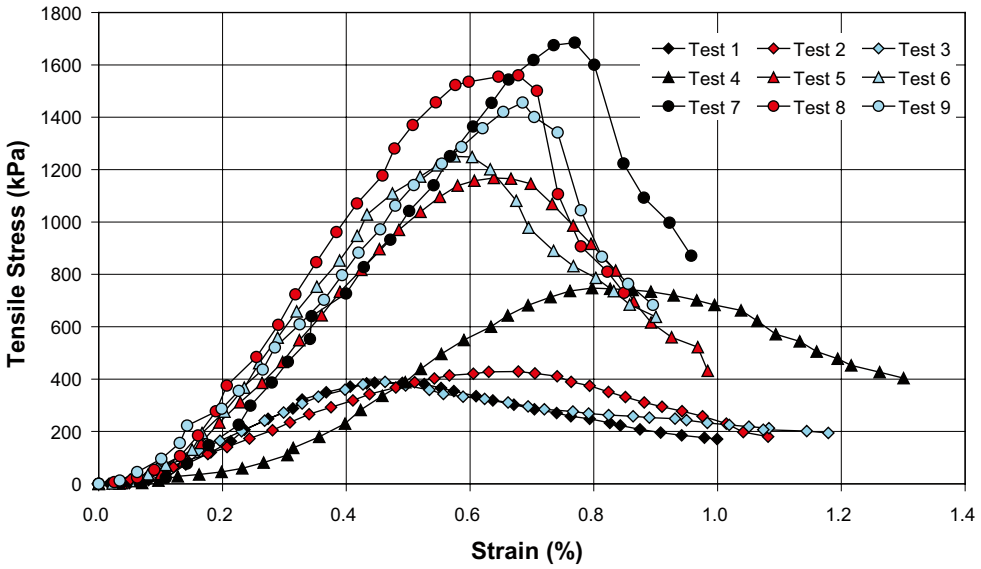

Figure 5-9. Results from beam tests made on IBECO-RWC-BF clay.

Table 5-4. Maximum tensile stress and strain at failure evaluated from beam tests.

Test no	Comp. Pressure (MPa)	Dry density (kg/m³)	Water cont.	Max Tensile stress (kPa)	Strain at failure (%)
1	25	1,594	0.183	386	0.45
2	25	1,600	0.183	429	0.68
3	25	1,596	0.179	389	0.46
4	50	1,654	0.183	747	0.80
5	50	1,646	0.181	1,168	0.64
6	50	1,677	0.181	1,251	0.57
7	100	1,723	0.178	1,685	0.77
8	100	1,722	0.181	1,560	0.68
9	100	1,732	0.177	1,456	0.68

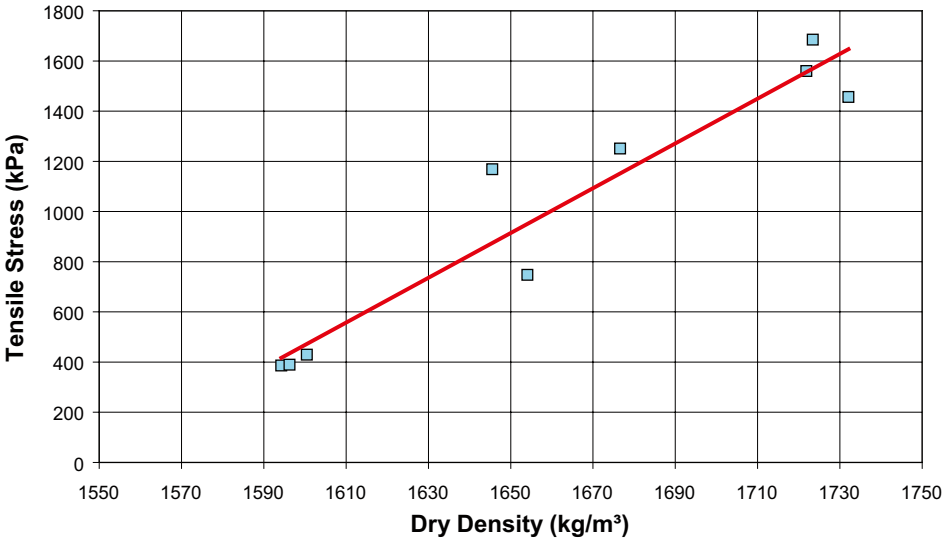

Figure 5-10. *The evaluated tensile stress at failure for the beam tests plotted as function of the dry density of the specimens.*

5.5 Compression properties of unsaturated filling of bentonite pellets

With the concept of backfilling the tunnels with pre-compacted blocks the slot between the blocks and the rock surface of the tunnel will be filled with pellets of bentonite as well as the bottom bed on the floor. It is of importance to know the compression properties of the clay pellets filling in order to be able to calculate the deformation of the filling caused by the swelling of the buffer in the deposition hole. The compression properties were investigated in a Procter cylinder. Two tests were made: The cylinder was filled with loose filled pellets (with the height of about 90 mm and a diameter of about 101 mm.). A piston was placed on the pellets, which were compressed up to a pressure of about 5,000 kPa at a constant rate of deformation (~1 mm/min). The results from the tests are plotted in Figure 5-11.

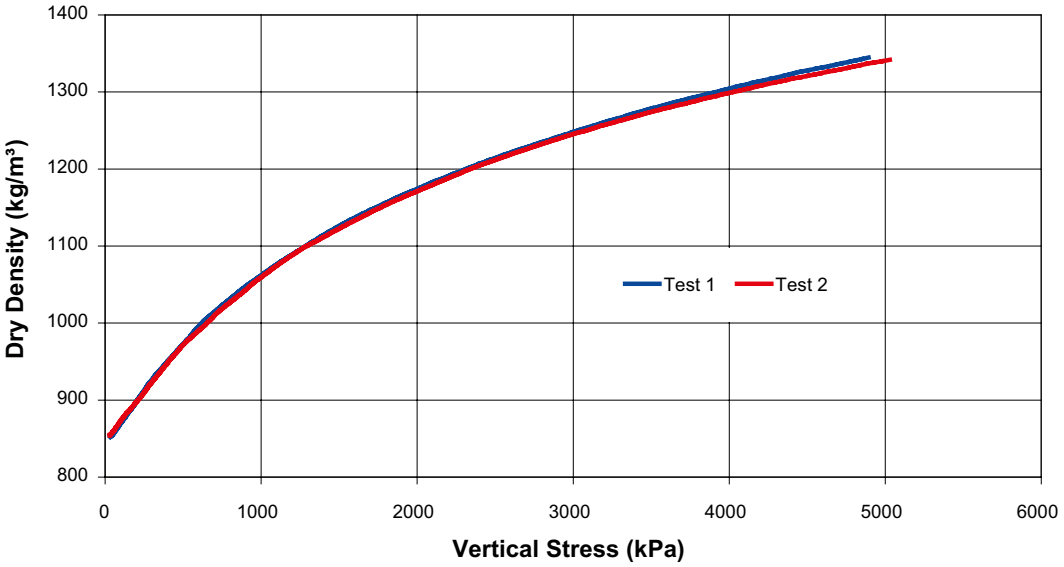

Figure 5-11. *The dry density as function of the applied vertical stress in compression tests made on pellets of IBECO-RWC-BF.*

5.6 Conclusions

The following conclusions can be made from the tests:

1. The compressibility of the water saturated backfill was tested with oedometer tests. The evaluated oedometer modulus from the four tests made of backfill with the dry density 1,800–1,850 kg/m^3 varied between 34 and 50 MPa.
2. Altogether three tests were made for determining Young´s modulus (E) and Poisson´s ratio (υ) of the unsaturated backfill blocks. The specimens had a dry density of about 1,710 kg/m^3 and the evaluated parameters were E = 231–263 MPa and υ 0.16–0.19 respectively.
3. The strength of the unsaturated backfill blocks, both the compressive strength and the tensile strength were measured on specimens compacted to different dry densities. The test results show that the strength is depending on the density of the specimens and that the tensile strength is about a factor of 4 lower than the compressive strength.
4. Two tests were made for evaluating the compressibility of loosely filled pellets. The tests show that from an initial dry density of ~850 kg/m^3 the filling was compressed to ~1,350 kg/m^3 at a compaction pressure of about 5,000 kPa.

6 Swelling pressure and hydraulic conductivity

The hydraulic conductivity and swelling pressure tests were made in oedometers with a diameter of 50 mm. The height of the samples was 20 mm. The tests were prepared and made in the following steps:

- The specimens were compacted into the oedometer (see Figure 6-1) to a specified dry density at the initial water content of the material of about 18.5%. The delivered material was rather coarse (see Figure 3-1). In order to find out if the granule size affects the swelling pressure and the hydraulic conductivity some of the tests were made with ground material.
- A piston was placed on top of the specimen which was saturated from both the top and bottom filters during continuous measurement of the swelling pressure with the load cell placed on top of the piston. The tests were performed with two different water salinities (1% and 3.5%).
- After saturation, a pore pressure gradient was applied over the specimens and the volume of out-flowing water measured. This volume was used for calculating the hydraulic conductivity of the specimens. The gradient during the tests varied between 250–5,000 (corresponding to a pore pressure difference over the specimen of Δu = 50–1,000 kPa). No backpressure was used.
- The specimen was pressed out of the oedometer after the test and the water ratio and density determined.
- The swelling pressure and the hydraulic conductivity are presented as function of the dry density.

6.1 Results from the measurements

Figure 6-2 shows the swelling pressure plotted versus the dry density and Figure 6-3 shows the hydraulic conductivity plotted vs. the dry density. A summary of all measured values is also provided in Table 6-1. The figures indicate that the water salinity and the granule size are not significantly affecting the measured swelling pressure and hydraulic conductivity.

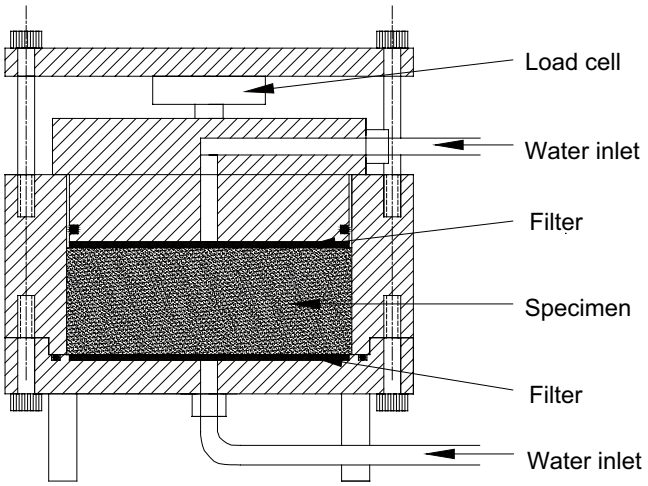

Figure 6-1. *A schematic drawing of an oedometer.*

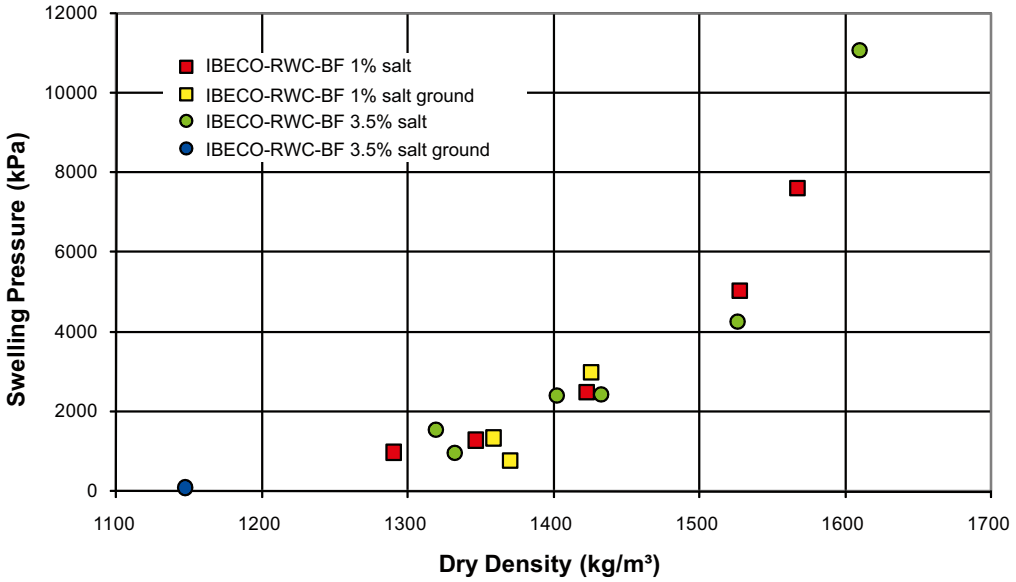

Figure 6-2. *The swelling pressure as function of the dry density.*

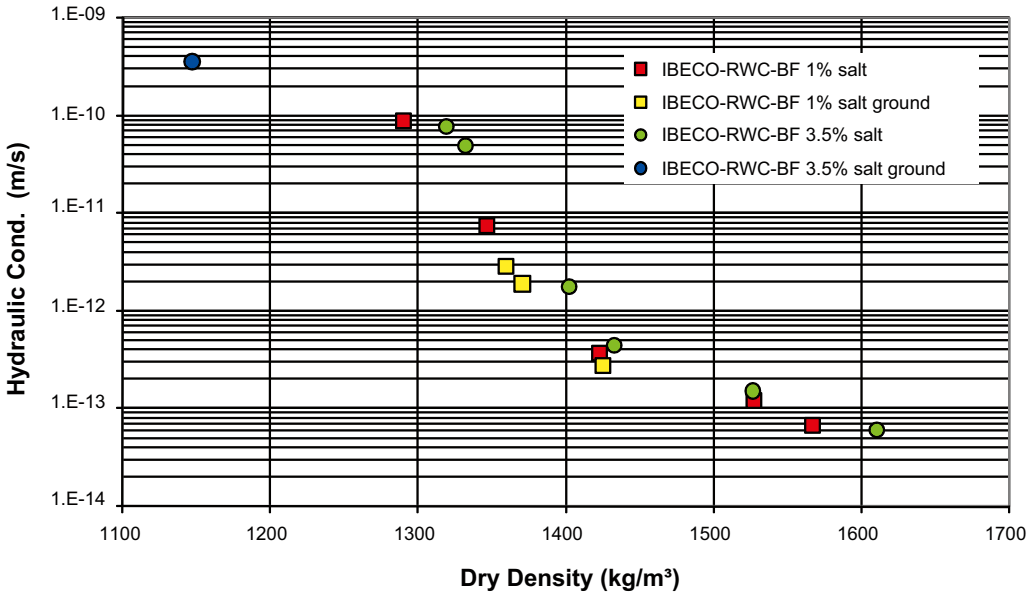

Figure 6-3. *The hydraulic conductivity as function of the dry density.*

Table 6-1. Results from the investigation of the hydraulic conductivity and swelling pressure of the backfill material IBECO-RWC-BF.

Dry density (kg/m³)	Gradient	Hydr. Cond. (m/s)	Swelling Pressure (kPa)	Note
1,043	25	1.25E–10	38	Pellets
1,290	250	8.9E–11	985	
1,346	400	7.59E–12	1,293	
1,359	250	2.86E–12	1,350	Ground
1,370	1,000	1.91E–12	780	Ground
1,423	5,000	3.70E–13	2,501	
1,425	1,000	2.79E–13	3,000	Ground
1,527	5,000	1.22E–13	5,035	
1,567	5,000	6.87E–14	7,604	
1,036	25	1.17E–10	44	Pellets
1,147	250	3.58E–10	100	Ground
1,319	250	7.73E–11	1,557	
1,332	400	4.98E–11	982	
1,402	400	1.81E–12	2,394	
1,433.	5,000	4.49E–13	2,430	
1,526	5,000	1.52E–13	4,260	
1,610	5,000	6.06E–14	11,089	

6.2 Conclusions

The measured swelling pressure and hydraulic conductivity show a very logical influence of the dry density, as expected, for this kind of material. The following conclusions can be made:

- **Granule size distribution**. There is no obvious influence of the granule size. The delivered material was rather coarse and in order to investigate the influence of the granule size a number of tests were performed with ground material but the results did not differ.
- **Salt content of the water**. The investigation was performed using water with a salt content of 1% and 3.5%. At the rather high dry densities, 1,300–1,600 kg/m³, there was no influence of the salt content regarding the determined swelling pressure or hydraulic conductivity. Only one measurement has been made at a low density, 1,150 kg/m³. More tests are needed in order to study the influence of the salt content at low densities.

7 Erosion

7.1 General

Backfilling of deposition tunnels is planned to be done by emplacement of pre-compacted blocks of bentonite, see Figure 7-1. The blocks will be stacked, filling up 60–80% of the tunnel volume. The remaining space between blocks and rock is to be filled with bentonite pellets. During and after emplacement of blocks and pellets a number of scenarios can develop due to water inflow from the rock. One of the most obvious scenarios is that water will flow and erode away material both from the blocks and the pellets. Investigations regarding erosion properties have been made earlier with different backfill candidate materials. In this investigation of the backfill material IBECO-RWC-BF, the same equipment and test layouts have been used as in the previous tests.

7.2 Erosion of blocks

7.2.1 General

Tests to study the erosion properties of blocks have been done in both Phase 2 and 3 of the Baclo project /Sandén et al. 2008/ and /Sandén and Börgesson 2008/. Those tests simulated the installation phase in a tunnel filled with blocks and pellets. The tests were performed using blocks of Friedland clay. The water inflow rate and the salt content in the water were varied. The results from these tests showed a large influence of the water salinity, while the water flow rate and the test length seemed to have a small impact on the erosion rate (amount of eroded material per liter water). The total number of tests performed was, however, limited.

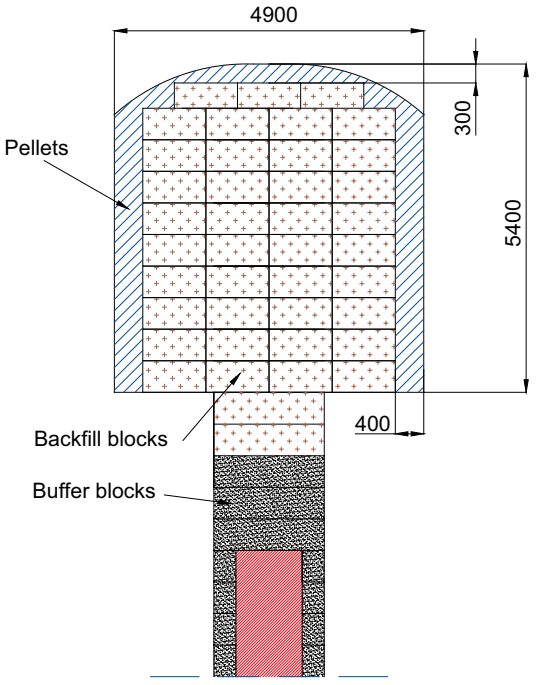

Figure 7-1. *Schematic drawing showing an example of the geometry of a deposition tunnel backfilled with blocks and pellets.*

7.2.2 Test description

The blocks used in the tests described in this chapter were made of IBECO-RWC-BF and have been manufactured at the same factory that produced the Friedland blocks (Höganäs Bjuf AB, see chapter 3). The blocks had a water content of about 18% and a dry density of 1,620 kg/m^3.

The tests were performed in the same way as the old test series /Sandén et al. 2008/ and /Sandén and Börgesson 2008/, using the same test equipment. The blocks were placed in a groove made of a steel profile, Figure 7-2. The length of the groove is 1 meter. A preselected water inflow was applied in one end and was allowed to travel along the block surface. The steel profile had an inclination of about 1%, close to that envisaged for an emplacement tunnel in a KBS-3V repository.

The following was controlled and measured during the tests:

Water flow

- **Water flow into the system.** This was set to a selected value on the microprocessor controlled pump used to supply water to the test.
- **Water outflow from the system.** Samples of exiting water were taken, weighed and then placed in an oven at 105° where the water was evaporated. After drying, the container was weighed again. With this procedure the amount of water flowing out per unit time could be calculated. When the flow rate was 0.1 l/min or higher, water samples were taken from the downstream exit at regular intervals. For flow rates of 0.01 l/min or lower all the water during a certain time period was collected as a single sample.

Erosion measurements

- **The amount of eroded material in the water**. The water samples taken from the exiting water were also used to determine the amount of clay contained in the water by evaporating the water in an oven at 105°C and determining the residue. The mass remaining was corrected for salt originally in the water. The determined erosion rate for a certain sample was used for the period between two samples when calculating the accumulated erosion.
- **Observing the material.** A digital camera was used in order to register the behavior.

Figure 7-2. *The blocks were placed in a steel profile. A constant water flow was applied in one end and the amount of eroded material in the other end was measured. The photo shows the start of the test with a water flow of 0.1 l/min and with water containing 3.5% salt.*

7.2.3 Results

General

Totally six tests were made in this test series:

1. Applied water flow: 0.1 l/min, 1% salt in water.
2. Applied water flow: 0.01 l/min, 1% salt in water.
3. Applied water flow: 0.1 l/min, 3.5% salt in water.
4. Applied water flow: 0.01 l/min, 3.5% salt in water.
5. Repetition of test 1.
6. Repetition of test 3.

Erosion

It was only possible to measure erosion in the four tests performed with the higher water flow rate i.e. 0.1 l/min. In the two tests performed with the lower water flow rate, 0.01 l/min, the blocks got time to swell and seal of the flow way. Before any water had reached the outflow point, the blocks were totally wetted and fell apart, see photos in Appendix 2.

In Figure 7-3 the accumulated amount of eroded material from the four tests where erosion was measured is plotted versus time. The test duration was set to about 8 hours. After this time the blocks were completely wetted and fell apart which means that it was impossible to continue the erosion measurements.

In Figure 7-4 the results from the erosion tests are presented as the accumulated dry mass of eroded material plotted vs. the accumulated water flow in logarithmic scales. The two black lines shows the boundary of the erosion model that was suggested in /Sandén et al. 2008/. The results from the measurements show that the erosion rate is close to the upper limit but the curves have the same inclination i.e. the erosion rate decreases by time.

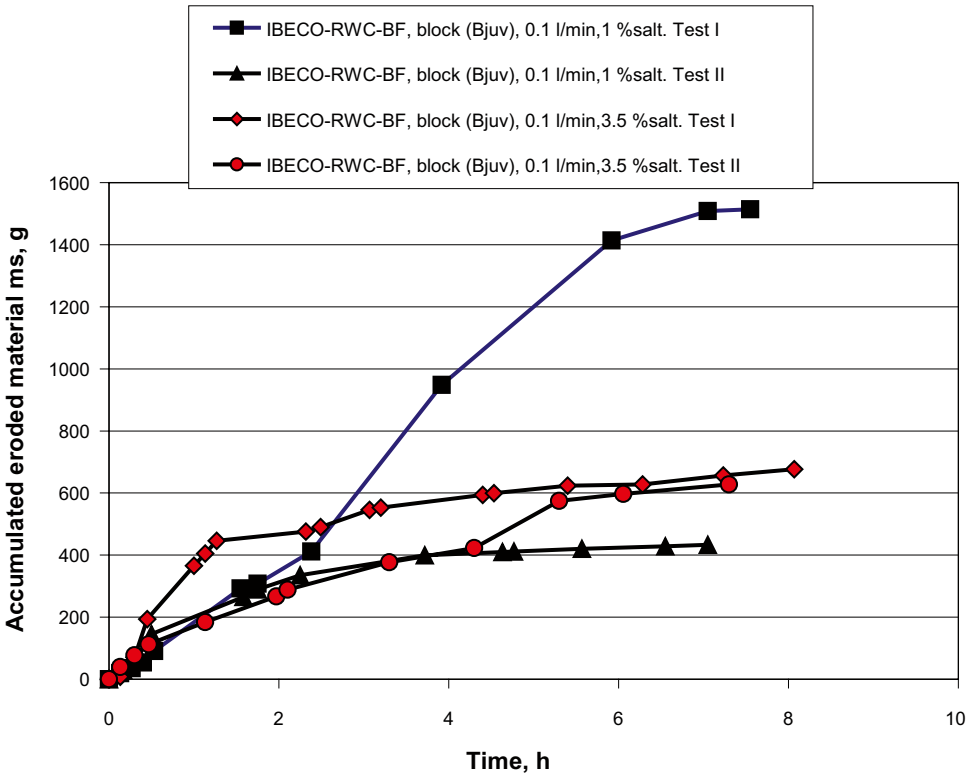

Figure 7-3. *The accumulated dry mass of eroded material plotted vs. time.*

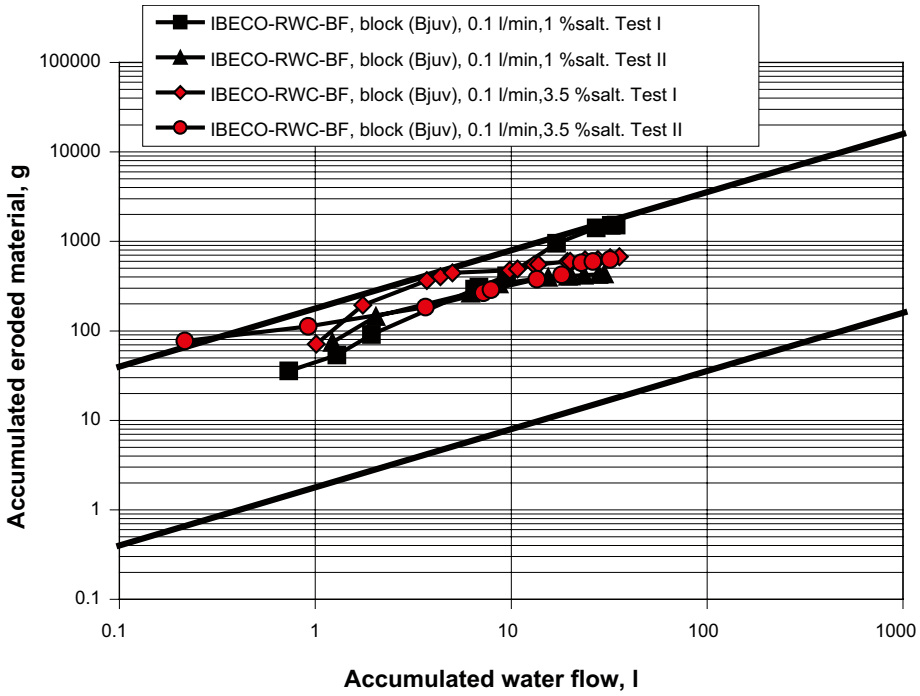

Figure 7-4. *Accumulated dry weight of eroded material plotted vs. the accumulated water flow in logarithmic scales. The two black lines shows the boundary of the suggested erosion model /Sandén et al. 2008/.*

The results of Test I with 1% salt are not logical. In the first test the erosion rate was significantly higher than in the second test. This depends probably on the difficulty to separate real erosion i.e. material transported away with the water, from the fact that parts of the blocks came loose during the wetting and fell down to the collector of the out-flowing water.

For the tests performed with a flow rate of 0.1 l/min more than 10 liters of water were taken up, stored, by the bentonite blocks, see Figure A2-4 in Appendix 2. The two tests performed with the lower flow rate, 0.01 l/min, were running for about 24 hours and during this time no water flew out from the test. This means that about 14.4 liters were stored by the bentonite. When finishing the tests it was found that all bentonite was wetted, see photos in Appendix 2, and that the bentonite had water content between 57 and 73%.

7.2.4 Conclusions and comments

The results from the erosion tests on pre-compacted blocks can be summarized as follows:

- It was only possible to measure erosion when the flow rate was 0.1 l/min. In the tests with the lower flow rate, 0.01 l/min, all water was sucked up by the bentonite blocks and after 24 hours test duration no water had left the test setup.
- In the first test with a flow rate of 0.1 l/min and using water with a salinity of 1%, the erosion rate was significantly higher than in the second test. This depends probably on the difficulty to separate real erosion i.e. material transported away with the water, from the fact that parts of the blocks came loose during the wetting and fell down to the collector of the out-flowing water.
- The two tests performed with 0.1 l/min and with 3.5% water salinity have somewhat higher erosion rate than one of the tests performed with 1% salt in the water. This is consistent with earlier results were higher salt contents in the water have resulted in higher erosion rate.
- The measured erosion rate decreases with time in all tests.
- Although the number of tests performed has been limited, the test method seems representative of what might be encountered in the field when water flows on the surface of the backfill blocks.

7.3 Erosion of pellets

7.3.1 General

The erosion properties of bentonite pellets have also been investigated in both Phase 2 and 3 of the Baclo project /Sandén et al. 2008/ and /Sandén and Börgesson 2008/. The main parts of the tests were made with MX-80 pellets but also other materials have been tested (Cebogel QSE, Minelco granules and Friedland granules). Some important conclusions/findings from these tests were:

1. The erosion rate decreases by time. The earlier tests (except some tests including pellets mixed with powder) have been used for the suggested erosion model.
2. For some materials high water counter pressure can be build up which may affect the ability of the pellet fill to "store" water and thereby delay the time before water will exit the backfilled volume into adjacent open areas. It is suggested that the dry pellets could be pushed forward and water filled cavities created. This phenomenon could probably also occur with the other materials if hydraulically unfavorable conditions exist. This type of behavior is probably controlled by factors such as the granule size distribution, the size of the available voids and the geometry of the confinement. With a large pellet size the voids are rather large and the water can flow in a channel that remains open for long time (MX-80). When the pellets are smaller the voids are smaller and flow resistance can be built up and at an unfavorable geometry this clogging process may occur (Friedland, Minelco and Cebogel QSE). However, it has only been observed in tubes where the stiff walls prevent radial flow and valve formation may occur.
3. A conceptual model that may be used to predict the eroded clay mass as a function of the mass of through-flowing water has been suggested.

7.3.2 Test description

The test equipment was the same as used earlier in the Baclo project. It consists of tubes made of Plexiglas so that the course of events could be followed from the outside and also photographed, Figure 7-5. Each tube had an inner diameter of 0.1 m and a length of 0.5 m. The tubes could be jointed end-to-end to produce test assemblies of any desired length. In this test series all tests were made with a length of 1 m.

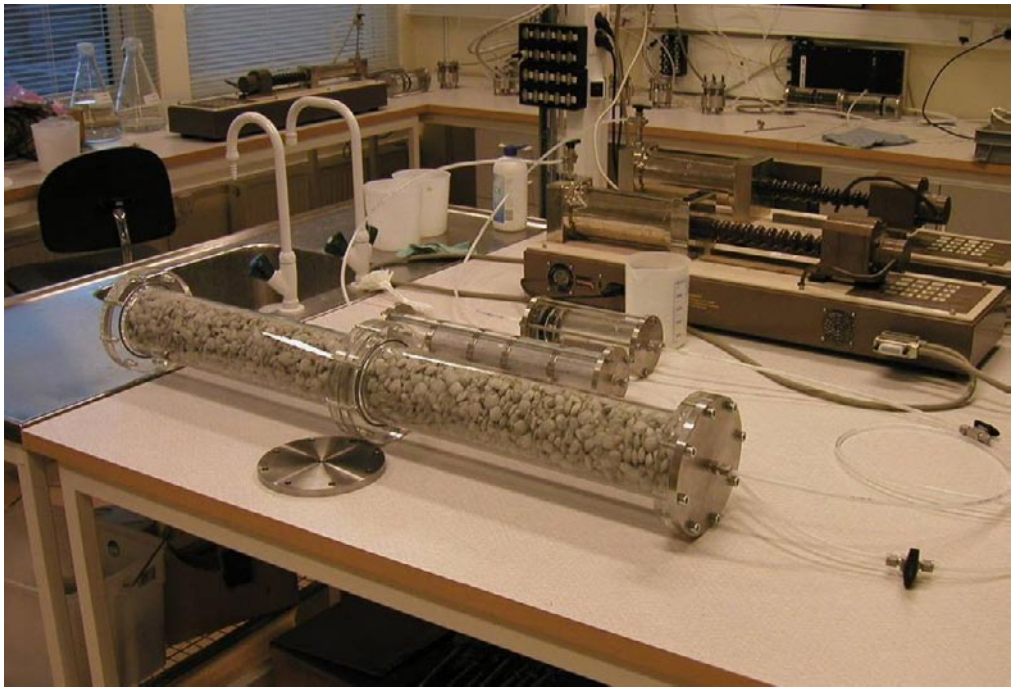

Figure 7-5. *The test equipment consists of Plexiglas tubes which are filled with the pellet material. A constant water flow was applied in one end and the discharging water collected in the other end.*

At the outflow ends of the Plexiglas-tube, a perforated plate was positioned, see photo in Figure A3-2 in Appendix 3, in order to keep the pellet material in position during the test. At the other side of the tube a point inflow was applied. Different water types were used in order to examine the effects of the water composition, see chapter 2.

Water flow and erosion measurements

The water flow and erosion measurements were controlled and measured in the same way as described in section 7.2. In addition, a separate pressure transducer was used to monitor possible water pressure built up in the system. The aim was to apply a constant inflow rate regardless of the resisting water pressure that was built up during the saturation of the pellet material.

7.3.3 Results

General

Four erosion tests have been performed. In all tests pellets of IBECO RWC BF material was used. The tests were performed with two water flow rates, 0.1 and 0.01 l/min, and with two water salinities, 1% and 3.5%.

Additional data and photos are provided in Appendix 3 to 6.

Erosion

The results from the four tests are presented in Figure 7-6 to 7-7. The erosion is strong in the beginning but decreases by time. The measured data can also be presented as the accumulated amount of eroded material plotted versus the accumulated water flow, see Figure 7-7. The results from the tests are well inside the limits of the suggested erosion model. However, the decrease in erosion rate in the pellets seems to be faster than in pellets made of MX-80.

Also the influence of the salt content in the water was clear (higher salt content caused higher erosion rate) but after a certain time, the differences between the tests had decreased and the erosion rate was for all tests settled on a rather similar rate.

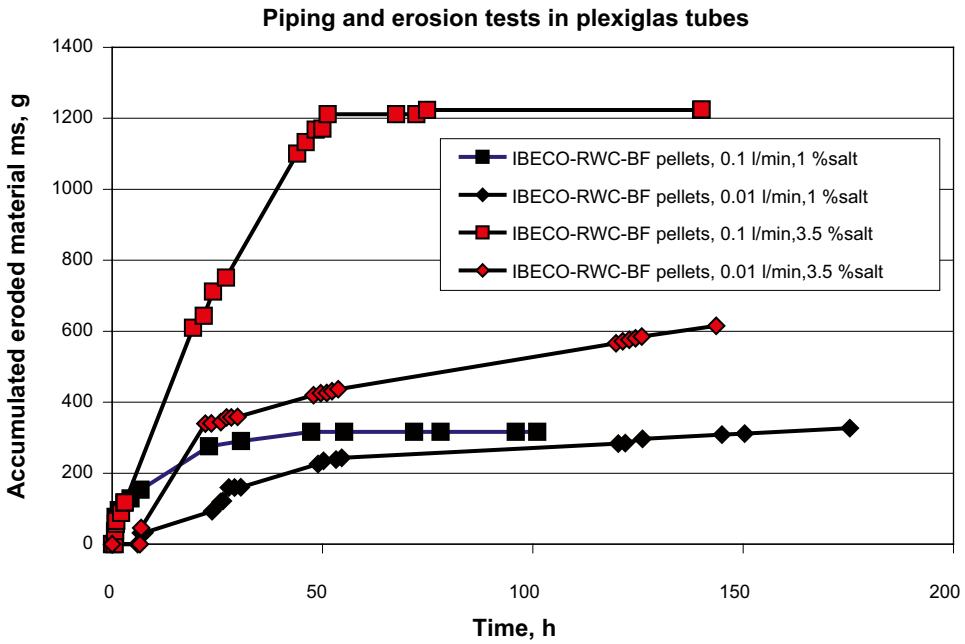

Figure 7-6. *The accumulated amount of eroded material plotted vs. time for the four tests. In the beginning of the tests is the erosion rate high but after 20–50 hours it has settled on much lower level.*

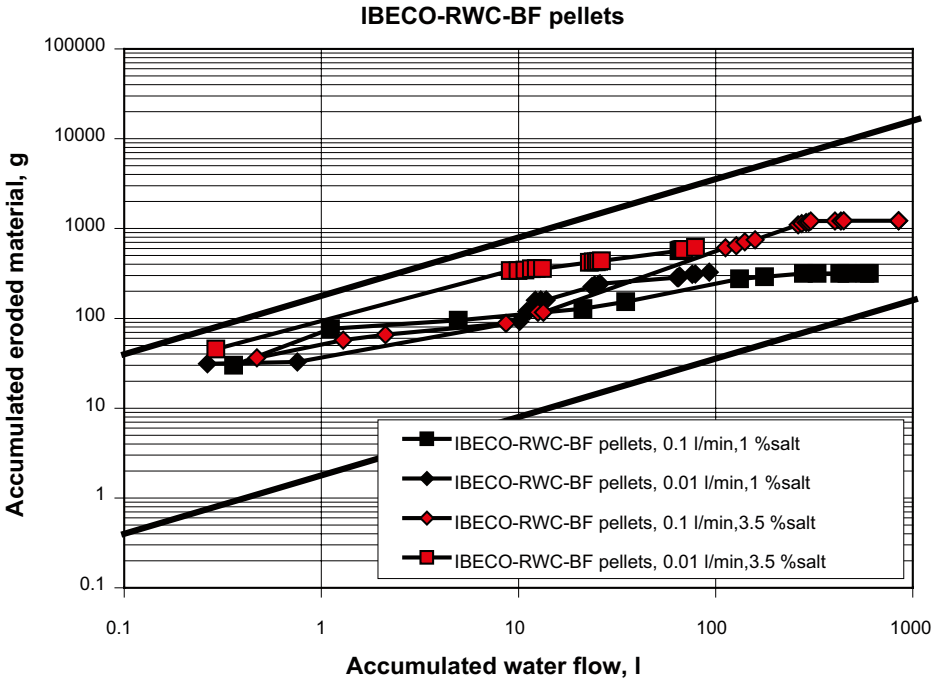

Figure 7-7. *The accumulated amount of eroded material plotted vs. the accumulated water flow in logarithmic scales.*

Resistance to water inflow

A compilation of flow and pressure measurements during the tests is presented in Appendix 3–6 together with pictures from the tests. In none of the tests performed with the higher water inflow rate (0.1 l/min), did a strong degree of resistance to water input build up during the test. However, a resistance to inflow was monitored in the tests performed with the lower water flow rate 0.01 l/min; see Figure 7-8 with both 1% and 3.5% salt in the water, especially in the beginning of the tests when up to 400 kPa water pressure was measured occasionally.

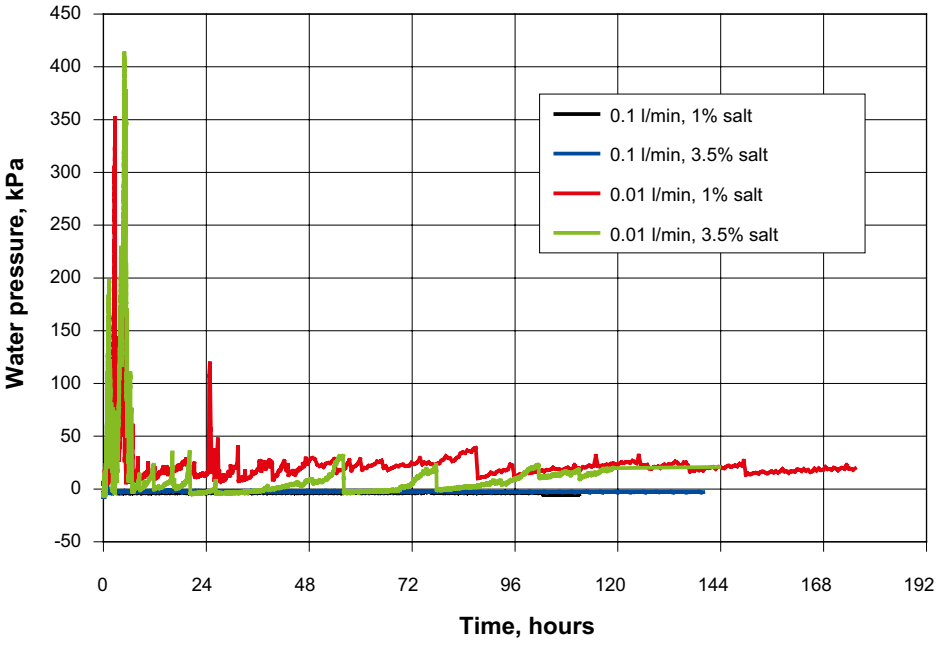

Figure 7-8. *The water pressure built up during tests plotted vs. time.*

7.3.4 Conclusions and comments

The results from the erosion tests on the IBECO-RWC-BF pellets can be summarized as follows:

- The results from the tests are well inside the limits of the suggested erosion model. However, the decrease in erosion rate in the pellets seems to be faster than in pellets made of MX-80.
- The erosion rate is higher for the eroding water with the high salt content. This effect is obvious in the beginning of the test but decreases by time.
- In the tests with low water flow rate, a resistance to the water flow was built up (up to 400 kPa). This behavior have been seen also in the earlier tests performed in phase 2 and 3 of the Baclo project /Sandén et al. 2008/ and /Sandén and Börgesson 2009/. The behavior probably depends on a combination of many factors such as salt content in water, water flow rate, granule size distribution and the size of the available voids. The main reason is however probably the geometry of the confinement.

8 Self healing ability

8.1 General

The aim of these tests was to study the healing ability of the backfill materials after piping. The same type of tests have been performed earlier using the same test equipment and with the same test layout but with different materials /Sandén et.al 2008/.

8.2 Test description

The tests were performed in oedometers, see Figure 8-1, where specimens with an outer diameter of 50 mm and a height of 50 mm could be tested (the tests with pellets were performed in a similar piece of equipment, but with an inner diameter of 101 mm and a specimen height of 85 mm). The tests with compacted material were performed at two different densities. Piping will probably not occur at the innermost parts of the block filling where the density is high but at the outermost parts of the deposition tunnel where the backfill has swollen and the density is lower. The higher density corresponds to an average dry density of the backfill material in a cross section. Based on this density gradation, the lower density condition was chosen for inclusion in the test matrix. The chosen density of the pellets specimens corresponds to the bulk density of the filling after pouring the pellets into the vessel without any additional compaction (the density is somewhat higher than expected depending on the fact that a vacuum pump was used in order to get rid of the air before water saturation and during this vacuum suction, the specimens were somewhat compacted). The test conditions represent, however, well the conditions anticipated to occur.

8.2.1 Saturation of samples

After preparation of the specimens they were placed in oedometers, Figure 8-1, and contacted to water via the steel filters placed on both sides of the samples. Tubes were connected to the oedometers in one end and to burettes in the other end. The burettes were set to provide a water pressure of about 1 meter during the saturation time. The saturation time lasted for about 1.5 to 2 months. The development of the swelling pressure was also measured.

8.2.2 Hole drilling and measurement of hydraulic conductivity

When the specimens were saturated, the hydraulic conductivity was determined by applying a water pressure in the bottom of the oedometer and measuring the volume of the discharged water on the other side per unit time. The applied pressure was different for the different materials (see Table 8-1), and there was no backpressure applied during the measurement of the hydraulic conductivity. When the measurements were finished, the lids of the oedometers were removed and a hole with the diameter 5 mm was drilled through the center of each specimen. The lids were then re-mounted and the specimens were again provided with passive access to water. A small through flow in the drilled hole was applied in the beginning in order to avoid air pockets and then a source of water was connected to the specimen, providing the specimen with free water. After a certain time of healing, about three weeks, the hydraulic conductivity was measured again with the same method as previously.

8.3 Test matrix

In this test series totally five tests have been performed, three with compacted specimens and two with pellets, see Table 8-1. Two of the compacted specimens had the dry density 1,331 and 1,345 kg/m^3 and they were tested with water with a salinity of 1% and 3.5% respectively. One sample was compacted to a dry density of 1,402 kg/m^3 and was tested with water with a salinity of 3.5%. The two pellets specimens were tested with water with 1% and 3.5% respectively.

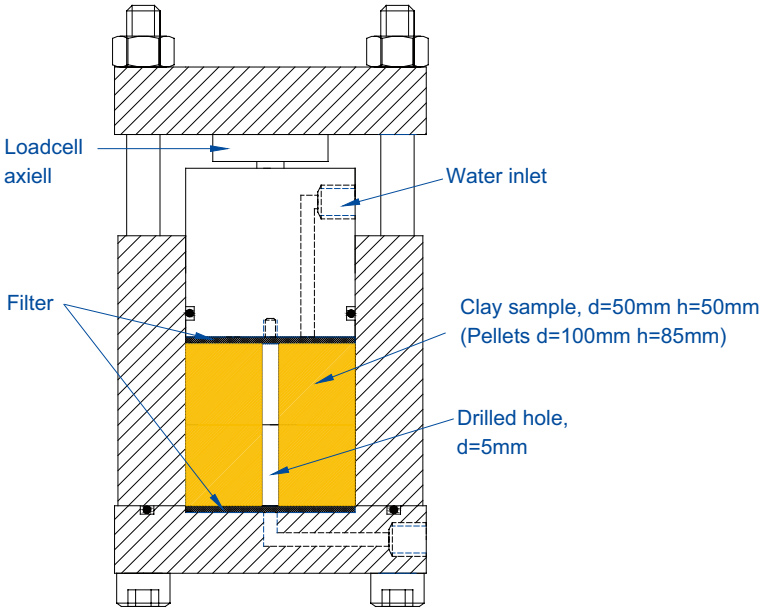

Figure 8-1. *Schematic drawing of the test equipment used in the self-healing tests. In the tests with pellets a larger test cell was used (inner diameter = 101 mm, height = 85 mm).*

Table 8-1. Data from the self healing tests.

Material	Measured sat.density/ dry density kg/m³	Water	Applied gradient	H.K. before drilling m/s	Healing time	H.K. after healing m/s	Remark
IBECO-RWC-BF	1862/1345	1% salt	400	7.6×10^{-12}	3 weeks	1.1×10^{-10}	5 mm hole
IBECO-RWC-BF	1852/1331	3.5% salt	400	5×10^{-11}	3 weeks	4.4×10^{-10}	5 mm hole
IBECO-RWC-BF	1897/1402	3.5% salt	400	1.8×10^{-12}	3 weeks	4.1×10^{-12}	5 mm hole
IBECO pellets	1668/1043	1% salt	25	1.3×10^{-10}	3 weeks	1.1×10^{-6}	5 mm hole
IBECO pellets	1663/1035	3.5% salt	25	1.2×10^{-10}	3 weeks	3.4×10^{-7}	5 mm hole

8.4 Results

8.4.1 General

A compilation of the test data is presented in Table 8-1. The time dependence of the healing ability was not tested in this investigation (all specimens had a healing time of 3 weeks). The loss of material caused by the drilling of the central hole was about 1% of the specimen's weight.

8.4.2 IBECO-RWC-BF blocks

The swelling pressure as a function of time is shown in Figure 8-2. The drop in swelling pressure was not recovered due to the decreased average density.

As shown in Table 8-1, the specimens had healed the drilled hole very well but there remained a distinct difference in hydraulic conductivity compared to the measurements made before the drilling. After finishing the tests, the specimens were cut in the middle exposing a cross-section of the middle, see example in Figure 8-3. It was still possible to see traces after the drilled hole. The water content was determined in a number of positions after termination of the tests, see Figure 8-4. The samples taken out were small, about 2 g, in order to see the differences between different parts of the specimens, but it was of course difficult to get perfectly representative values of the water content in the former hole. The measurements showed, however, that there were still differences with a few percentage units, between the central parts and the outer parts of the specimens.

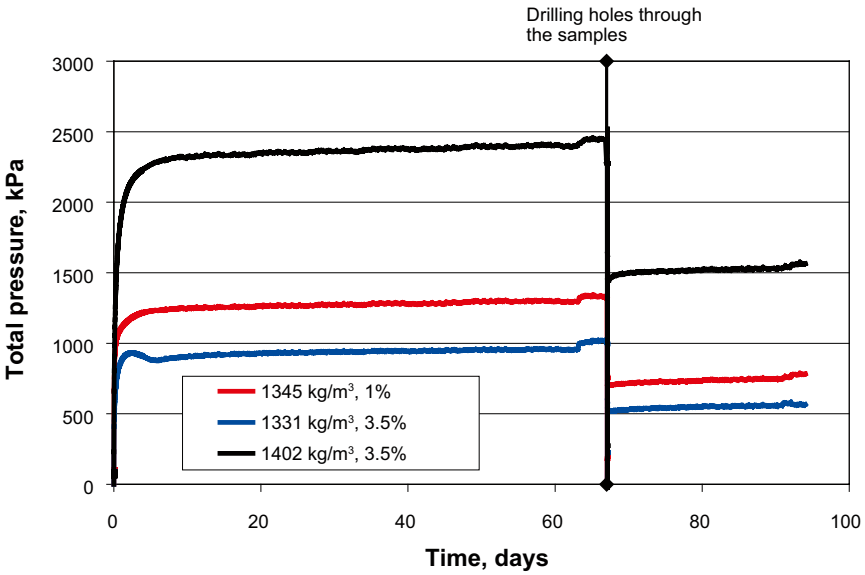

Figure 8-2. *Development of swelling pressure for the three block specimens plotted versus time.*

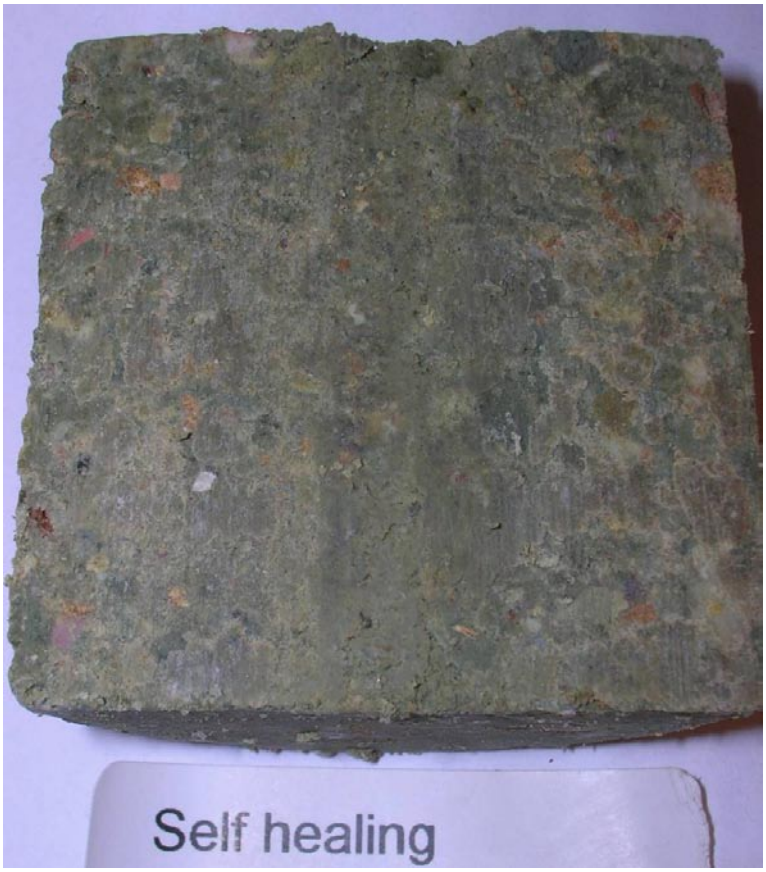

Figure 8-3. *After finishing the tests the specimens were cut in the middle along the cylinder. Note that it is still possible to see tracks from the drilled hole. The photo shows the sample with a dry density of 1,345 kg/m³ and saturated with water with 1% salt.*

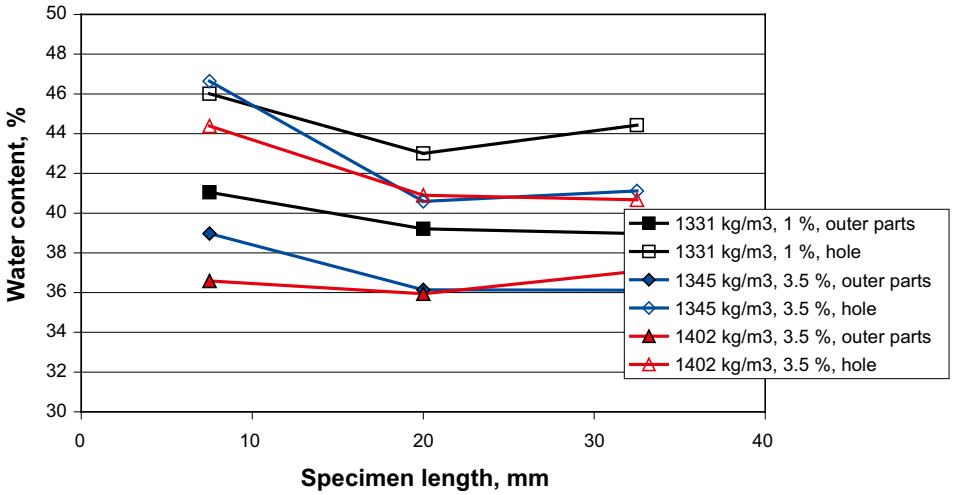

Figure 8-4. Water content distribution in the three block specimens after termination. There is still a small difference in water content between the central parts and the outer parts.

8.4.3 IBECO-RWC-BF pellets

The development of swelling pressure measured during saturation is shown in Figure 8-5. After about 40 days a water pressure of 20 kPa was applied in the bottom of the specimens in order to measure the hydraulic conductivity. After determination of the hydraulic conductivity, the cells were opened and a hole was drilled through the middle of the specimens. Then the cells were closed and the specimens had again access to water. After three weeks of healing the hydraulic conductivity was measured again.

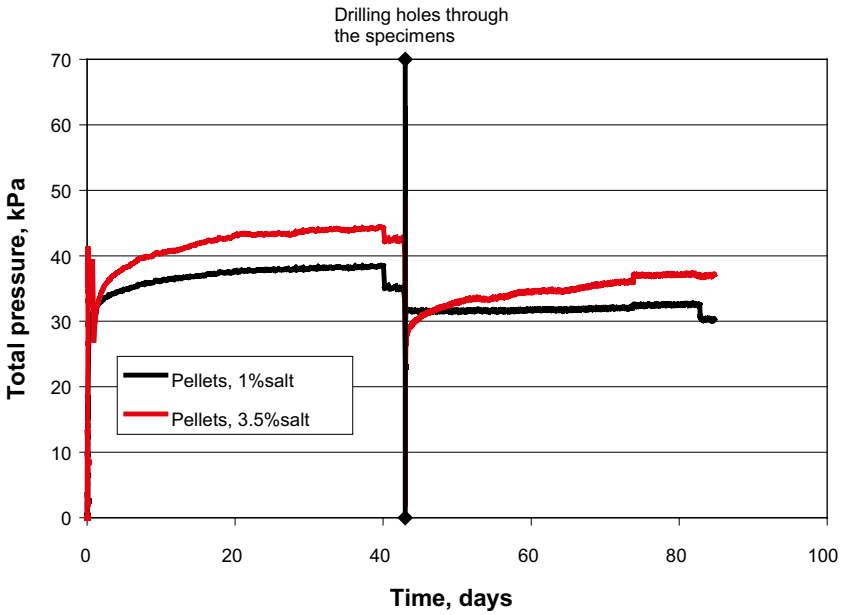

Figure 8-5. Development of swelling pressure for the IBECO RWC BF pellets with time.

At termination of the tests both specimens had the drilled hole still clearly visible and it was filled with a gel with noticeable lower density than the surroundings, see Figure 8-6 and 8-7. The water contents were determined at three levels in each specimen; close to the drilled hole and at the extreme perimeter, see Figure 8-8. The sampling of the clay in the former hole was difficult depending on the loose consistency and the measurements showed that there was almost no difference between the inner parts and the outer parts in none of the two tests. This depends probably on the fact that the samples taken were too big and didn't give representative values of the water content. The parts of the specimens closest to the end lids had, however, for both specimens evidently higher water content.

The dry density of the pellet fills tested was much lower compared to the other materials examined in this investigation. This is the explanation for the low healing during the tested three weeks period, see Figure 8-9

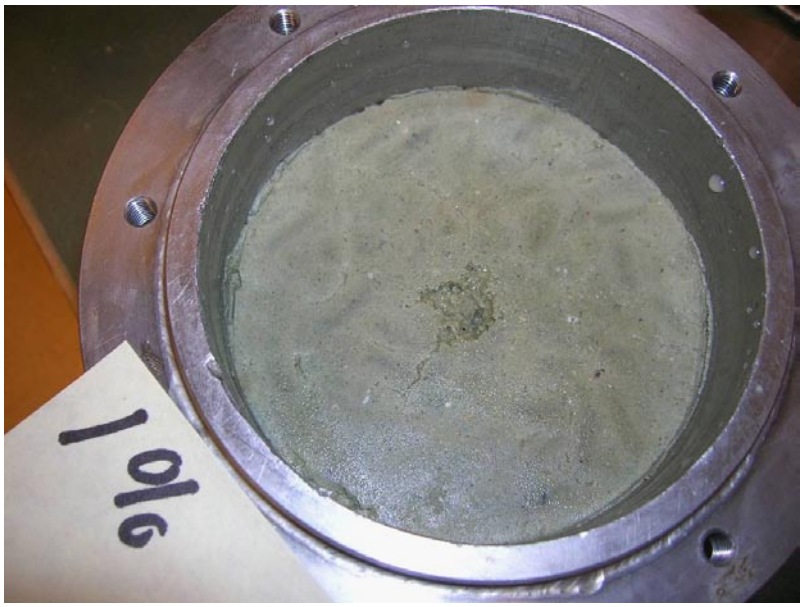

Figure 8-6. *Picture of the specimen saturated with 1% salinity in the water. The photo is taken during dismantling. The drilled hole can still be seen. The hole is filled with gel with higher water content than the surroundings.*

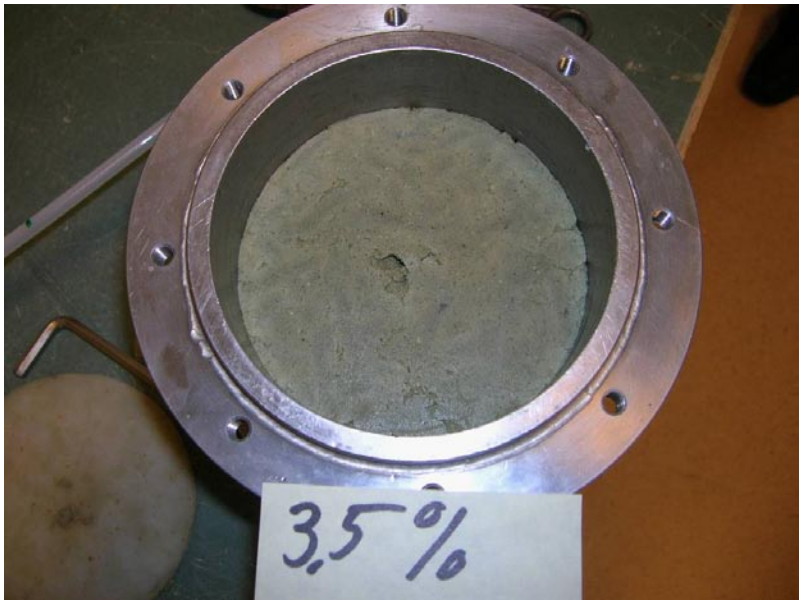

Figure 8-7. *Picture of the specimen saturated with 3.5% salinity in the water. The photo is taken during dismantling.*

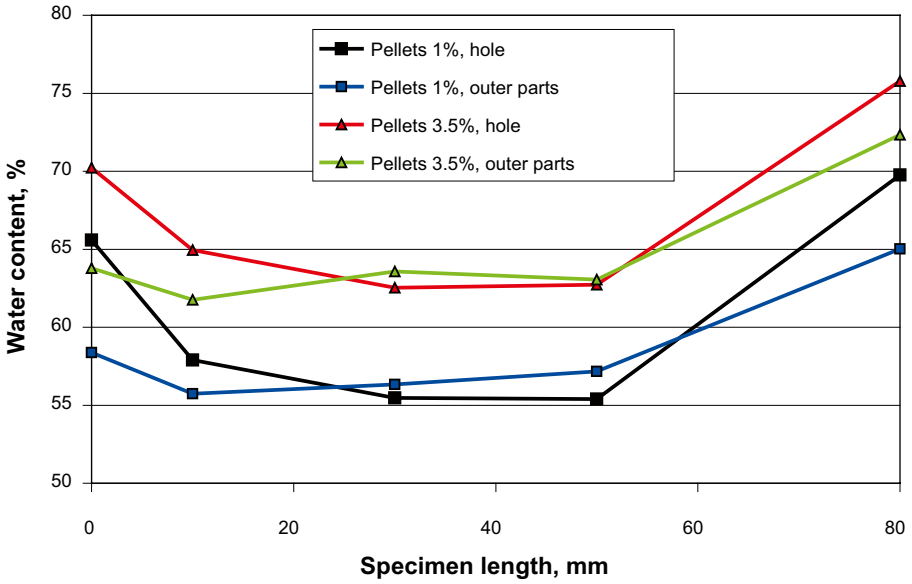

Figure 8-8. *Water content distribution measured in the two tests performed with pellets. The differences in water content between the outer parts and around the drilled hole are very small.*

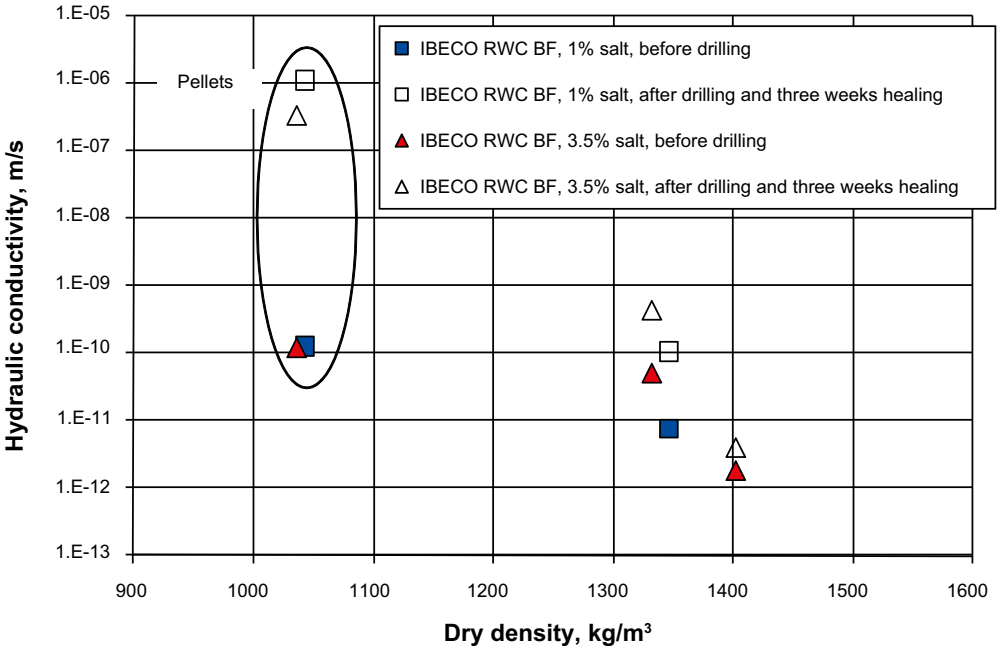

Figure 8-9. *Compilation of self healing test results. The diagram shows the average axial hydraulic conductivity determined before drilling (filled dots) and after drilling the axial hole with the diameter 5 mm.*

8.5 Conclusions

The diagram in Figure 8-9 shows the measured hydraulic conductivity before and after drilling the central hole. The hydraulic conductivity, measured before drilling of the central hole and after three weeks of healing for each specimen, is plotted versus the average dry density of the specimen (including the drilled hole). Each specimen is represented by two dots, one showing the hydraulic conductivity before drilling the hole (filled dots) and one showing the average hydraulic conductivity after three weeks healing time (empty dots). The results before drilling are consistent with the measured hydraulic conductivity shown in Figure 6-3.

The values provided in the diagram of the hydraulic conductivity after drilling and healing, are plotted versus the average dry density of the specimens. However, since the main part of the water is flowing in the drilled hole, where the density is lower, the figures for the density are not representative, especially not for the pellet filling, where the healing proceeds with lower rate and it also could be seen that the former hole was filled with loose gel; see Figures 8-6 and 8-7. The diagram gives, however, a good picture of how the self healing process has proceeded after a three week period of healing for the different start densities.

The design of the experiments, with drilled holes in saturated samples, is for the pellet filling not very realistic on mainly two reasons:

1 The pipe is drilled after saturation and homogenization of the pellet filling. In reality the erosion channels will go in the existing open voids between the pellets and be better homogenized by swelling of the high density pellets.

2 During saturation of the backfill in the tunnel, the blocks will swell and compress the pellet filling i.e. the density of the pellet filling will increase with time during the saturation/homogenization of the system.

However, additional tests of the self sealing properties of erosion channels should be made.

The method used for determining the self healing ability of the materials is not a standard method as no standards for determining such behavior exist. The results are however consistent and the ability of the backfill material to self-heal can be summarized as follows:

- The increase in hydraulic conductivity determined after the healing time depends on an incomplete homogenization. The decrease in density depending on the drilling of the hole is 1% for the high density specimens and 0.2% for the pellets tests. This decrease in density is too small in order to influence the hydraulic conductivity more than marginally.
- The fact that the water after the healing period mainly is flowing in the former hole, where the density is lower (especially for the pellet filling) has not been considered when calculating the hydraulic conductivity. This means that the figures given for the dry density in Figure 8-9 and in Table 8-2 are not representative for the corresponding values of hydraulic conductivity (after healing).
- **Compacted blocks**. The specimens had largely healed but there were still visual traces of the drilled hole that could be seen after finishing the tests as well as a small remaining increased hydraulic conductivity.
- **Pellet**. The drilled holes were after three weeks of healing visibly filled with gel; see Figure 8-6 and 8-7, which means that the healing process was rather incomplete. Depending on this fact, there was a strong increase of the determined hydraulic conductivity after the healing period. The influence of salt content in the water was small.

A general conclusion is that the self healing capacity is rather good at high densities corresponding to the average density expected in the tunnels but also that the pellets filling alone has a rather poor healing capacity but will be significantly helped by the swelling of the backfill blocks.

9 Homogenization of backfill blocks/pellets

9.1 General

The backfill concept includes compacted bentonite blocks that are piled on the tunnel floor. After piling there will be a remaining slot between the blocks and the rock wall which will be filled with bentonite pellets. During the saturation phase the blocks will swell and homogenization of the blocks and the pellets will start.

The pellets filling alone are not good enough to function as backfill material but needs to be compressed by the swelling blocks. The ability of the filling to homogenize is an important issue.

Homogenization tests have been performed earlier using the same test equipment and with the same test layout but with different materials (Friedland and Asha blocks combined with different pellets) /Johannesson et.al 2008/. In this earlier test series, that included a large number of tests, the following was concluded:

- *Influence of time*. Tests were performed with test durations of two weeks, two months and four months. It was concluded that the main part regarding homogenization in this scale takes part during the first two weeks.
- *Influence of wall friction*. The influence of wall friction regarding the homogenization was tested by performing tests with lubricated walls and then compares the result with the standard tests. It was in these tests not possible to detect any differences in the homogenization process.
- *Access to water*. The influence of access to water was also investigated by letting one sample have access to water from both the pellets side, the rock, and also from the block side. The tests showed that there was a small difference in water content at the outer most part.
- *Influence of salt content in the water*. Tests were performed using water with different salinities (1% and 3.5%). The results showed that the influence of salt regarding the homogenization was small.
- *Influence of different slot widths.* The influence of the slot width regarding the homogenization rate was as expected rather large. In the performed test series, tests with different slot widths (4, 8 and 12 mm width) were performed. The results showed that in the test with the 4 mm slot the time to completed homogenization had been considerable shorter.

With the experience from these earlier tests it was possible to minimize the test matrix and focus on the important parameter i.e. the slot width.

9.2 Test description

The tests were performed using oedometers of standard type, see Figure 9-1. Block specimens (d = 50 mm and h = 40 mm) were manufactured in the laboratory using a hydraulic press. The specimens were compacted at the water content the material had at delivery to a bulk density of 1,600 kg/m^3. The compacted specimen was placed in an oedometer and then a pellet filling of different thickness (4, 8 or 12 mm) was placed above. The pellets were crushed to a maximum diameter of about 4 mm. After preparation the sample got access to water from the pellets side i.e. the simulated rock wall for 60 days. The axial force was continuously measured with a load cell. No lubrication of the inner cylinder wall was done.

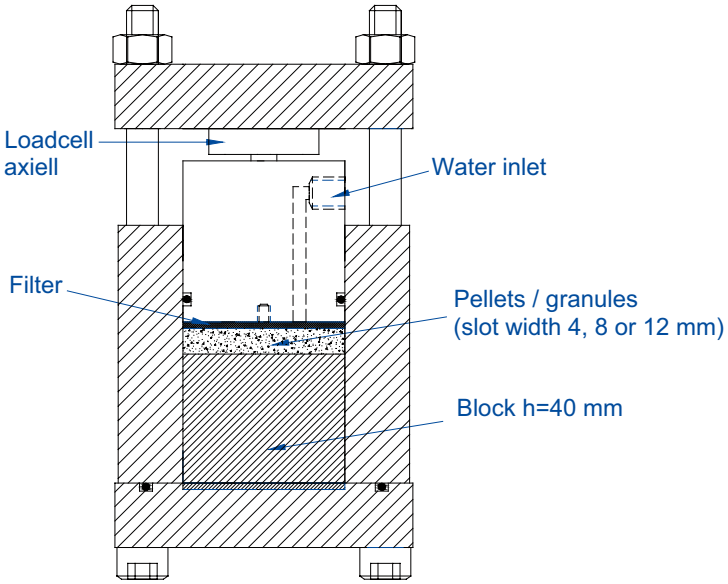

Figure 9-1. *Schematic view of the test equipment. An oedometer of standard type was used.*

Test variables

Three tests have been performed. In all tests water with a salinity of 3.5% was used. The slot widths 4, 8 and 12 mm were used.

Laboratory determinations

After termination of the tests, the specimens were divided in slices with a thickness of 5 mm (2.5 mm in some positions). Density and water content of each slice was then determined.

Water content

Half part of each slice was placed in an aluminum baking tin and the bulk mass (m_b) of the specimen determined by use of a laboratory balance. The specimen was dried in an oven for 24 hours at a temperature of 105°C. The dry solid mass (m_s) of the specimen was then determined immediately after removal and the water mass (m_w) was calculated according to Equation 9-1:

$$m_w = m_b = m_s \tag{9-1}$$

The water content (w) of the specimen determined according to Equation 9-2:

$$w = \frac{m_w}{m_s} \tag{9-2}$$

Density

The other half of each slice was used for determining the bulk density. The specimen was weighed, first in air (m_b) and then submerged into paraffin oil (m_{bp}). The volume of the specimen was then calculated

$$V = \frac{(m_b - m_{bp})}{\rho_p} \tag{9-3}$$

where ρ_p is the paraffin oil density. The bulk density of the specimen was calculated according to Equation 9-4:

$$\rho_b = \frac{m_b}{V} \tag{9-4}$$

Dry density and degree of saturation

After determining the water content and the bulk density of each specimen it was possible to calculate the dry density (ρ_d):

$$\rho_d = \frac{\rho_b}{1+w} \tag{9-5}$$

Since the density of the particles (ρ_s), the bulk density of the sample (ρ_b) and the density of water (ρ_w) are known the degree of saturation (S_r) can be calculated:

$$Sr = \frac{w \cdot \rho_b \cdot \rho_s}{[\rho_s \cdot [1+w] - \rho_b]\rho_w} \tag{9-6}$$

The density of the particles (ρ_s) used in the calculations is 2,780 kg/m^3.

9.3 Results

9.3.1 General

In Table 9-1 data is provided from specimen preparation and also measurements done after finishing the tests. An attempt to measure the width of the former pellets filled slot was done on each sample after finishing. The accuracy of these measurements is rather rough depending on the difficulties to determine the interface between pellets and block, see photos in Figure 9-2. The results from these measurements are also provided in Table 9-1.

In the following a brief analysis of the results will be done. However, in order to fully evaluate and accomplish the results from the tests they need to be modeled.

9.3.2 Homogenization

The diagrams in Figure 9-3 show the distribution of water content, dry density and the degree of saturation determined after finishing the tests. The black straight line shows the initial conditions at test start.

Swelling pressure

A diagram showing the swelling pressure development during the test is provided in Figure 9-4. The final pressure varied between 750 and 2,000 kPa. The differences depends of course on the fact that there is a difference in the average dry density between the samples, see Figure 9-3. The results are very logical. The swelling pressure agrees well with the measurements shown in Figure 6-2 if the dry density of the upper part of the pellets filling is used for the comparison.

The diagram in Figure 9-4 also shows that after about four weeks test duration, the swelling pressure has reached its maximum and after that there are only small changes.

9.4 Conclusions

The results from the homogenization tests will be used for modeling purposes. With the experience from the old tests it was possible to focus on the important parameter i.e. the slot width. The tests with the IBECO-RWC-BF material have shown that the homogenization of the specimens after two months testing had gone far even if there is a clear difference between the specimens depending on the initial slot width. The initial large gradient in density between the compacted specimen and the pellets filled slot has evened out and the remaining density gradient within the specimens is almost similar for all three tests even if there is a difference in the average density between the specimens. This difference depends on the different initial slot widths.

One example of the homogenization rate is that the differences in dry density at test start (block = 1,600 kg/m^3, pellets = 885 kg /m^3) has evened out to a density gradient from 1,250–1,400 kg/m^3 (12 mm initial width of pellets slot) after two months. The degree of saturation was for all three specimens between 92 and 100% at termination.

Table 9-1. Table showing data from material, preparation, after finishing and calculated average dry density.

	Specimen preparation											After finishing the tests			
	Block						Pellets					Specimen (block and pellets)			
Specimen	Material	w initial %	m g	h mm	Dry density g/cm³	d mm	Material	w initial %	m g	h mm	Dry density g/cm³	m g	h mm	d mm	Pellets slot** mm
IBECO-4mm	IBECO-RWC-BF	18.40	146.94	40.09	1.595	49.68	IBECO-RWC-BF	14.80	8.60	4	0.958	173.40	45.80	50.20	3.5
IBECO-8mm	IBECO-RWC-BF	18.40	146.60	39.81	1.595	49.70	IBECO-RWC-BF	14.80	17.30	8	0.958	185.58	49.97	50.29	7
IBECO-12mm	IBECO-RWC-BF	18.40	146.42	40.00	1.595	49.70	IBECO-RWC-BF	14.80	26.00	12	0.958	200.48	54.48	50.24	12

* Calculated average dry density

** Estimated width of the former slot. The accuaracy of this measurement is low.

Figure 9-2. *Photos taken after dismantling of the specimens. The former pellets filled slot can easily be seen but the width after homogenization is very difficult to determine.*

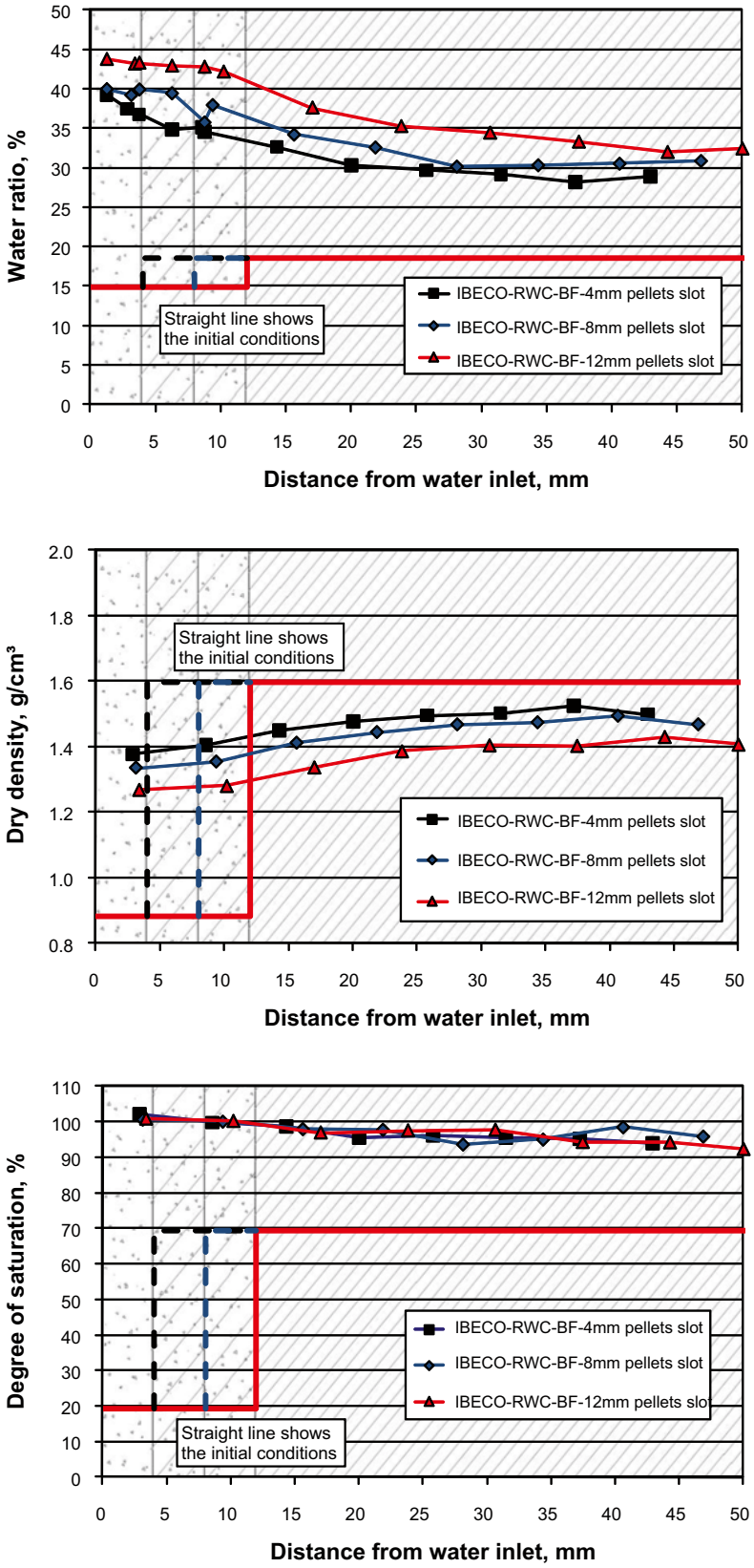

Figure 9-3. *Water content (upper), dry density (middle) and degree of saturation (lower) plotted as function of the distance from water inlet for the three specimens.*

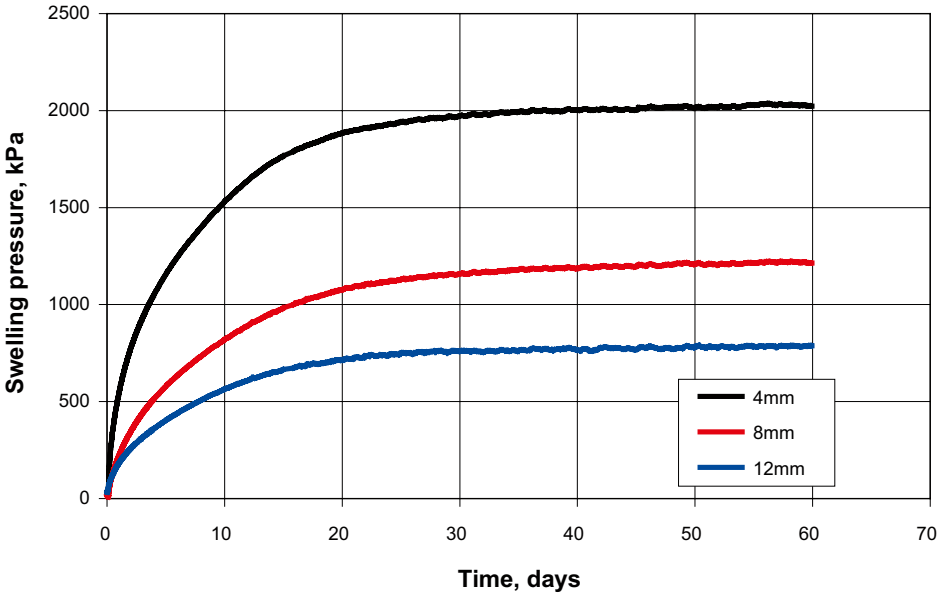

Figure 9-4. *Swelling pressure as function of time for the three specimens.*

10 Water uptake tests

10.1 General

In order to simulate and calculate the water uptake and the homogenization of a backfill consisting of pre-compacted blocks it is of great importance to study how and at with which rate the backfill material can take up water. In the laboratory it is possible to vary parameters which affect the water uptake and homogenization processes, such as material type, initial density and water content and the chemistry of the water. This type of tests can also be used as "benchmark tests" where different models and model parameters can be tested for simulating the water uptake and homogenization.

10.2 Test description

The tests were performed as follows:

- Material was compacted into a cylinder (ø = 101 mm and h = 100 mm) in five layers (see Figure 10-1).
- The specimens had access to water from the bottom during a specified time. The water was not pressurized (less than 10 kPa pressure). During the water uptake the sample was prevented to expand.
- After the water uptake phase the specimen was removed from the cylinder and the density and water content of the material were determined. The determinations were made on every 10 mm of the specimen. The results from the measurements were plotted as function of the distance from the water inlet.

The material was compacted to two different densities, one representing the assumed density of the blocks and one representing the average density of the backfilling after saturation. Furthermore the tests were made with a water salinity of 1%.

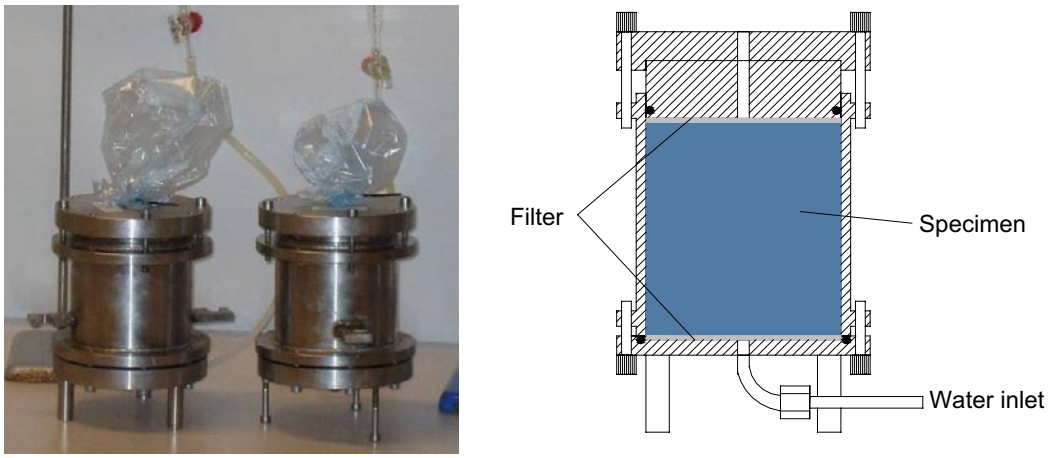

Figure 10-1. *The equipment used for the tests.*

10.3 Test matrix

The complete test matrix for the water uptake tests is shown in Table 10-1. The six preformed tests are shaded in the tables. The average dry densities of the specimens together with target densities (Density 1 and Density 2) are also shown.

10.4 Test results

The measured water content for specimens no. 21, 22 ,23 and 24 with the average dry density about 1,610 kg/m^3 and saturated with water of 1% salinity, are plotted in Figure 10-2a as function of the distance from the water inlet i.e. from the bottom of the specimens. The water content is increasing with time and after 4 weeks the water content had increased in all parts of the specimens (also close to the top of the sample although less than 1%) but they are still far from completely water saturated.

In Figure 10-2b the effect of the initial dry density of the material on the water uptake is shown. For the two samples which have had access to water for 7 days the difference in water content is visual up to a distance of about 25 mm from the water inlet. The figure also indicates that the material has taken up water up to a distance of about 50 mm. For the specimens that had had access to water for 56 days the difference in the final water content is large through the whole samples.

10.5 Conclusions and comments

The following conclusions can be made from the tests:

- The water uptake rate of a material depends on the initial dry density. As expected, the specimens with lower density take up water faster than the samples with higher density.
- The water uptake tests can be used as “bench mark” tests for evaluating different models and model parameters for simulating the water uptake process.

Table 10-1. Full test matrix for the water uptake tests on IBECO-RWC-BF. The test numbers in shaded boxes were performed. The target densities were: Density 1 = 1,460 kg/m^3 and Density 2 = 1,650 kg/m^3 (dry densities).

	Duration 7 days	14 days	43 days	56 days
Density 1, 1% salt	IBECO 11: ρ_d = 1,425 kg/m^3	IBECO 12:	IBECO 13:	IBECO 14: ρ_d = 1,417 kg/m^3
Density 2, 1% salt	IBECO 21: ρ_d = 1,607 kg/m^3	IBECO 22: ρ_d = 1,611 kg/m^3	IBECO 23: ρ_d = 1,610 kg/m^3	IBECO 24: ρ_d = 1,612 kg/m^3

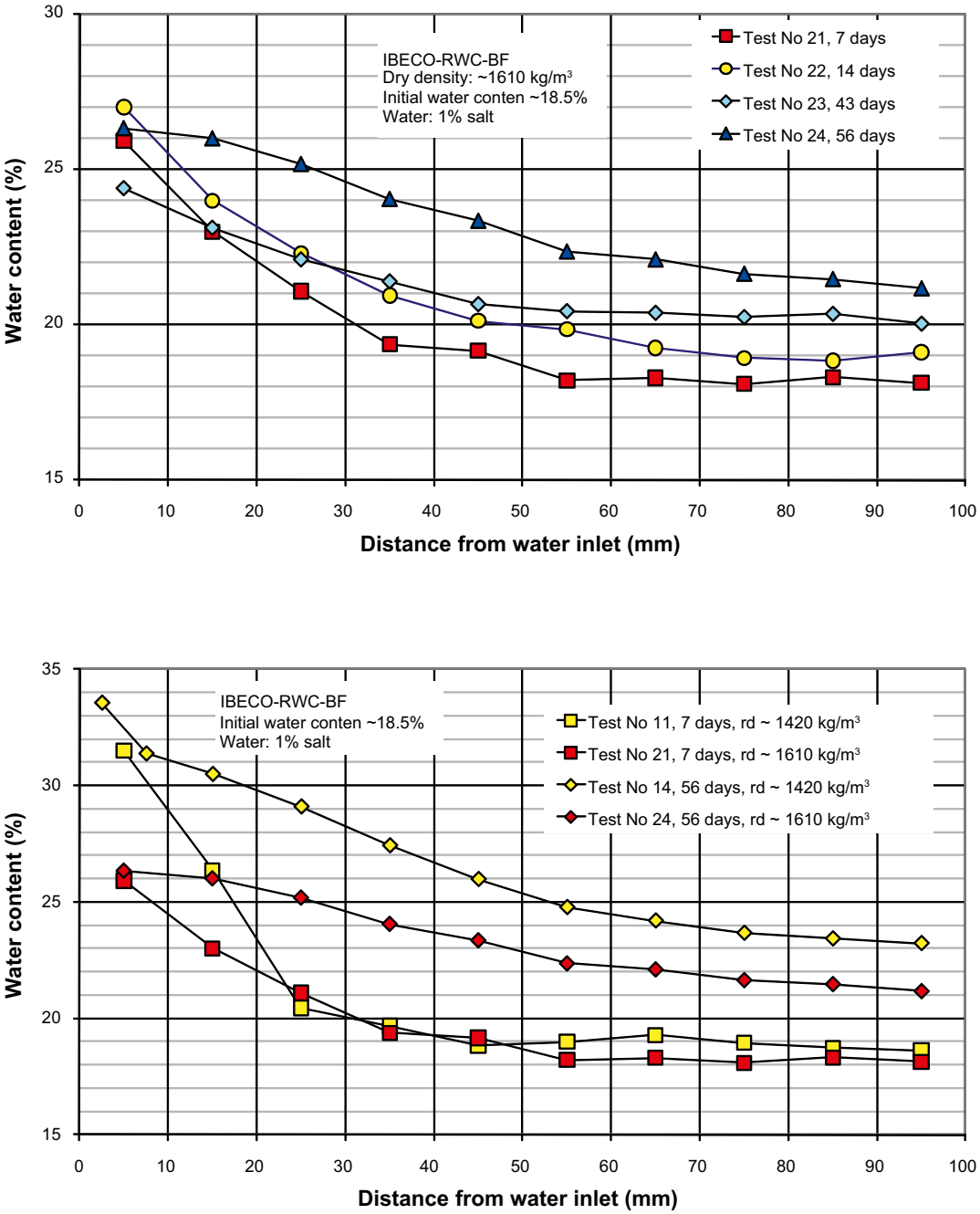

Figure 10-2. *Water content as function of the distance from water inlet for the tests made with IBECO-RWC-BF material: a) Upper diagram shows the influence of time and b) Lower diagram shows the influence of the specimen density.*

11 Relative humidity induced swelling

11.1 General

The backfill blocks can absorb water from the atmosphere after emplacement (depending on local humidity conditions). This may cause swelling and cracking of the blocks. The swelling and cracking of the blocks may affect the ability to stack blocks in a stable manner and thereby influence the ability to fill the tunnel with the required number of blocks. This issue is also investigated in the KBS-3H project regarding the buffer material and the same test equipment was used for the backfill specimens in a number of tests /Sandén et al. 2008/. See also /Johannesson et al. 2008/.

11.2 Experimental set-up

11.2.1 General

Specimens of IBECO RWC-BF were compacted with different compaction pressures but with the same initial water content. The water content, w, is defined as mass of water per mass of dry substance. The dry mass is obtained from drying the wet specimen at 105˚C for 24h.

After compaction the specimens were exposed to a high relative humidity from a free water surface. The water uptake and swelling (volume expansion) were measured continuously. Three identical specimens were made for each compaction pressure;

- one specimen was used to determine the water absorption rate (no suffix),
- one specimen was used for studying the swelling/volume expansion (suffix -V),
- one reference specimen was used for measurement of the initial density and water content (suffix -E).

The specimens were compacted in a mould with diameter 50 mm to a height of about 40 mm. Each specimen was subsequently sawn to the desired height 30 mm. At the end of testing each specimen was divided into three disks: closest to the water surface, middle and top (furthest from water). One half of each disk was used to determine the water content and the other half to determine the density. The density was calculated from a volume determined by weighing the specimens above and submerged into paraffin oil.

11.2.2 Test equipment

Water absorption test. The prepared specimens were suspended in a special vessel (jar made of acrylic plastic with a tight lid), which is shown in Figure 11-1. The bottom of the vessel was filled with de-ionized water. The specimen was covered with a rubber membrane to expose only the horizontal surface to the air above the water surface. Two O-rings were used to prevent the specimen from slipping. The specimen was attached to a vertical rod, which passed through the lid. This design made it possible to weigh the specimen without taking it out of the jar. In order to seal off the hole when no weighing was made a sealing washer was mounted. The distance between the exposed bentonite surface and the water surface was held constant during the test period. The tests were performed at room temperature. The specimens were weighed at selected intervals and after each weighing the amount of absorbed water could be calculated and hence the water absorption rate determined.

Swelling test. The specimens used in this test were placed in a cage on a fine net over a free water surface (Figure 11-2) in the same type of vessel made of acrylic plastic as described above. The specimens were weighed and taken out and measured with a slide calliper at preselected intervals. In this test the specimens had access to humid air at all surfaces in contrast to the water absorption test where access to humid air was only allowed at the lower horizontal surface.

The height and diameter of each specimen were measured at two locations. The heights were measured from the bottom of the specimen holder to the top of the specimen on the opposite sides of the specimen. The diameters were measured a few millimeters from the bottom of the specimen and a few millimeters from the top. The results are displayed as the average of each measurement pair.

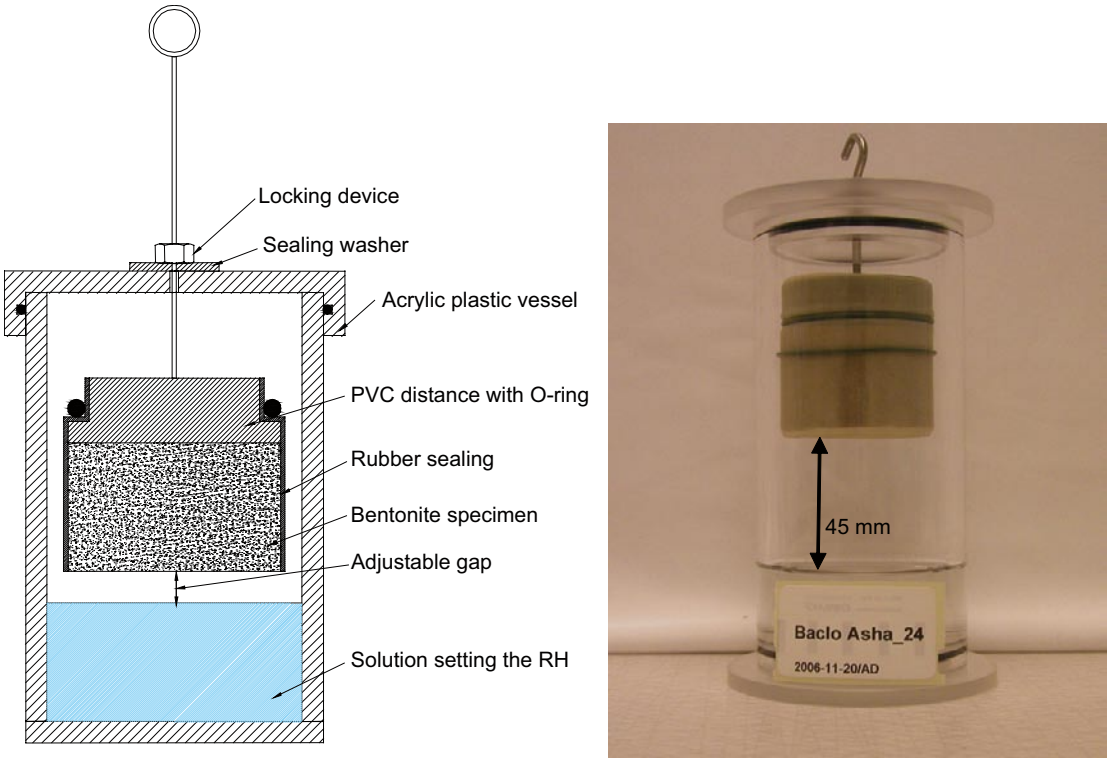

Figure 11-1. *Schematic view showing the test equipment to the left and a photo of the equipment used for measuring water absorption rate to the right.*

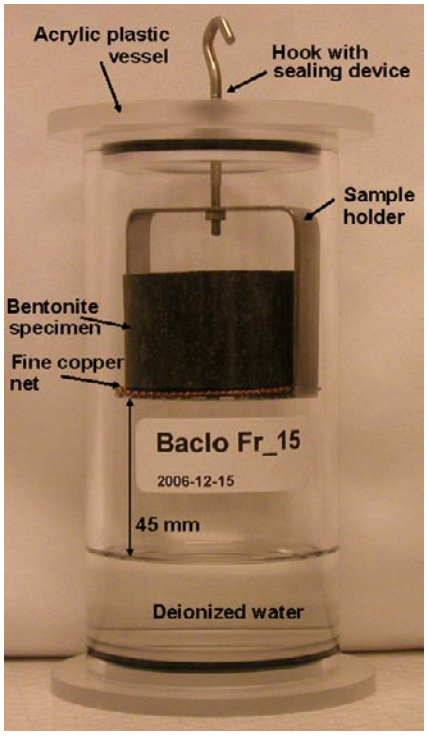

Figure 11-2. *Photo of the equipment used for measuring swelling.*

11.2.3 Test matrix

Three different series with IBECO RWC-BF material were preformed where the specimens were compacted with a uniaxial compaction pressure of 25, 50 and 75 MPa, respectively. From the relation between compaction pressure and dry density in Figure 4-2 the initial bulk densities in Table 11-1 were calculated. The initial water content for all specimens was 18.4%.

11.3 Results

11.3.1 General

The tests were run for about 100 days and the samples were not assumed to have reached steady state or equilibrium.

11.3.2 Water absorption test

Figure 11-3 shows the cumulative mass of water absorbed in the specimens that were only weighed. In the diagrams the initial weight at time zero corresponds to the specimens' weight directly after compaction and before they were placed in the vessels and water was added. The total increases in mass were also calculated from the initial and final mass of the specimens. Good agreement was seen and the difference was less than 0.3 g for the three specimens shown in Figure 11-3.

The initial and final water contents of the specimens shown in Figure 11-3 are shown in Figure 11-4. The initial values were determined on the extra specimens.

Table 11-1. Test matrix for the RH induced swelling. Initial bulk densities.

Material	Compaction pressure		
water content (%)	25 MPa density (kg/m³)	50 MPa density (kg/m³)	75 MPa density (kg/m³)
IBECO RWC-BF 18.4	1,870	1,970	2,010

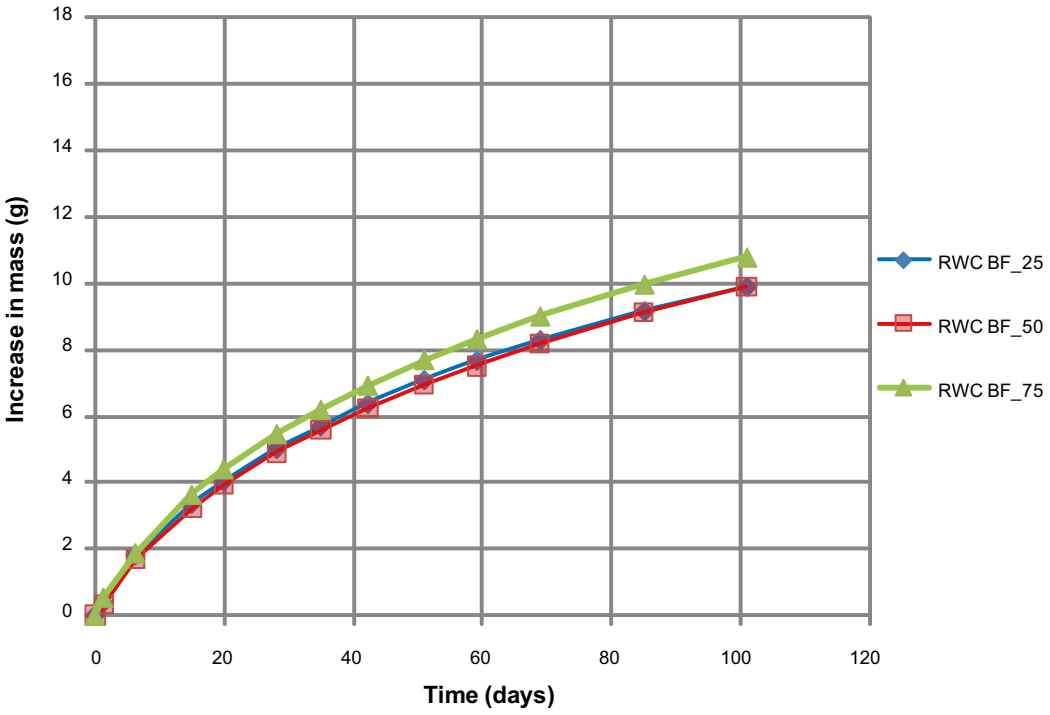

Figure 11-3. Water absorption rate.

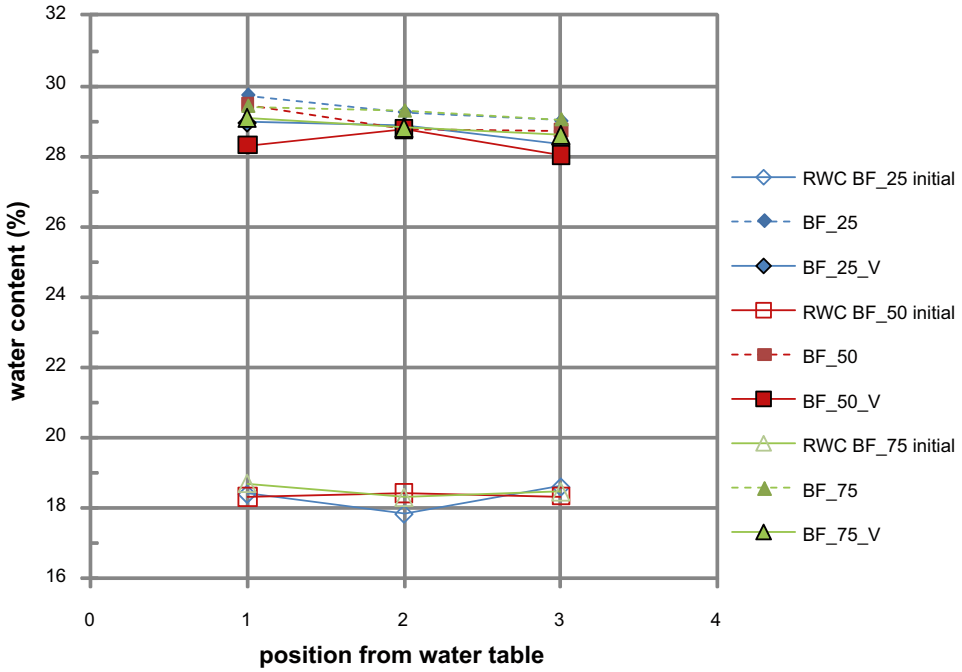

Figure 11-4. *Initial and final water contents. The values are plotted versus position from the water table where the numbers 1, 2 and 3 mean near the water table, in the middle and on top, respectively.*

11.3.3 Swelling test

Figures 11-5 and 11-6 show the changes in height and diameter of the specimens in the swelling test. The height and diameter at time zero correspond to measurements of the specimens before water was added to the vessel.

The final height and diameter were measured and could also be calculated from the initial values and added to the changes shown in Figure 11-5 and 11-6. The differences between the calculated and measured values were less than 0.6 mm and 0.1 mm for the height and diameter, respectively.

Figure 11-7 shows the densities before and at the end of the tests determined by the method with paraffin oil. The initial values were determined on the extra specimens. The specimens compacted to 25 MPa were very crumbly and tended to break after the tests so the density could not be measured.

In Figure 11-7 the average densities determined from measured height and diameter are shown on the y-axis, i.e. at the position from water table equal to zero. Both the initial values, open symbols, and the final values, solid symbols, are shown. No large difference in swelling can be seen between the different series having different compaction pressures.

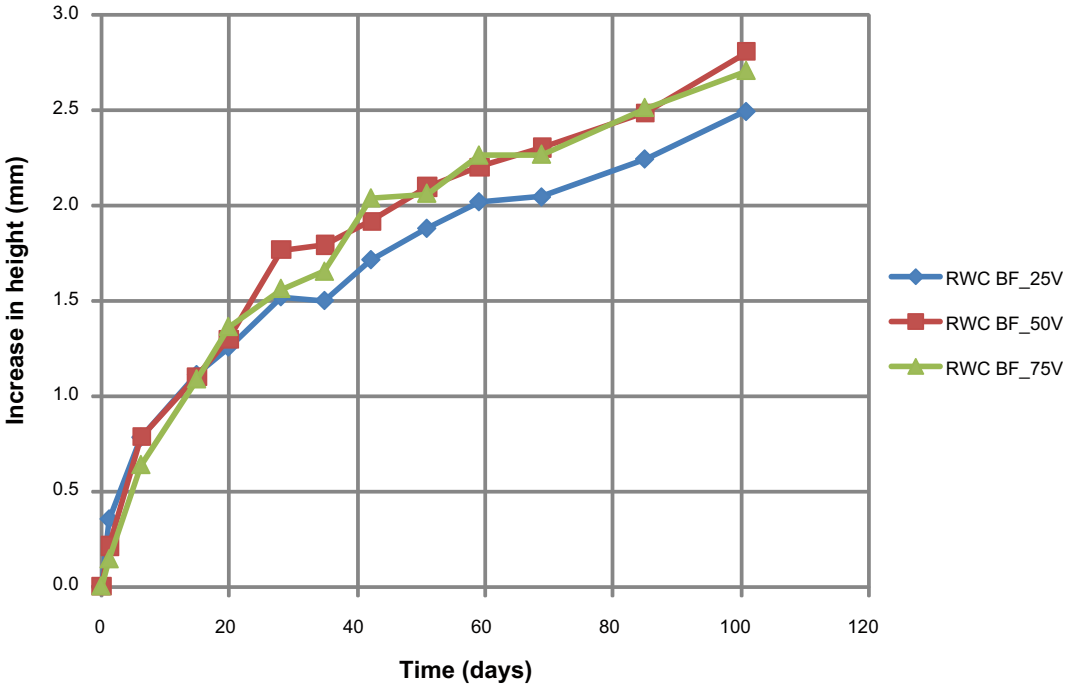

Figure 11-5. *Change in specimen height as result of water absorption. (The diagram shows the average of the measurements taken at each time.)*

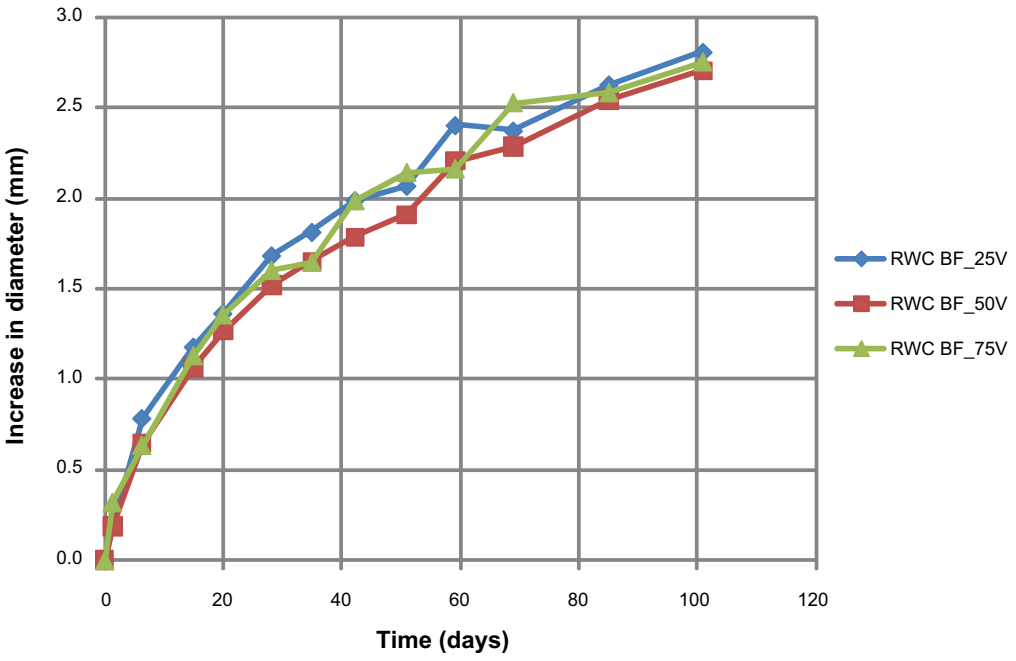

Figure 11-6. *Change in specimen diameter as result of water absorption. (The diagram shows the average of the measurements taken at each time.)*

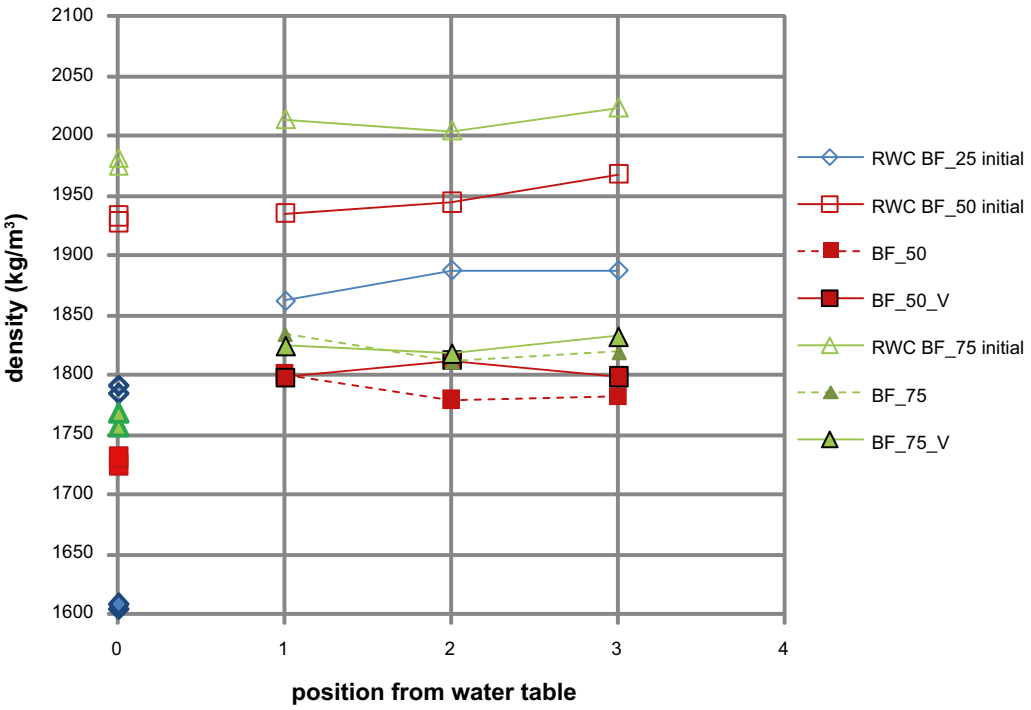

Figure 11-7. *Initial densities compared with the corresponding densities at the end of the tests. The label initial refer to determinations made on extra specimens. On the y-axis initial (open symbols) and final (solid symbols) values calculated from measured heights and diameter, are shown.*

11.4 Conclusions

In general the test results will be used for checking and calibrating material models and parameters but the following specific observations could be made:

Absorption test

- The absorption rate was about the same for the specimens studied irrespective of initial density.
- After 100 days the water content gradient in the specimens was less than 1% along all the initially 3 cm high specimens.

Swelling test

- No large difference in swelling was seen between the specimens studied.
- The specimens compacted to 25 MPa were very crumbly and tended to break after the test so the densities could not be determined.
- After 100 days the density difference in the specimens was less than 20 kg/m^3 along all the initially 3 cm high specimens.

12 Determination of retention curve

12.1 General

The water retention curve is a relation between the water content and the energy state or potential of the soil water expressed as relative humidity or suction. The retention curve is here presented as water content vs. relative humidity. The so called specific retention curve is determined under free swelling condition and starting with an initial water content deviating from 0%.

The method used is an experimentally simple method, jar method, described below; see also /Wadsö et al. 2004/.

12.2 Terminology

The water content, *w*, used is defined as mass of water per mass of dry substance. The dry mass is obtained from drying the wet specimen at 105˚C for 24h. The relative humidity is the ratio between the partial vapor pressure p and the vapor pressure at saturation p_s in %, $RH = 100 \cdot \frac{p}{p_s}$

12.3 Experimental set up

12.3.1 General

The specific retention curve was determined for IBECO RWC-BF. The initial water content was 18.4%. The specimens were placed in jars with tight lids at different controlled *RH* for about 9 months when a steady state equilibrium was reached. The jars were placed in an oven with a constant temperature of 25°C. During the course of the experiment, the specimens were weighed at regular intervals and the development of increase in mass was monitored.

The specimens were determined to have reached an equilibrium state when two specified conditions were fulfilled:

- the parameter $|\Omega|$ (Eq.12-1) was less than $5 \cdot 10^{-9}$ s^{-1}.
- the rate of change of water content per 100 h was less than 0.02%.

$$\Omega = \frac{dm}{dt} \times \frac{(RH_f - RH_i)/100}{m(t) - m_i} \qquad 12\text{-}1$$

Here, m is the mass (g) and t is the time (s). The parameter Ω and the limit value of this parameter were suggested by /Wadsö et al. 2004/. The subscripts *f* and *i* refer to the initial and final states, respectively.

At the end of the experiment, the final water content was measured on each of the specimens.

12.3.2 Test equipment

About 10 g of RWC-BF (granules) was used for each test. The specimens were placed in metal cages and hung inside glass jars with a tight lid. A rod passing through the lid made it possible to weigh the specimens below the balance without having to remove them from the jars. A plastic sealing washer was placed around the rod such that the generated *RH* was maintained during the course of the experiment. The design is presented in Figure 12-1. The same equipment was used and described by /Johannesson et al. 2008/.

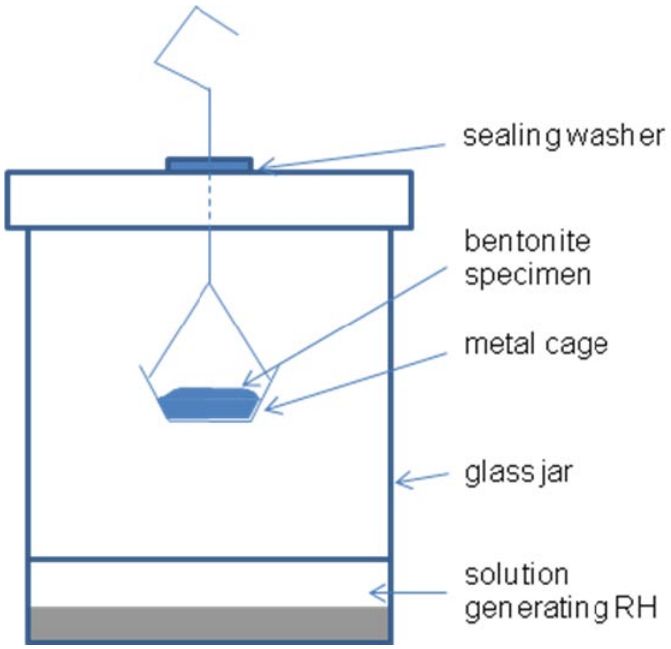

Figure 12-1. *Schematic view showing the test equipment.*

Each jar contained a salt solution, which generated a constant relative humidity. The measurements were carried out at eight different *RH* values (0%, 11%, 33%, 58%, 76%, 84%, 93%, 97%). These *RH* values were achieved using various saturated salt solutions (LiCl, $MgCl_2$, NaBr, NaCl, KCl, K_2SO_4) except in the cases of *RH* = 0% and 93% were molecular sieve and an unsaturated NaCl solution, respectively, were used. The *RH* values for the saturated salt solutions were taken from /Greenspan 1977/ and the vapour pressure above the 2 molal NaCl solution was taken from /Clarke and Glew 1985/. The jars were placed in an oven at a constant temperature of 25°C. The unsaturated solution was replaced with a new mixture on a weekly basis such that a constant humidity would be maintained in the jar.

12.3.3 Test matrix

The test matrix is presented in Table 12-1. One specimen was made for each *RH*, with the exception of the jar with saturated NaCl solution, where an extra specimen was added for comparison.

Table 12-1. Test matrix and labels.

Chemical	RH at 25°C (%)	RWC-BF
Molecular sieve	0	1
LiCl (saturated)	11.3	2
$MgCl_2$ (saturated)	32.8	3
NaBr (saturated)	57.6	4
NaCl (saturated)	75.3	5 and 5II
KCl (saturated)	84.4	6
NaCl (2 molal)	93.1	7
K_2SO_4 (saturated)	97.3	8

12.4 Results

The retention curve for the RWC-BF obtained at 25°C is presented in tabular form in Table 12-2. The result is also shown in Figure 12-2. In this figure results for the materials Asha and Friedland /Johannesson et al. 2008/ are also shown together with results for MX-80 /Dueck and Nilsson 2008/. These results are shown for comparison reason. The initial water contents of the Asha, Friedland and MX-80 were 1.5%, 7.8% and 9.8%, respectively, i.e. this is much lower than for RWC-BF, which partly explains the difference at $RH < 70\%$. The methodology used for these three materials was the same as the one used for RWC-BF but the temperature deviated for MX-80, which was 20°C.

Table 12-2. Retention curve for the RWC-BF material obtained at 25°C.

RH at 25°C (%)	Water content RWC-BF (%)
0	0.6
11.3	4.0
32.8	9.3
57.6	16.1
75.3	19.1*
75.3	19.5*
84.4	20.8
93.1	25.0
97.3	28.4

*doublet samples

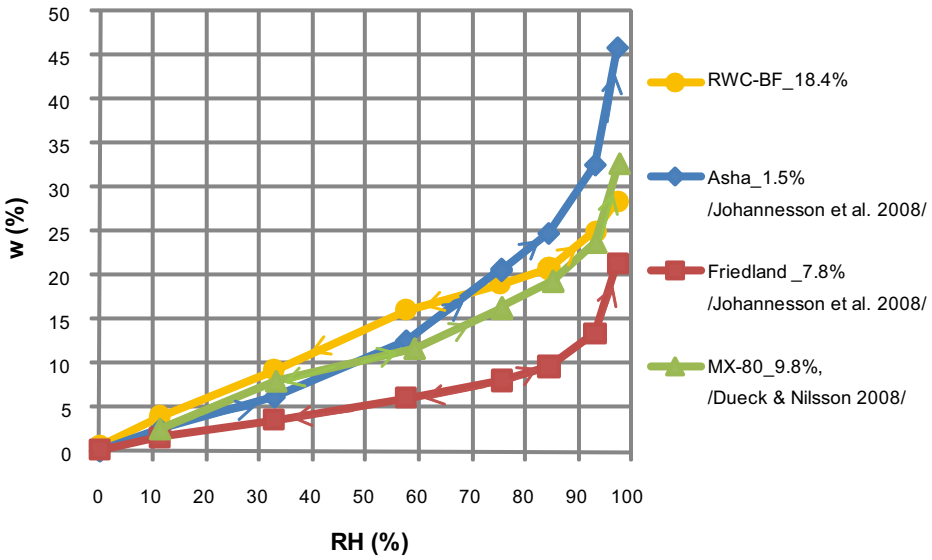

Figure 12-2. *Specific retention curve for the RWC-BF material obtained at 25°C shown together with previous results for Asha and Friedland at 25˚C and MX-80 at 20°C. The labels show material and initial water content (%). The arrows show the moisture paths.*

12.5 Time criteria

The very long testing time led to that the two conditions given in section 13.2.1 were fulfilled. The parameters Ω and dw/dt are given in Table 12-3 for the last measurements. For one salt $MgCl_2$ the condition was fulfilled during the last months except just the last one shown below.

12.6 Discussion

The specific retention curve for RWC-BF with the initial water content of 18.4% has been determined with the jar method and will be used for modeling purpose. The results show that at absorption the four materials RWC-BF, Asha, Friedland and MX-80 will reach different water contents at equilibrium with a specific relative humidity.

Each series had one doublet specimen and the deviation in the results for this specimen was less than 0.4% units, cf. Table 12-2. Uncertainties of the method with jars were discussed by /Wadsö et al. 2004/.

Table 12-3. Equilibrium-determining parameters for the RWC-BF material.

	RWC-BF		
Specimen	RH at 25°C (%)	Ω (s^{-1})	100·(dw/dt) (%/100 h)
1	0	0	0
2	11.3	0	0
3	32.8	–3.1E–09	–2.5E–02
4	57.6	–2.0E–09	–1.2E–02
5	75.3	–1.7E–09	1.3E–02
5II	75.3	0	0
6	84.4	0	0
7	93.1	–1.1E–10	–1.3E–02
8	97.3	8.0E–10	1.3E–02

13 Summary and conclusions

13.1 General

The tests described in this report were made in order to investigate several important properties of a material, considered for use for backfilling of tunnels in the KBS-3V concept. The investigations will be used to evaluate if the material is suitable and to determine parameters needed for modeling.

This chapter summarizes the main conclusions from these tests.

13.2 Standard laboratory tests

The material was delivered both as granules and as pellets. The granulated material was delivered with a water content of 18.5% and the pellets material with a water content of 14.8%. The raw material should according to specifications from the supplier be the same for the granules and for the pellets, but the results of the measurements of the liquid limit and the swelling capacity were quite different for the two materials. The granules had a liquid limit of 122% compared to 208% for the pellets. The swelling capacity was determined to 4.4 ml for the granules and 9.1 ml for the pellets. These results indicate that the amount of swelling minerals is considerably higher in the pellets material.

13.3 Block compaction

The block compaction properties were investigated in two steps. Before the large amount of material (60 tons) was ordered a minor amount was delivered from the supplier and with this material, a number of compaction tests were done in the laboratory. The pretests indicated that the maximum dry density at a compaction pressure of 25 MPa was reached at a water content of about 19%. The material was therefore ordered with this water content. Tests with the new material showed, however, a completely different behavior. There was no clear maximum density at the water content interval (12–22%) tested. The achieved density was also lower than expected.

In spite of the unexpected differences, it is still considered that blocks of a suitable density and quality can be manufactured with this material. The density demands of the blocks are very much depending on the final design of the tunnel filling, i.e. mainly the relation between blocks and pellets filling.

The manufacturing of 60 tons of blocks that should be used in large scale laboratory tests at Äspö HRL was successful. The block quality was good i.e. the amount of cracks was very small and the variation of density within the blocks, but also between the blocks, was very small.

13.4 Mechanical parameters

In order to describe the behavior of the backfill material both during and after installation in the tunnel, a number of laboratory tests were made. The following conclusions can be drawn from these tests:

1. The oedometer modulus evaluated from four made oedometer tests varied between 34 and 50 MPa.
2. Altogether three tests were made for determining Young´s modulus (E) and Poisson´s ratio (υ). The specimens tested had a dry density of about 1,710 kg/m^3 and the evaluated parameters were E= 231–263 MPa and υ= 0.16–0.19 respectively.
3. The strength of the material, both the compressive strength and the tensile strength were measured on samples compacted to different dry densities. The test results yielded a relation between density and the two types of strength.
4. Two tests were made for evaluating the compressibility of loosely filled pellets. The tests show that from an initial dry density of ~850 kg/m^3 the filling was compressed to ~1,350 kg/m^3 at a compaction pressure of about 5,000 kPa.

13.5 Swelling pressure and hydraulic conductivity

The measured swelling pressures and hydraulic conductivities show as expected a strong influence of the dry density. The following conclusions can be drawn:

- **Granule size distribution**. There is no clear influence of the granule size. The delivered material was rather coarse and in order to investigate the influence of the granule size a number of tests were also performed with grinded material which showed insignificant differences.
- **Salt content of the water**. The investigation was performed using water with a salt content of 1% and 3.5%. At the rather high dry densities, 1,300–1,600 kg/m^3, there was no influence of the salt content regarding the determined swelling pressure or hydraulic conductivity. Only one measurement has been done at a low density, 1,150 kg/m3. More tests are needed in order to study the influence of the salt content.

13.6 Erosion

Erosion tests have been performed both with compacted blocks but also with the pellets material. From the tests performed the following conclusions can be drawn:

- **Time dependence**. The results from the tests are well inside the limits of the suggested erosion model with the block properties at the upper limit and the pellets properties in the middle. However, the decrease in erosion rate in the pellets seems to be faster than in pellets made of MX-80.
- **Water flow rate**. The erosion rate determined as the amount of eroded material per liter water is not influenced by the water flow rate. There is, however, the following problem with erosion measurements on bentonite blocks or in a bentonite pellets filling when the water flow rate is low:
  1. Blocks: If the water flow rate is low, e.g. 0.01 l/min, all water is sucked up by the blocks, which starts to swell. After 24 hours test duration, no water had left the test setup and depending on the swelling it was not possible to continue the tests. This phenomenon has been observed also with other bentonite materials /Sandén et al. 2008/.
  2. Pellets: If the water flow rate is low (e.g. 0.01 l/min), a resistance to the water flow were built up in some tests and sealed the bentonite which led to separation and that the water pressure started to act on a "wall" of bentonite. If the resistant pressure got too high it was difficult to finalize the measurements. The phenomena depends mainly on the geometry of the confinement but also on many factors such as water flow rate, salt content in water and granule size distribution.
- **Salt content in water**. There is an influence of the salt content in the water on the erosion rate. The effect is obvious in the beginning of the tests but decreases by time.

13.7 Self healing ability

The self healing ability has been tested for both blocks and pellets. Two block densities were used:

1. A density corresponding to the calculated average density of a cross section.
2. A density corresponding to a lower density close to the rock wall.

In addition also the properties of a pellet filling were tested. The tests were performed using water with 1% and 3.5% salinity.

The self healing ability was tested by drilling holes in saturated specimens and then letting them have access to water again for three weeks. The hydraulic conductivity was measured before drilling of the central hole and then again after three weeks of healing. The method used for determining the self healing ability of the materials is not a standard method as no standards for determining such behavior exists. The results are however consistent and the ability of the material to self-heal can be summarized as follows:

- The increase in hydraulic conductivity determined after the healing time depends on an incomplete homogenization. The decrease in density depending on the drilling of the hole is 1% for the high density specimens and 0.2% for the pellets tests. This decrease in density is too small in order to influence the hydraulic conductivity more than marginally.
- **Compacted blocks**. The specimens had largely healed but there were still visual traces of the drilled hole that could be seen after finishing the tests. For the two specimens with the lower density, an increase in hydraulic conductivity was measured after the healing time when comparing to the hydraulic conductivity measured before drilling.
- **Pellets**. The drilled holes were visibly filled with gel. There was a strong increase of hydraulic conductivity after the healing time. The influence of salt content in the water was small.

13.8 Homogenization tests

Three tests investigating how the homogenization of high density backfill blocks and pellets will proceed have been performed. Compacted specimens with a diameter of 50 mm and a height of 40 mm were placed in an oedometer, At the top of each specimen, pellets (somewhat crushed) were placed to a thickness of 4.8 and 12 mm respectively. The specimens had access to water only from the pellets side i.e. the simulated rock wall.

When different materials are used together e.g. for backfilling of a deposition tunnel the different retention and mechanical properties imply that at otherwise similar conditions regarding load and suction different water contents and densities will be reached at equilibrium. During the saturation the low density part will be compressed by the swelling pressure from the high density part.

Similar tests have been performed earlier using the same test equipment and with the same test layout but with different materials /Johannesson et.al 2008/. In this earlier test series, that included a large number of tests, the following was concluded:

- *Influence of time*. Tests were performed with test durations of two weeks, two months and four months. It was concluded that the main part regarding homogenization in this scale takes part during the first two weeks.
- *Influence of wall friction*. The influence of wall friction regarding the homogenization was tested by performing tests with lubricated walls and the compare the result with the standard tests. It was in these tests not possible to detect any differences in the rate of homogenization.
- *Access to water*. The influence of access to water was also investigated by letting one sample have access to water from both the pellets side, the rock, and also from the block side. The tests showed that there was a small difference in water content at the outermost part.
- *Influence of salt content in the water*. Tests were performed using water with different salinities (1% and 3.5%). The results showed that the influence of salt regarding the homogenization was small.
- *Influence of different slot widths.* The influence of the slot width regarding the homogenization rate was as expected rather large. In the performed test series, tests with different slot widths (4, 8 and 12 mm width) were performed. The results showed that in the test with the 4 mm slot the time to completed homogenization had been considerable shorter.

With the experience from the old tests it was possible to focus on the important parameter i.e. the slot width. The new tests with the IBECO-RWC-BF material show that the homogenization of the specimens after two months testing had gone far even if there is a very clear difference between the specimens depending on the initial slot width. The tests with the IBECO-RWC-BF material have shown that the homogenization of the specimens after two months testing had gone far even if there is a clear difference between the specimens depending on the initial slot width. The initial large gradient in density between the compacted specimen and the pellets filled slot has evened out and the remaining density gradient within the specimens is almost similar for all three tests even if there is a difference in the average density between the specimens. This difference depends on the different initial slot widths.

One example of the homogenization rate is that the differences in dry density at test start (block = 1,600 kg/m^3, pellets = 885 kg /m^3) has evened out to a density gradient from 1,250–1,400 kg/m^3 (12 mm initial width of pellets slot) after two months. The degree of saturation was for all three specimens between 92 and 100% at termination.

13.9 Water uptake tests

This type of test was made in order to study how the backfill material will take up water and which parameters affect this process. From the performed tests the following conclusions have been made:

- The water uptake rate of a material is depending on the initial dry density. As expected, the samples with lower density take up water faster compared to the samples with higher density.
- The water uptake tests can be used as “bench mark” tests for evaluating different models for simulating the water uptake.

13.10 Relative humidity induced swelling

The tests results will be used for checking and calibrating material models and parameters but the following are example of specific observations made:

- The specimens compacted to 25 MPa were very crumbly after the tests.
- After 100 days the density difference in the specimens was less than 20 kg/m^3 along the initially 3 cm high specimens.

13.11 Determination of the retention curve

The specific retention curve for the IBECO_RWC-BF with the initial water content of 18.4% was determined by the jar method and will be used for modeling purpose.

13.12 Further work and recommendations

The reported tests have yielded a lot of information regarding the IBECO-RWC-BF material. One question that has been raised is, however, how the raw material should be controlled and checked both before and after delivery. The properties of the sample sent in advance and which served as a base for the following order of 60 ton bentonite was not the same as for the main delivery.

References

SKB's (Svensk Kärnbränslehantering AB) publications can be found at www.skb.se/publications.

Clarke E C W, Glew D N, 1985. Evaluation of the Thermodynamic Functions for Aqueous Sodium Cloride from Equilibrium and Calorimetric Measurements below 154˚C, J. Phys. Chem. Ref. Data, Vol 14, No 2, pp 536–537.

Dueck A, Nilsson U, 2008. Hydro-mechanical properties of unsaturated MX-80, laboratory study 2005–2007. SKB report in progress.

Greenspan L, 1977. Humidity fixed points of binary saturated aqueous solutions, Journal of research of the national Bureau of Standards A. Physics and Chemistry, Vol 81A, No 1, pp 89–96.

Johannesson L, Nilsson U, 2006. Geotechnical properties of candidate backfill material for deep repository. SKB R-06-73, Svensk Kärnbränslehantering AB.

Johannesson L, 2008. Geotechnical investigations made on unsaturated backfill materials. SKB-R-08-131, Svensk Kärnbränslehantering AB.

Johannesson L, Sandén T, Dueck A, 2008. Deep repository-Engineered barrier system. Wetting and homogenization processes in backfill materials. SKB R-08-136, Svensk Kärnbränslehantering AB.

Pastina B, Hellä P, 2006. Expected evolution of a spent nuclear fuel repository at Olkiluoto. Posiva 2006-05.

Sandén T, Börgesson L, 2008. Deep repository-Engineered barrier system. Laboratory tests to understand processes during early water uptake. SKB R-06-72, Svensk Kärnbränslehantering AB.

Sandén T, Börgesson L, Dueck A, Goudarzi R, Lönnqvist M, 2008. Deep repository-Engineered barrier system. Erosion and sealing processes in tunnel backfill materials investigated in laboratory. Baclo project-phase 3. SKB R-08-135, Svensk Kärnbränslehantering AB.

Wadsö L, Svennberg K, Dueck A, 2004. An experimentally simple method for measuring sorption isotherms. Drying Technology 22(10): 2427-2440.

Appendicies

Appendix 1 Data sheet IBECO RWC BF

Appendix 2 Erosion-block

Appendix 3 Erosion pellets, 0.1 l/min, 1% salt

Appendix 4 Erosion pellets, 0.01 l/min, 1% salt

Appendix 5 Erosion pellets, 0.1 l/min, 3.5% salt

Appendix 6 Erosion pellets, 0.01 l/min, 3.5% salt

Appendix 7 Block compaction in Bjuv

Appendix 8 Data from oedometer tests

Appendix 9 Evaluation of elastic parameters of unsaturated blocks-data

Data sheet from the supplier of the raw material

IBECO RWC-BF

Beschreibung	Description	Description
Natürlicher Calziumbentonit mit mittlerem Montmorillonitgehalt	Calcium bentonite natural with a medium montmorillonite content	Bentonite calcique naturelle à moyen teneur en montmorillonite

Anwendung	Application	Application
Für Verfüllmaßnahmen im Tunnelbau.	For backfilling of tunnel constructions.	Pour des mesures de remplissage dans la construction de tunnels

	Technische Durchschnittswerte	Technical values (average)	Valeur techniques (moyenne)		
w	Wassergehalt ISO 787/2	Water content	Teneur d'eau	16 ± 1,5	%
ρ_s	Dichte DIN 51057	Specific density	Poids spécifique	2,65	g/cm³
	Schüttdichte DIN 53466	Bulk density	Densité apparente tassée	1020 ± 50	g/l
	Körnung	Grain size	Granulation	0 – 5	mm
	Siebrückstand auf Sieb 0,063 mm DIN 53734	Dry screen residue on sieve 0,063 mm	Refus au tamis (voie sèche) 0,063 mm	> 80	%
	Methylenblau-Adsorption VDG P69	Methylen-blue-adsorption	Adsorption du bleu de méthylène	300 ± 30	mg/g
CEC	Kationenaustauschkapazität	Cation exchange capacity	Capacité d'échange de cations	60 ± 10	mval/ 100g
w_A	Wasseraufnahmevermögen Enslin-Neff, DIN 18132	Water absorption capacity	Capacité d'absorption d'eau	150± 30	%
	Quellvolumen	Swelling index	Gonflement	≥ 7	ml/2g
w_L	Fließgrenze DIN 18122	Liquid limit	Limite de liquidité	115	%
wp	Ausrollgrenze DIN 18122	Plastic limit	Limite de plasticité	33	%
I_p	Plastizitätszahl (errechnet)	Plasticity index (calculated)	Indice de plasticité (calculée)	82	%

Lieferform	Delivery	Livraison
• Lose per Silo-Lkw • In Säcken, auf Paletten, geschrumpft • In Big Bags	• Bulk per road tanker • In bags on pallets, shrink wrapped • In big bags	• Vrac en camion-silo • En sacs sur palette filmée • En big bags

Da wir auf die Verwendung unseres Produktes keinen Einfluss nehmen können, beschränkt sich unsere Haftung auf diese Produktinformation.	The values listed are indicative and are not to be construed as rigid specifications.	Les renseignements contenus dans cette fiche technique sont fournis à titre indicatif et ne peuvent engager notre responsabilité.

S&B Industrial Minerals GmbH
- Geschäftsbereich IBECO -
Ruhrorter Straße 72 • D – 68219 Mannheim • Tel.+49 6 21 / 8 04 27-0 • Fax +49 6 21 / 8 04 27-50

AMAN/HSPE 0310

Appendix 2

Erosion-block

Figure A2-1. Left: *0.1 l/min and water with 1% salt.* ***Right:*** *0.1 l/min and water with 3.5% salt.*

Figure A2-2. *Block erosion test with 0.01 l/min and 1% salt in the water. It was not possible to measure erosion depending on the fact that with this rather low water flow the blocks had time to suck up all water, swell and prevent all flowing of water. The result was the same for the test with 0.01 l/min and 3.5% salt in the water.*

Erosion-block

Figure A2-3. *Block erosion test with 0.01 l/min and 1% salt in the water. A picture of a cross section shows that all bentonite was wetted. The result was the same for the test with 0.01 l/min and 3.5% salt in the water.*

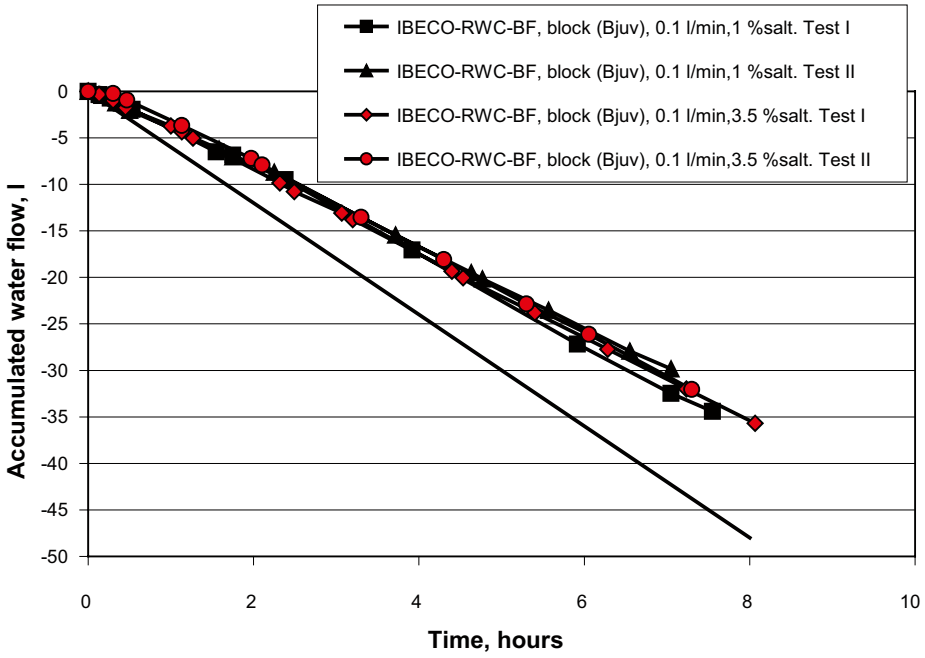

Figure A2-4. *The measured water outflow from the tests performed with 0.1 l/min. The black line shows the applied water flow. In all tests more than 10 liters have been taken up, or been stored, by the bentonite blocks during the test time.*

Appendix 3

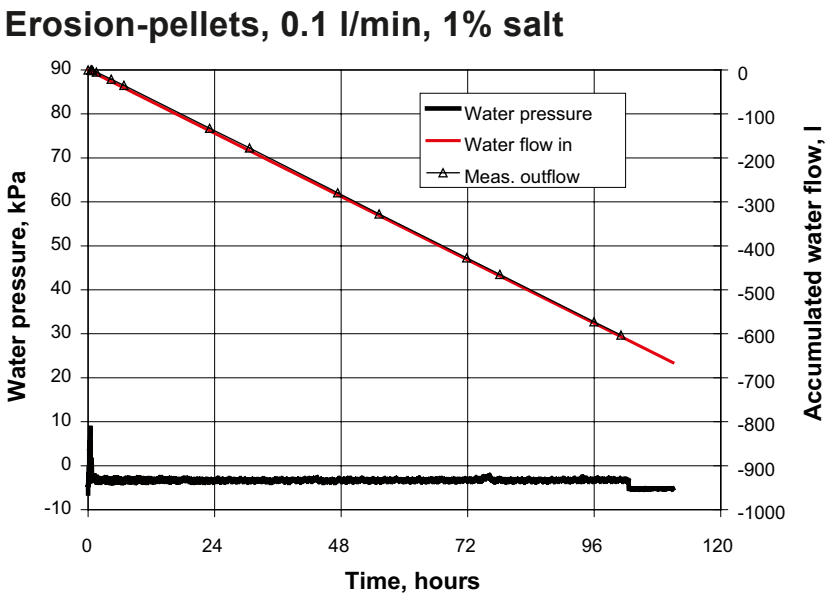

Figure A3-1. *The measured water pressure, the applied water inflow and the measured outflow plotted vs. time.*

Figure A3-2. *After a few hours, all water is flowing in one clear channel.*

Appendix 4

Erosion-pellets, 0.01 l/min, 1% salt

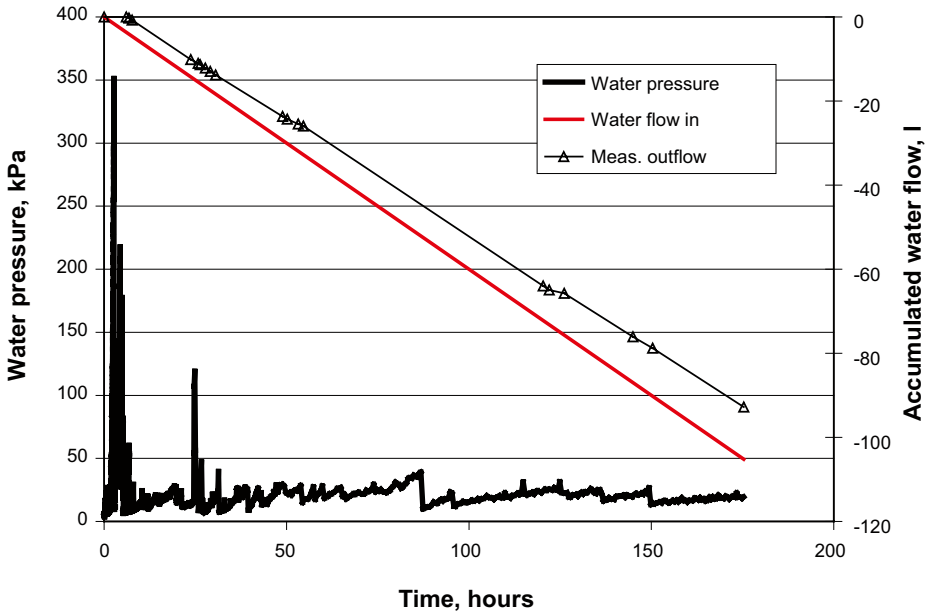

Figure A4-1. *The measured water pressure, the applied water inflow and the measured outflow plotted vs. time.*

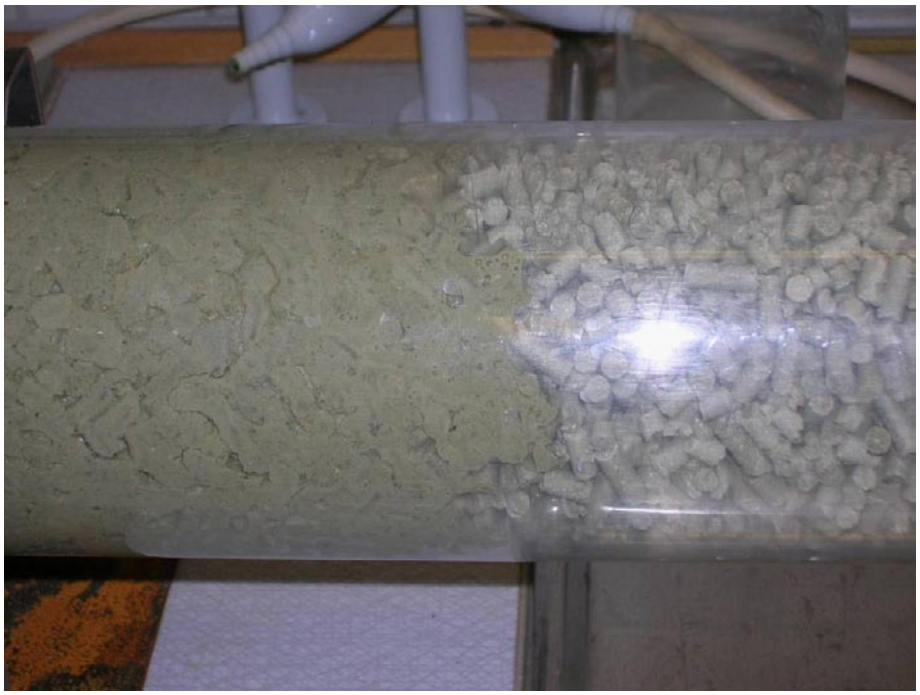

Figure A4-2. *With the lower flow rates is the wetting proceeding as a front.*

Appendix 5

Erosion-pellets, 0.1 l/min, 3.5% salt

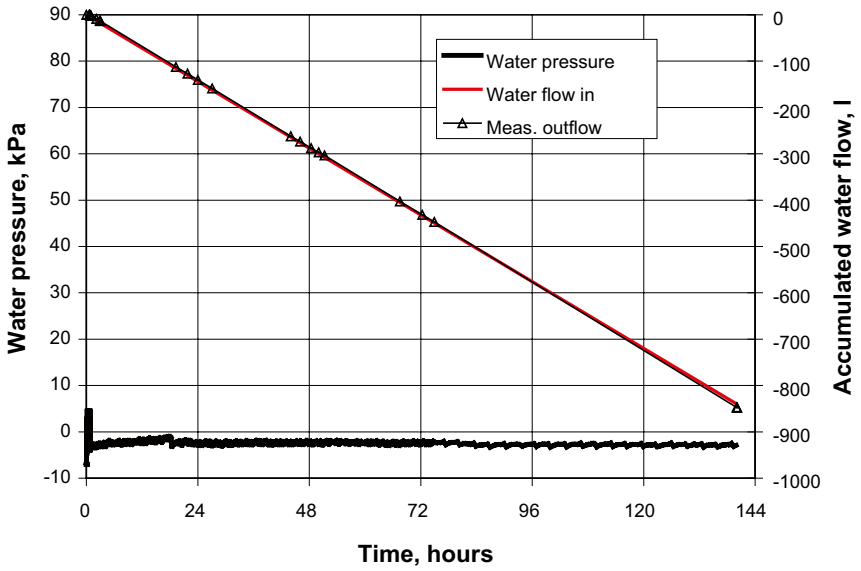

Figure A5-1. *The measured water pressure, the applied water inflow and the measured outflow plotted vs. time.*

Figure A5-2. *The water is flowing in one channel situated at the top of the test tube.*

Appendix 6

Erosion-pellets, 0.01 l/min, 3.5% salt

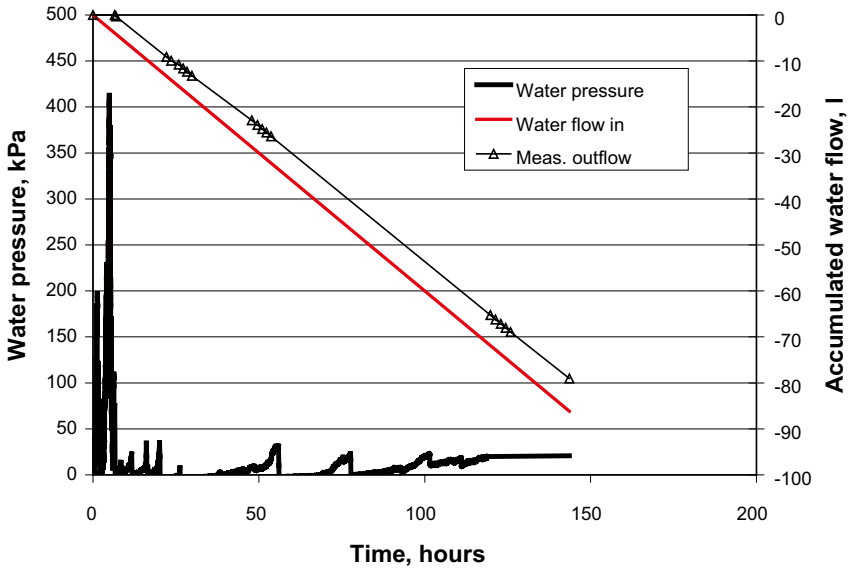

Figure A6-1. *The measured water pressure, the applied water inflow and the measured outflow plotted vs. time.*

Figure A6-2. *With the lower flow rates, the water is not flowing in a clear channel.*

Appendix 7

Evaluation of bentonite blocks compacted from material IBECO RWC BF in Bjuv during February 2009

Lars Ohlsson

2009 07 17, Lund, Sweden

Supervised by Torbjörn Sandén, Clay Technology AB

This report summarise the examination of a 20 block sample of bentonite, more precise IBECO RWC BF, blocks compacted in Bjuv during February 2009.

By sawing out pieces at the corner and side of the blocks, density and water content at four different positions were determined, allowing evaluation of the dry density variations to conclude if the blocks are homogeneous or not.

A7.1 THEORY

To evaluate a large series from only a small sample, it is necessary to use statistical arguments when one wants to impose the characteristics of the sample on the series as a whole. The mathematical arguments for all of the distribution theory above can be found in /Blom et al. 2005/. Also used during the statistical evaluation of the data was /NIST/SEMATECH 2003/, particularly chapter 1.3.5. Quantitative Techniques.

A7.1.1 Gaussian distributed stochastic variables

The *Gaussian distribution* class $N(\mu,\sigma)$, also known as the *normal distribution*, is centred on the *expectation value* μ, commonly referred to as the mean, and its spreading is characterised with the *standard deviation* σ.

If the stochastic variable of interest Y is a linear combination of N independent and normal distributed stochastic variables $X_1 \ldots X_N$, i.e.

$$Y = a_1X_1 + a_2X_2 + ...a_NX_N + b \quad \text{(A7-1)}$$

the expectation value will also be a linear combination of the expectation values $\mu_{X,i}$

$$\mu_Y = \sum_{i=1}^{N} a_i \mu_{X,i} + b \quad \text{(A7-2)}$$

while the standard deviation is constructed from the sum of squared standard deviations $\sigma_{X,i}$

$$\sigma_Y = \sqrt{\sum_{i=1}^{N} a_i^2 \sigma_{X,i}^2} \quad \text{(A7-3)}$$

As a consequence, the arithmetic mean of the independent and normal distributed stochastic variables $X_1 \ldots X_N$ having *equal standard deviations* σ_X,

$$\overline{X} = \frac{1}{N}\sum_{i=1}^{N} X_i \quad \text{(A7-4)}$$

will also be normal distributed with expectation value

$$\mu_{\overline{X}} = \frac{1}{N}\sum_{i=1}^{N} \mu_{X,i} \quad \text{(A7-5)}$$

and the standard deviation of the mean simplifies to

$$\sigma_{\overline{X}} = \sqrt{\sum_{i=1}^{N} \frac{1}{N^2}\sigma_{X,i}^2} = \frac{1}{\sqrt{N}}\sigma_X \quad \text{(A7-6)}$$

Note that the averaging of data reduces the standard deviation. This would be applicable for the distribution of the mean value of N sized samples of a larger distribution.

At last, subtracting the expectation value from a Gaussian distributed stochastic variable X and dividing it by its standard deviation produces a new stochastic variable of the *standard normal distribution* class $N(0.1)$, i.e.

$$\frac{X-\mu}{\sigma} \in N(0.1) \quad \text{(A7-7)}$$

The α-quantiles of the standard normal distribution is well known, describing the α probability limit of finding the stochastic variable at a deviating value in a sample, making it ideal for hypothesis testing in normal distributions with well known characteristics.

A7.1.2 Estimated distribution characteristics

Assume that a variable X is normally distributed, e.g. the dry density of M bentonite blocks compacted with a single target density. If the characteristics of X are not well known, one may want to estimate the expectation value from a random sample $x_1 \ldots x_N$. This is done by simply taking the arithmetic mean of the sample,

$$\hat{\mu} = \frac{1}{N}\sum_{i=1}^{N} x_i \tag{A7-8}$$

where $N < M$ is the sample size and ^ denotes an estimated entity, i.e. not necessarily the true value of μ. Similar, the standard deviation of the sample may be estimated from

$$\hat{\sigma} = \sqrt{\frac{1}{N-1}\sum_{i=1}^{N}(x_i - \hat{\mu})^2} \tag{A7-9}$$

where one should observe that the denominator N-1 is used instead of the full sample size.

A7.1.3 The t-distribution

Trying to form the standard normal distribution in (A7-7) for a sample mean with estimated distribution characteristics will instead produce a stochastic variable in the very similar *t-distribution* class,

$$\frac{X - \hat{\mu}_{\bar{X}}}{\hat{\sigma}_{\bar{X}}} \in t(\nu) \tag{A7-10}$$

where the argument ν of the t-distribution is its degrees of freedom. For a one sample test, the degrees of freedom is the sample size reduced by one,

$$\nu = N - 1 \tag{A7-11}$$

A more general definition must be used if a linear combination of M stochastic variables is under study,

$$\nu = \left[\sum_{i=1}^{M}\frac{\hat{\sigma}_i^2}{N_i}\right]^2 \Bigg/ \sum_{i=1}^{M}\left[\left(\frac{\hat{\sigma}_i^2}{N_i}\right)^2 \Big/ (N_i - 1)\right] \tag{A7-12}$$

which simplifies into (11) for $M = 1$.

A7.1.4 T-tests

To evaluate the probability that a sample $x_1 \ldots x_N$ originates from a distribution clustered around a specific value, a *t-test* may be used. The t-test utilises a *confidence interval* within which it is 1-α probability to find the mean of a sample from a normal distribution. The parameter α is called the *significance level*, which is easiest to think of as the level of risk to draw the wrong conclusion.

To start with, a *zero hypotesis* H_0 for the expectation value should be assumed, e.g. that the expectation value of the tested distribution is equal to 0,

$$\mu_0 = 0 \tag{A7-13}$$

Then, the expectation value and standard deviation of the sample is estimated using (A7-7) and (A7-8). The corresponding expectation value and standard deviation of the mean distribution may now be calculated using (A7-5) and (A7-6), yielding

$$\hat{\mu}_{\bar{X}} = \frac{1}{N}\sum_{j=1}^{N}\hat{\mu} = \hat{\mu} \tag{A7-14}$$

and

$$\hat{\sigma}_{\bar{X}} = \frac{1}{\sqrt{N}}\hat{\sigma} \tag{A7-15}$$

respectively, resulting in the t-distributed test variable

$$T = \frac{\hat{\mu}_{\bar{X}} - \mu_0}{\hat{\sigma}_{\bar{X}}} = \frac{\hat{\mu} - \mu_0}{\hat{\sigma}/\sqrt{N}} \tag{A7-16}$$

Again, if the variable under test is a linear combination of stochastic variables, the expression of the test variable T will have to be constructed in a more general way. Testing the difference between two stochastic variables X and Y will result in

$$T = \frac{\hat{\mu}_X - \hat{\mu}_Y - \mu_0}{\sqrt{\frac{\hat{\sigma}_X^2}{N_X} + \frac{\hat{\sigma}_Y^2}{N_Y}}} \tag{A7-17}$$

Due to the symmetry of the t-distribution, the $\alpha/2$-quantiles $t_{\alpha/2}(\nu)$ of the t-distribution is used in a two-sided t-test to acquire confident α-risk of error limits for the confidence interval, telling within which number of standard deviations from the expectation value μ_0 a sample mean is likely to be found if H_0 is true, i.e. the inequality

$$-t_{\alpha/2}(\nu) < T < t_{\alpha/2}(\nu) \tag{A7-18}$$

is true with 1-α probability if the expectation value of the sampled distribution corresponds to the expectation value assumed in H_0. In other words, at least 1-α of the times an equal sized sample is drawn, the t-test will show the same result.

If the inequality (A7-18) fails, the zero hypothesis may be discarded on a significance level of α, and repeated tests of the distribution will almost exclusively show a mean difference from H_0 i.e. the absolute value of T is, in at least 1-α of the times, larger than $t_{\alpha/2}(\nu)$.

A7.1.5 Calculation of dry density

With both density ρ and water content w, i.e. the mass ratio between water and solid, of the clay known, the dry density ρ_d may be calculated from standard soil mechanics

$$\rho_d = \frac{\rho}{1+e} \tag{A7-19}$$

where the void ratio e may be calculated from the degree of saturation S_r, and the densities of clay solid $\rho_s = 2.750$ g/cm^3 and water $\rho_w = 1.000$ g/cm^3, according to

$$e = \frac{\rho_s - \rho}{\rho - S_r \rho_w} \tag{A7-20}$$

The degree of saturation is defined as the volume fraction of pores in the clay that are filled with water, calculated through

$$S_r = \frac{w \rho \rho_s}{\rho_s (1+w) - \rho} \tag{A7-21}$$

A7.2 EXPERIMENTAL METHODS

Four samples, labelled 1, 2, 3 and 4, were sawed out of 20 IBECO RWC BF blocks according to Figure A7-1. Also shown is that each sample were split in two so that one part could be used for determination of water ratio and the other part was used for determination of density, the relative position of the two pieces within each sample was not kept track of.

The water content was determined by measuring the mass difference of the sample piece before and after drying in a 105 C hot oven for 24 hours. To determine the density, the other sample piece was weighed hanging in air and a second time submerged in paraffin oil allowing the calculation of density through Archimedes principle.

The measured data was then used to calculate the dry density in each position of the 20 blocks in the sample.

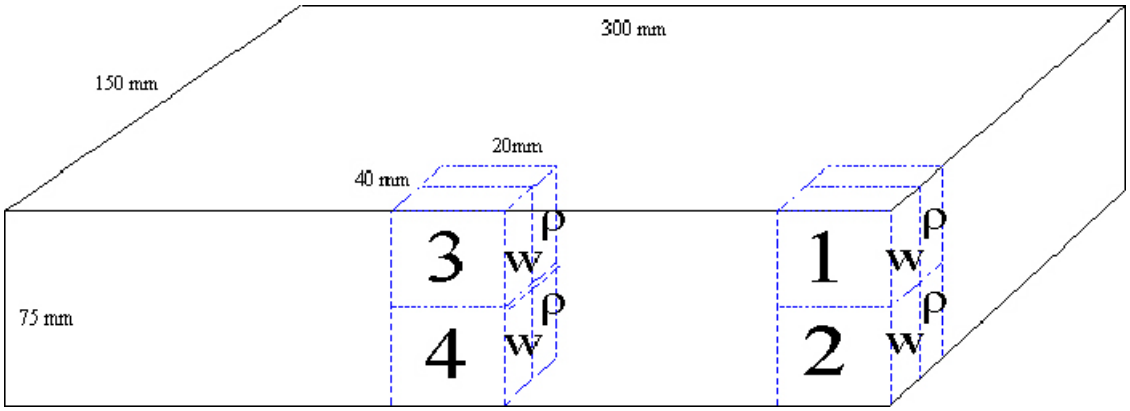

Figure A7-1. *Schematic picture of the bentonite blocks and where the samples were taken.*

A7.3 RESULTS

The calculated dry densities at each position of the bentonite blocks in the 20 block sample are presented in Figure A7-2. Smoothed trendlines have been inserted to make it easier to follow the data from one block.

If one studies the distribution of the data, it is readily observed that the trends of the data from block 3, 5, 8, 9, 15 and 18 deviates heavily from the rest of the blocks. If instead the data at position 1 and 2 are interchanged and the same is done for the data at position 3 and 4 so that it appears that the block was measured flipped upside down, all blocks show similar trends.

This manipulation is motivated from the fact that the blocks don't have any indication on them which direction they have been inside the compaction equipment and the assumption that the source of the density trend is the same for all blocks.

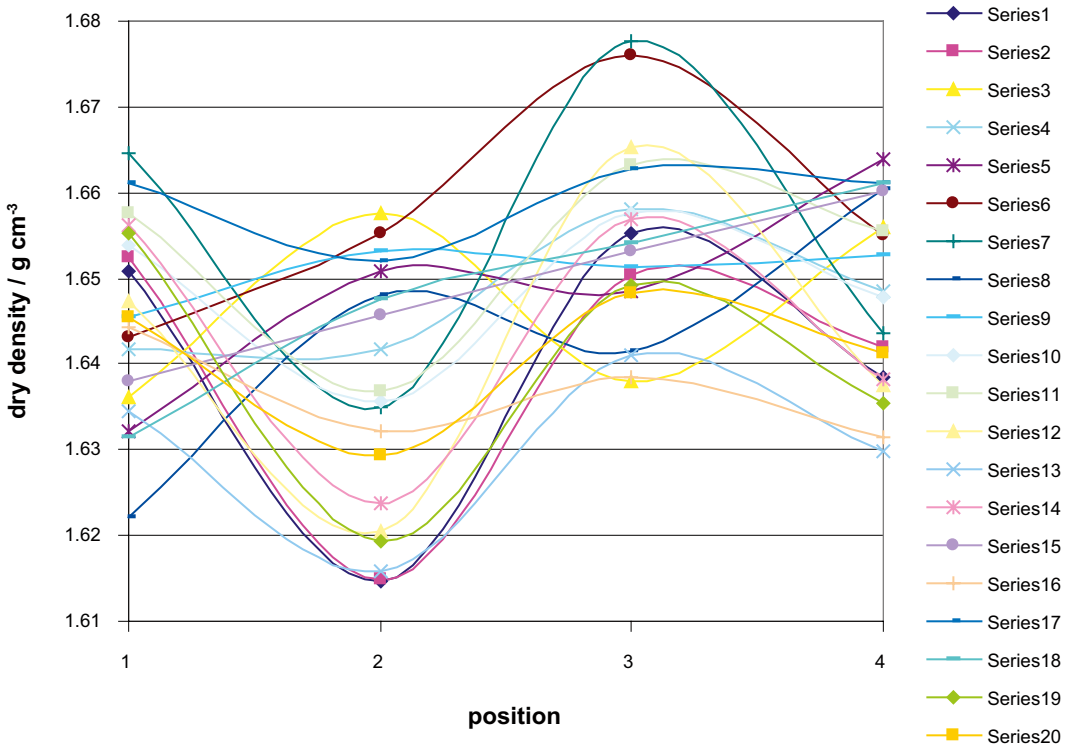

Figure A7-2. *Calculated dry densities in the blocks plotted as series over the different measurement positions.*

In Figure A7-3, the reordered dry density data from the bentonite blocks is plotted once again, with the condition that the dry density at position 3 should be larger than that of position 4 (i.e. flipping block 3, 5, 8, 9, 15 and 18), now showing a similar trend in each block.

The corresponding numerical data is presented in Appendix 7A, where manipulated blocks are marked with "F" for flipped.

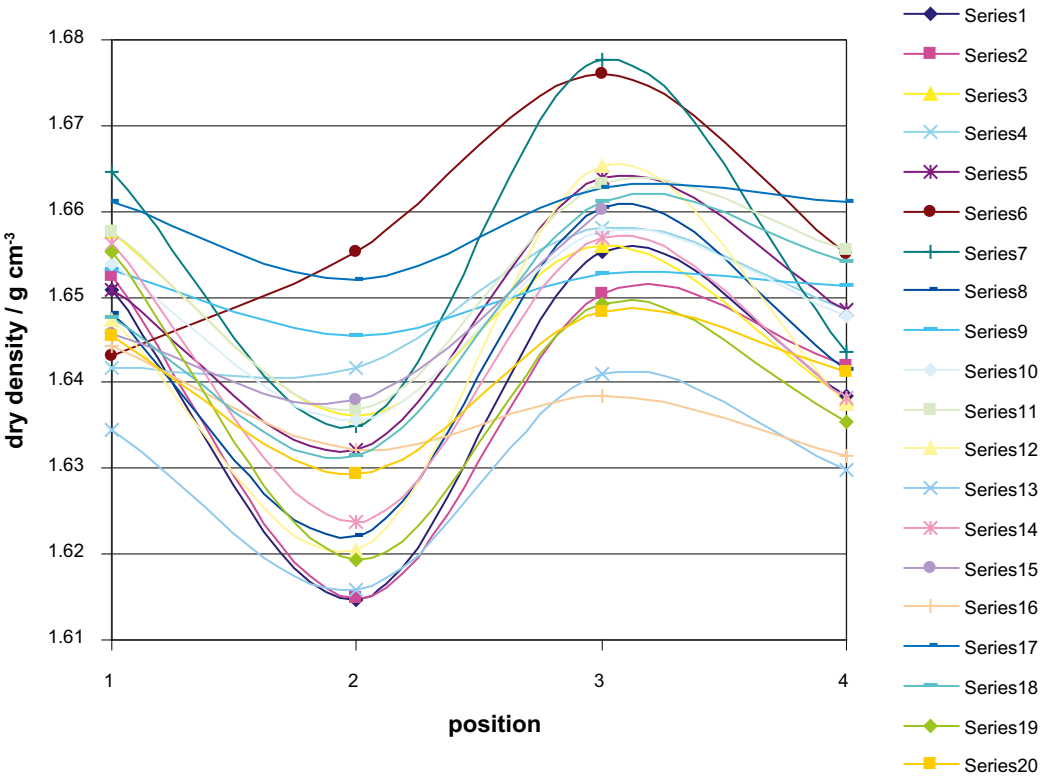

Figure A7-3. *Calculated dry densities in the blocks, reordered to show the same trend in every block, as series over the different measurement positions.*

A7.4 T-TESTS

To examine the homogeneity of the compacted blocks, the hypothesis of homogenous blocks may be divided into several hypotheses to be tested separately;

- the mean dry density at a position is equal to the overall mean dry density,
- the mean dry density at a position is equal to the corresponding block mean,
- the mean dry density do not differ between the different measurement positions,
- the mean dry density do not differ between top (position 1 and 3) and bottom,
- the mean dry density do not differ between side and corner.

A7.4.1 Dry density mean deviation

The dry density deviation from the overall mean ρ_{md} was studied by simply subtracting the overall mean value of the dry density from all data, Figure A7-4.

To satisfy the zero hypothesis, the mean value of the data in each point must be smaller than $t_{\alpha/2}(v)$ standard deviations. In Table A7-1, a t-test of the dry density mean deviation at 1% risk is performed. The test shows a significant difference for position 2 and 3. Worth to mention is that Microsoft Excel's built in function for averaging and standard deviation estimation in the raw data has been used.

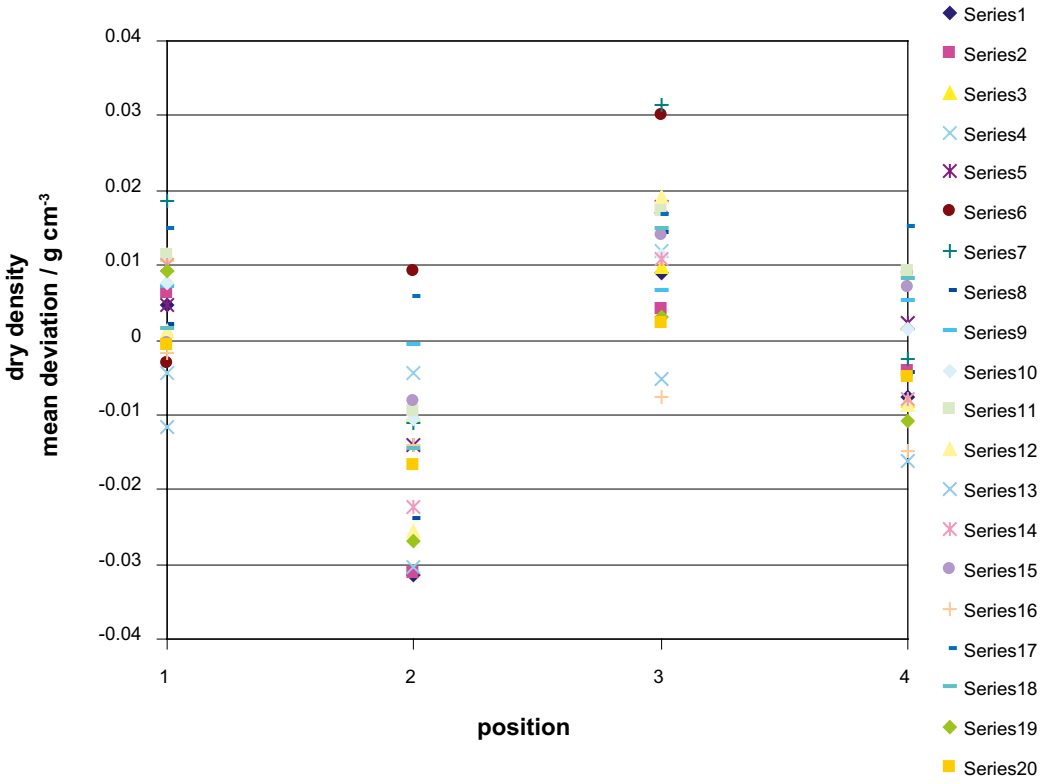

Figure A7-4. *Dry density mean deviation in the blocks as series over the different measurement positions.*

Table A7-1. T-test of the dry density mean deviation at significance level 1%.

	rho_md			
	1	2	3	4
mean of samples	0,00445	-0,01452	0,011586	-0,00152
stdev of samples	0,007175	0,011776	0,009775	0,008657
v	19	19	19	19
t_alpha/2(v)	2,861	2,861	2,861	2,861
stdev of mean distribution	0,001604	0,002633	0,002186	0,001936
t_alpha/2(v)*stdev of mean	0,00459	0,007534	0,006253	0,005538
significant difference?	NO	YES	YES	NO

A7.4.2 Dry density block mean deviation

The dry density deviation from each block mean ρ_{bmd} was studied by subtracting the corresponding block mean value of the dry density from each block series, Figure A7-5.

For the data to satisfy the zero hypothesis, the mean value of the data in each position must once again be small. In Table A7-2, a t-test of the dry density block mean deviation at 1% risk is performed. The test shows, once again, a significant difference for position 2 and 3.

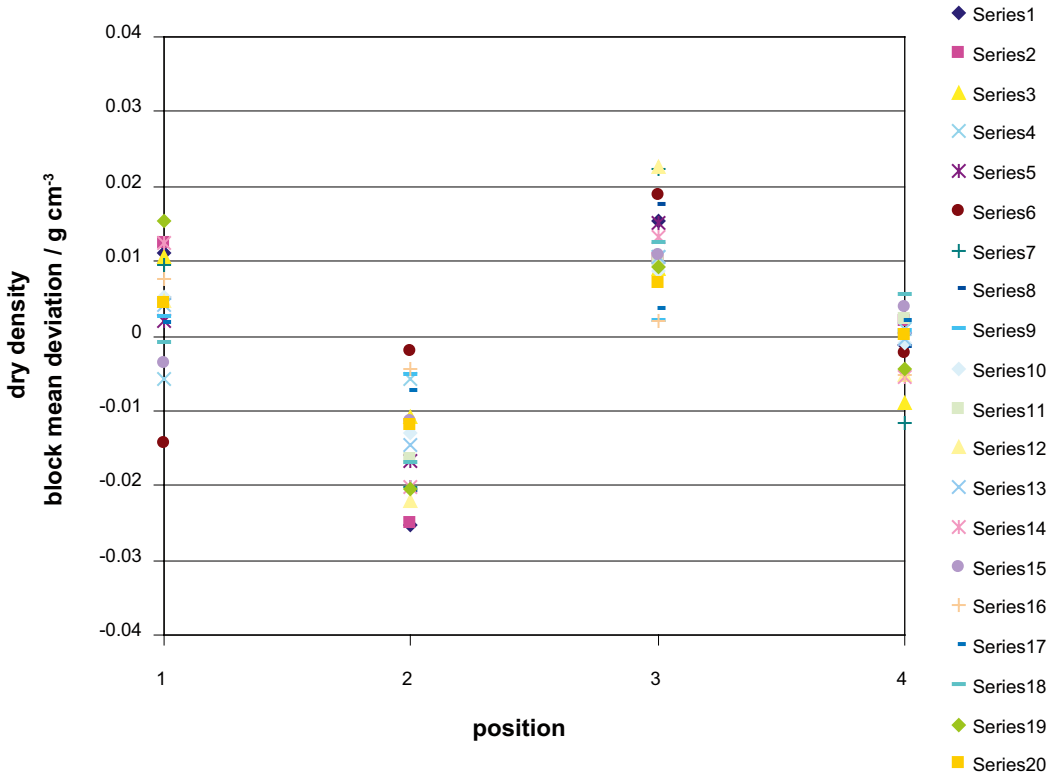

Figure A7-5. *Dry density block mean deviation in the blocks as series over the different measurement positions.*

Table A7-2. T-test of the dry density block mean deviation at significance level 1%.

		rho_bmd			
		1	2	3	4
mean of samples		0,00445	-0,01452	0,011586	-0,00152
stdev of samples		0,007002	0,007047	0,005835	0,004248
v		19	19	19	19
t_alpha/2(v)		2,861	2,861	2,861	2,861
stdev of mean distribution		0,001566	0,001576	0,001305	0,00095
t_alpha/2(v)*stdev of mean		0,00448	0,004509	0,003733	0,002717
significant difference?		NO	YES	YES	NO

A7.4.3 Dry density deviation between different positions on the block

At last, the dry density variations between different positions are examined with a 1% risk of error t-test in Table A7-3. The test variables consist of the density difference between position 1 and 2 (denoted 1-2), the density difference between position 3 and 4 (3-4), the difference between mean density at "side" and "corner" (12-34) and the difference between mean density at "top" and "bottom" (13-24).

The raw data of this calculation is presented in Appendix 7B.

Table A7-3. T-test of the dry density deviation between different positions at significance level 1%.

	rho_dp			
	1-2	3-4	12-34	13-24
mean of samples	0,018971	0,013102	0,01007	0,016036
stdev of samples A	0,007175	0,009775	0,006895	0,006063
stdev of samples B	0,011776	0,008657	0,006529	0,007308
v	31,397	37,45288	37,88738	36,74696
t_alpha/2(v)	2,744	2,715	2,715	2,719
stdev of mean distribution	0,003083	0,00292	0,002123	0,002123
t_alpha/2(v)*stdev of mean	0,008461	0,007927	0,005765	0,005773
significant difference?	YES	YES	YES	YES

A7.5 CONCLUSIONS

Differences from most parts of the zero hypothesis assuming that the blocks are homogenous have been shown at significance level 1%. The expectation values of the dry density at the different block positions are not equal and the dry density at position 2 and 3 deviates in different directions from each block mean. Although the deviations are small, it is clear that the preparation method of the blocks does not produce uniform density profiles.

A7.5.1 Mean values

The mean dry density of position 1, 2, 3 and 4 deviate 0.004 g/cm^3, –0.015 g/cm^3, 0.012 g/cm^3 and –0.002 g/cm^3 respectively from the overall mean, or equivalent, each block mean.

Also, the mean density is higher at one side of the block and it is also higher at the side than at the corner of the block. For the examined blocks, those deviations were on average 0.010 g/cm^3 and 0.016 g/cm^3, respectively.

A7.5.2 T-tests

The hypothesis that there are no mean deviation in dry density from the overall mean, block mean and that there are no difference in dry density between different positions may, at a significance level of 1%, be discarded in all cases except for the mean deviation of position 1 and 4. There will be 99% consequent mean deviations from homogeneity in all other positions and position comparisons if this evaluation should be repeated.

References

Blom, Enger, Englund, Grandell, Holst, 2005. Sannolikhetslära och statistikteori med tillämpningar. Studentlitteratur, fifth edition.

NIST/SEMATECH, 2003. e-handbook of statistical methods. [Online]. Available at: http://www.itl.nist.gov/div898/handbook/.

Appendix 7A

Calculated dry densities and statistics over the blocks and positions.

DRY DENSITY						
		position				
	roh_d	1	2	3	4	mean
block	1	1,650841	1,614598	1,655219	1,638517	1,639794
	2	1,652423	1,614876	1,6503	1,641878	1,639869
	3F	1,657593	1,63618	1,655963	1,637998	1,646933
	4	1,641838	1,641833	1,657971	1,648501	1,647536
	5F	1,650934	1,632159	1,663951	1,648492	1,648884
	6	1,643111	1,655272	1,676141	1,654995	1,65738
	7	1,664596	1,63494	1,677658	1,643622	1,655204
	8F	1,648058	1,62223	1,660497	1,641584	1,643092
	9F	1,653157	1,645506	1,652633	1,651285	1,650645
	10	1,653857	1,635583	1,657484	1,647722	1,648662
	11	1,657524	1,63672	1,663305	1,655395	1,653236
	12	1,647374	1,620608	1,665233	1,637537	1,642688
	13	1,634581	1,61579	1,640991	1,629894	1,630314
	14	1,656196	1,623673	1,656965	1,638212	1,643761
	15F	1,645749	1,637953	1,660153	1,653203	1,649264
	16	1,644268	1,63215	1,638567	1,631405	1,636598
	17	1,660993	1,651951	1,662847	1,661128	1,65923
	18F	1,647664	1,631508	1,661032	1,654202	1,648601
	19	1,655234	1,619278	1,649101	1,635374	1,639747
	20	1,645571	1,629339	1,648269	1,641294	1,641118
	mean	1,650578	1,631607	1,657714	1,644612	1,646128
	stdev	0,007175	0,011776	0,009775	0,008657	0,007243

Appendix 7B

Raw data in the position comparison tests.

DENSITY VARIATIONS BETWEEN DIFFERENT POSITIONS					
		position			
	rho_dp	1-2	3-4	34-12	13-24
block	1	0,036242	0,016701	0,014148	0,026472
	2	0,037547	0,008422	0,012440	0,022984
	3	0,021413	0,017965	0,000094	0,019689
	4	0,000005	0,009470	0,011401	0,004737
	5	0,018775	0,015459	0,014675	0,017117
	6	-0,012162	0,021146	0,016377	0,004492
	7	0,029656	0,034036	0,010872	0,031846
	8	0,025828	0,018914	0,015897	0,022371
	9	0,007651	0,001347	0,002628	0,004499
	10	0,018275	0,009762	0,007883	0,014018
	11	0,020804	0,007910	0,012228	0,014357
	12	0,026766	0,027696	0,017394	0,027231
	13	0,018791	0,011097	0,010257	0,014944
	14	0,032523	0,018753	0,007654	0,025638
	15	0,007796	0,006950	0,014827	0,007373
	16	0,012118	0,007162	-0,003223	0,009640
	17	0,009042	0,001719	0,005516	0,005381
	18	0,016156	0,006830	0,018031	0,011493
	19	0,035956	0,013727	0,004981	0,024841
	20	0,016232	0,006976	0,007327	0,011604
	mean	0,018971	0,013102	0,010070	0,016036
	stdev	0,012753	0,008332	0,005895	0,008672

1-2 = density difference in the corner
3-4 = density difference at the side
34-12 = mean density difference between side and corner
13-24 = mean density difference between "top" and "bottom"

Data from oedometer tests

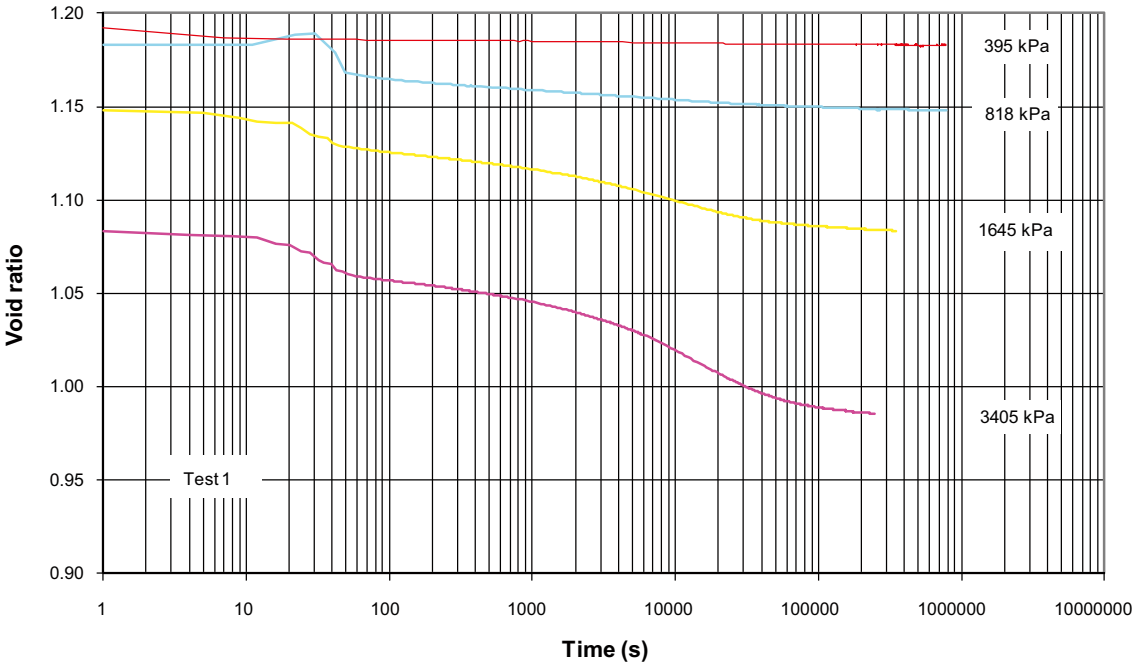

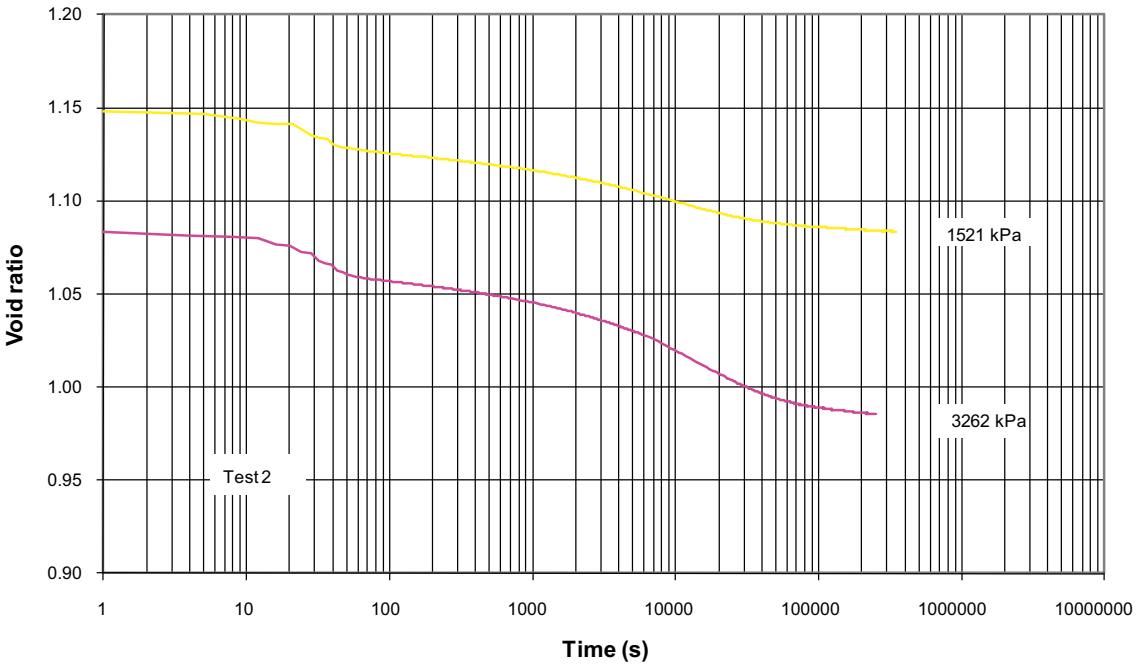

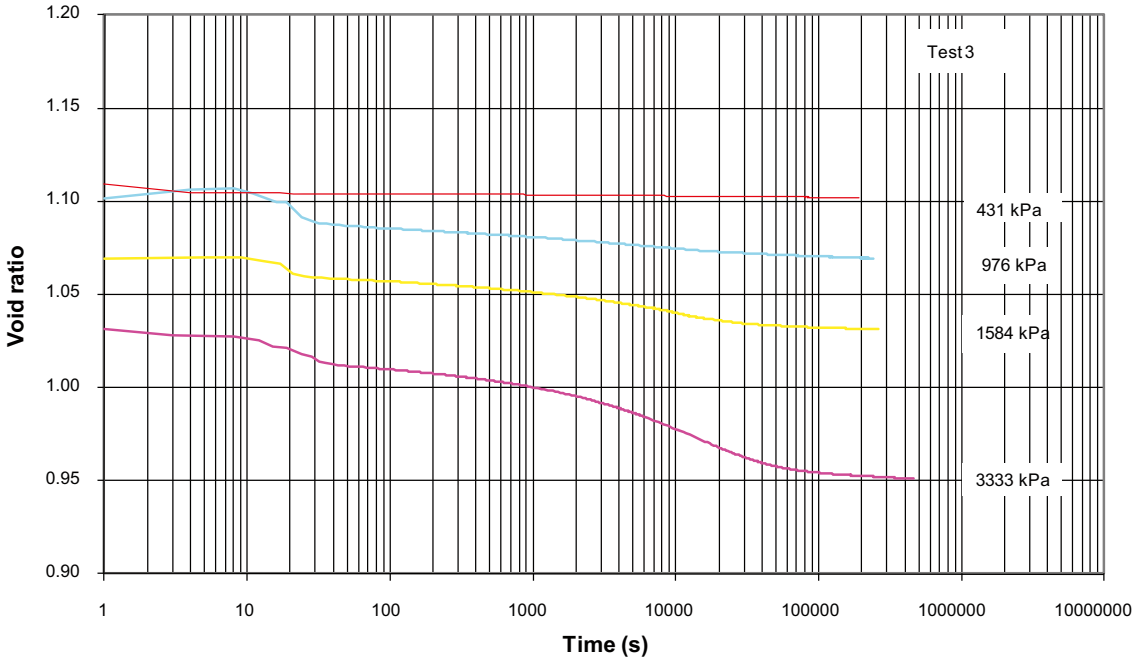
Test 3
431 kPa
976 kPa
1584 kPa
3333 kPa
Void ratio
Time (s)
1.20
1.15
1.10
1.05
1.00
0.95
0.90
1
10
100
1000
10000
100000
1000000
10000000

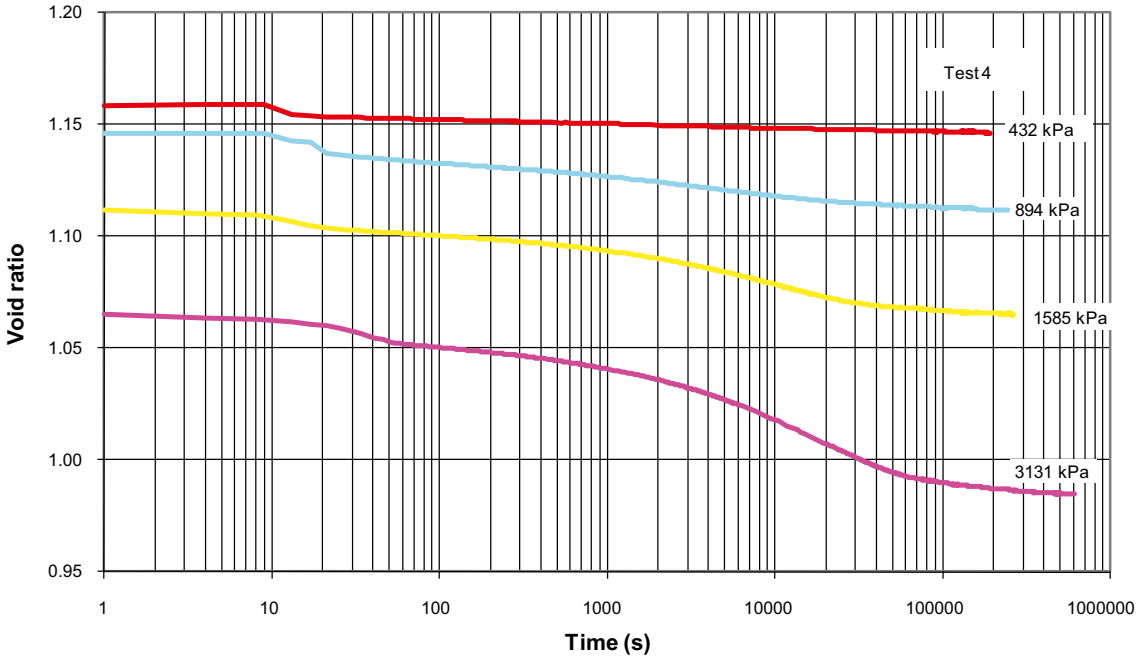
Test 4
432 kPa
894 kPa
1585 kPa
3131 kPa
Void ratio
Time (s)
1.20
1.15
1.10
1.05
1.00
0.95
1
10
100
1000
10000
100000
1000000

Evaluation of elastic parameters of unsaturated blocks-data

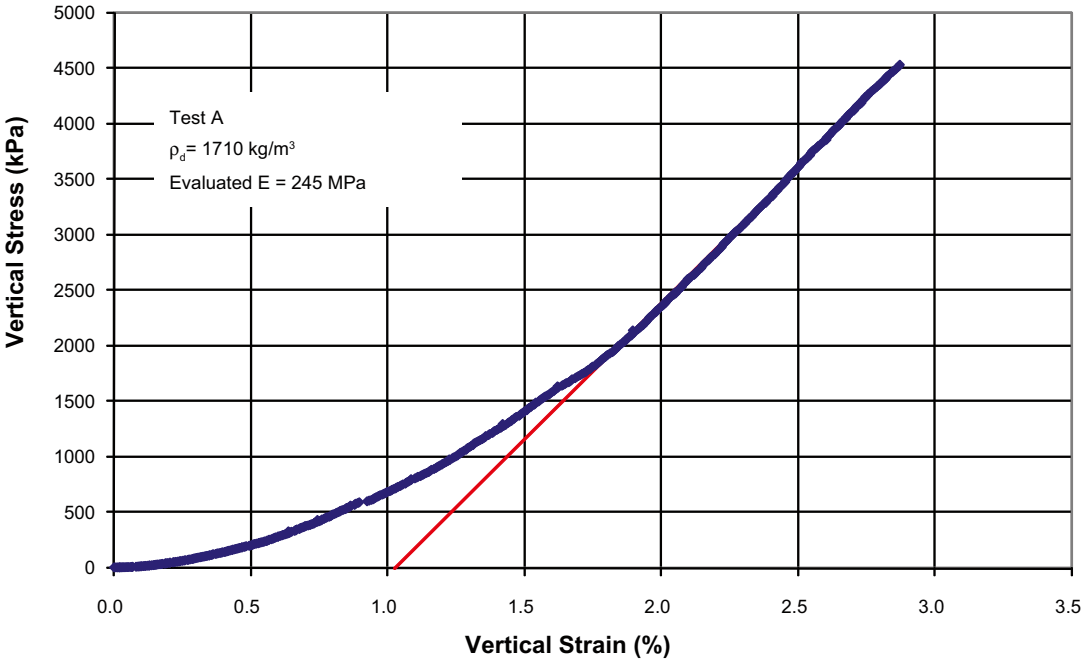

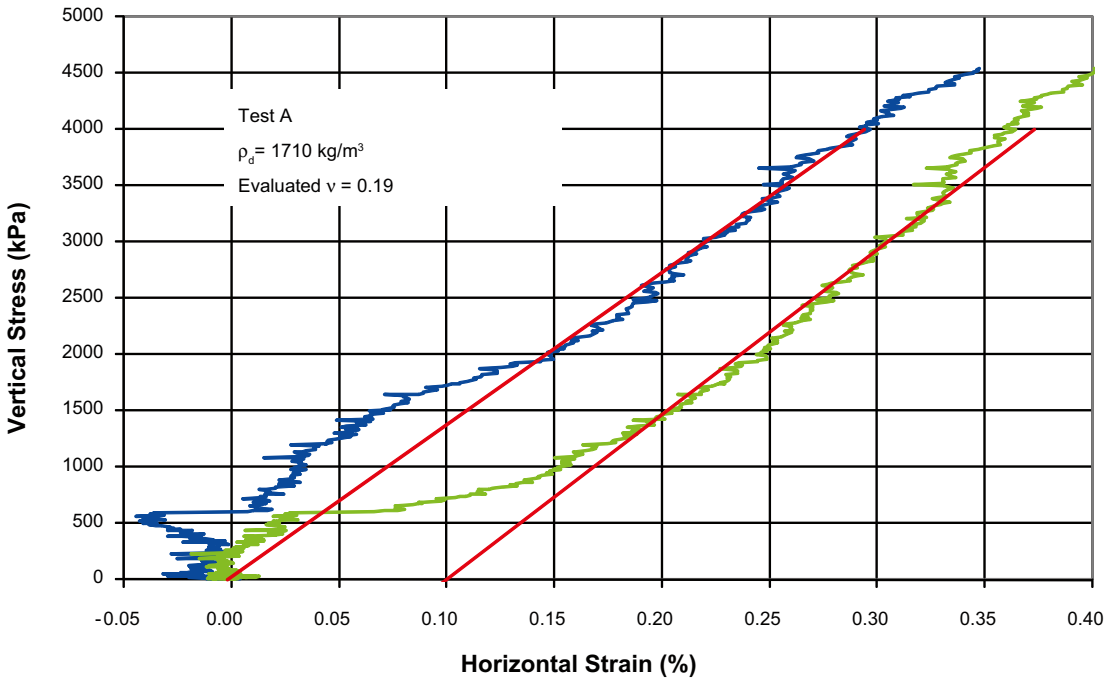

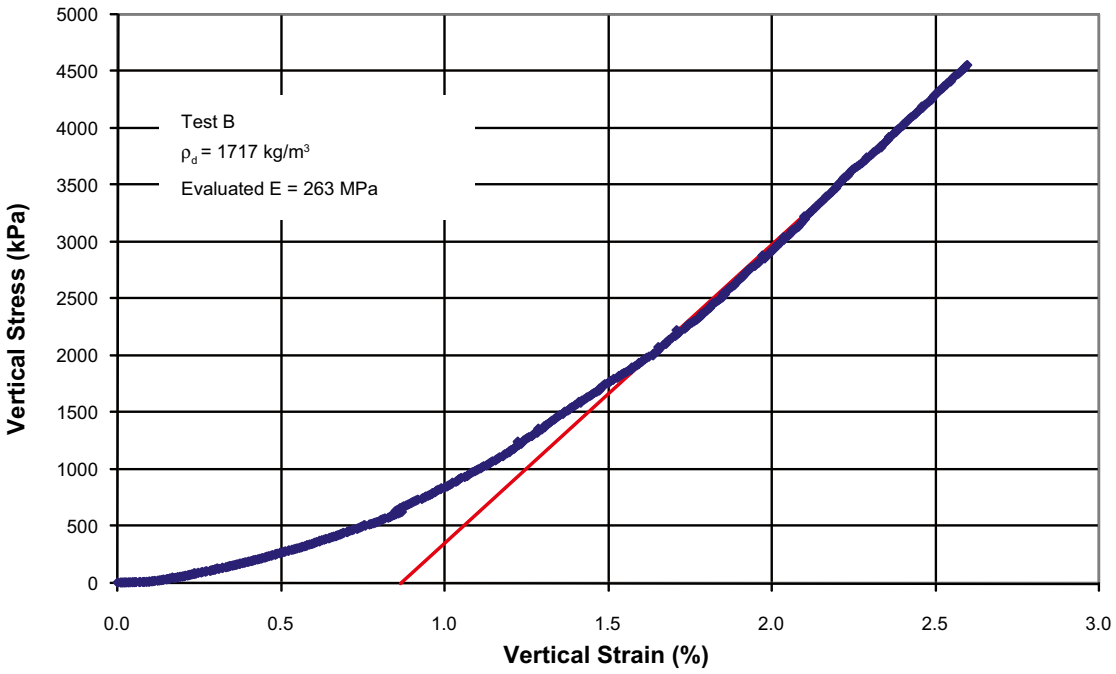
Test B
ρ_d = 1717 kg/m^3
Evaluated E = 263 MPa
Vertical Stress (kPa)
Vertical Strain (%)
5000
4500
4000
3500
3000
2500
2000
1500
1000
500
0
0.0
0.5
1.0
1.5
2.0
2.5
3.0

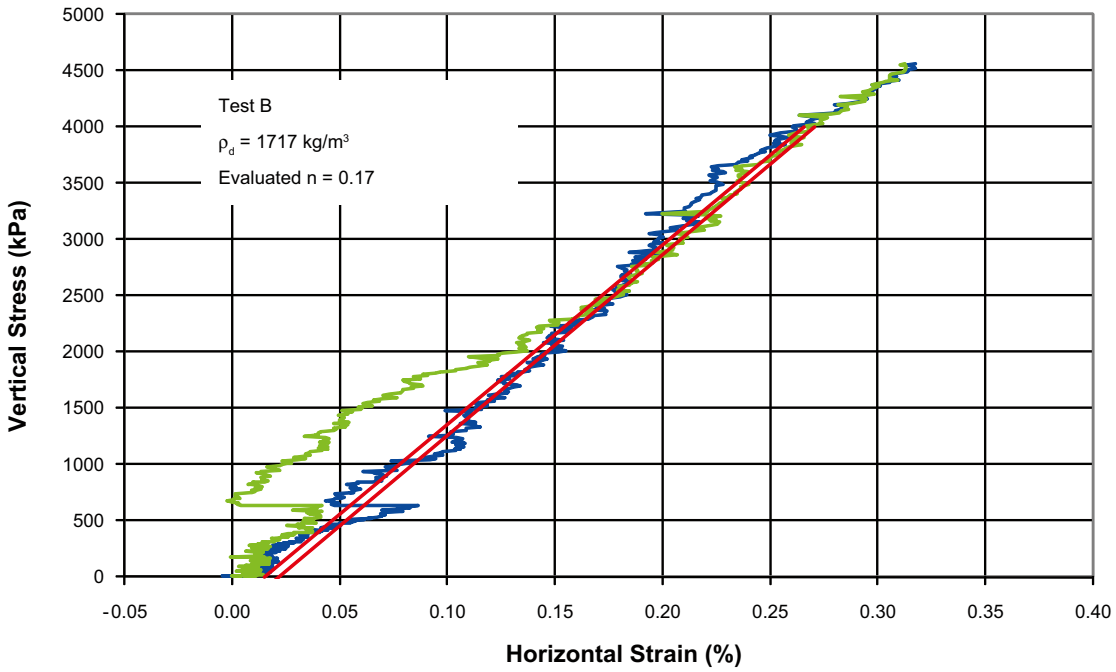
Test B
ρ_d = 1717 kg/m^3
Evaluated n = 0.17
Vertical Stress (kPa)
Horizontal Strain (%)
5000
4500
4000
3500
3000
2500
2000
1500
1000
500
0
-0.05
0.00
0.05
0.10
0.15
0.20
0.25
0.30
0.35
0.40

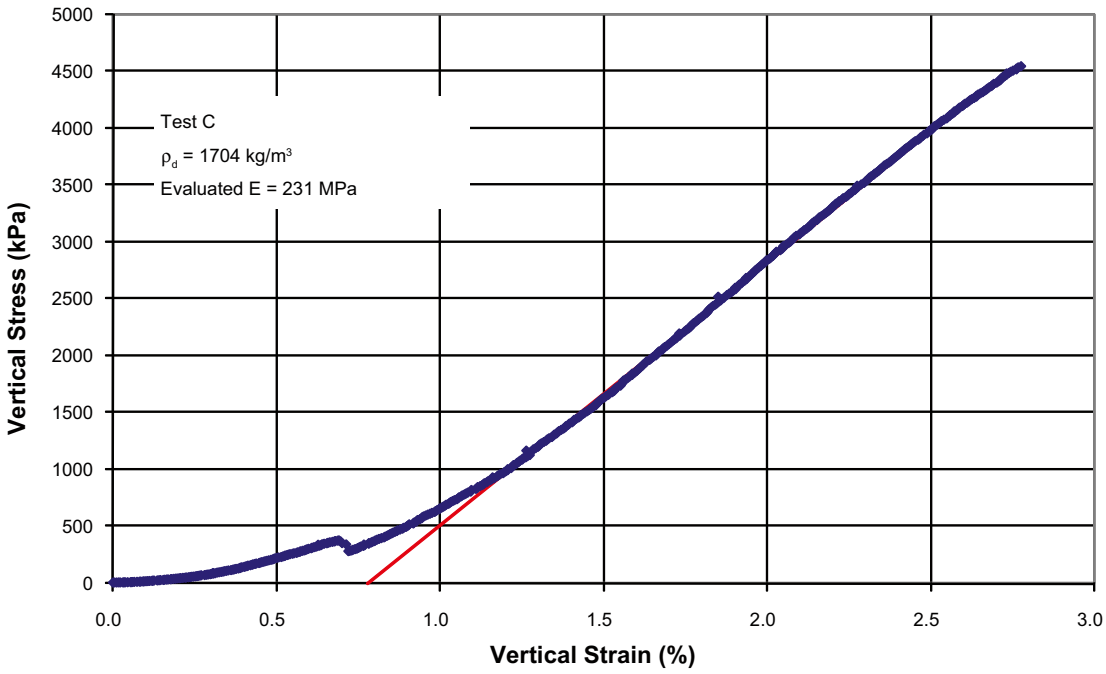
Test C
ρ_d = 1704 kg/m^3
Evaluated E = 231 MPa
Vertical Stress (kPa)
Vertical Strain (%)
5000
4500
4000
3500
3000
2500
2000
1500
1000
500
0
0.0
0.5
1.0
1.5
2.0
2.5
3.0

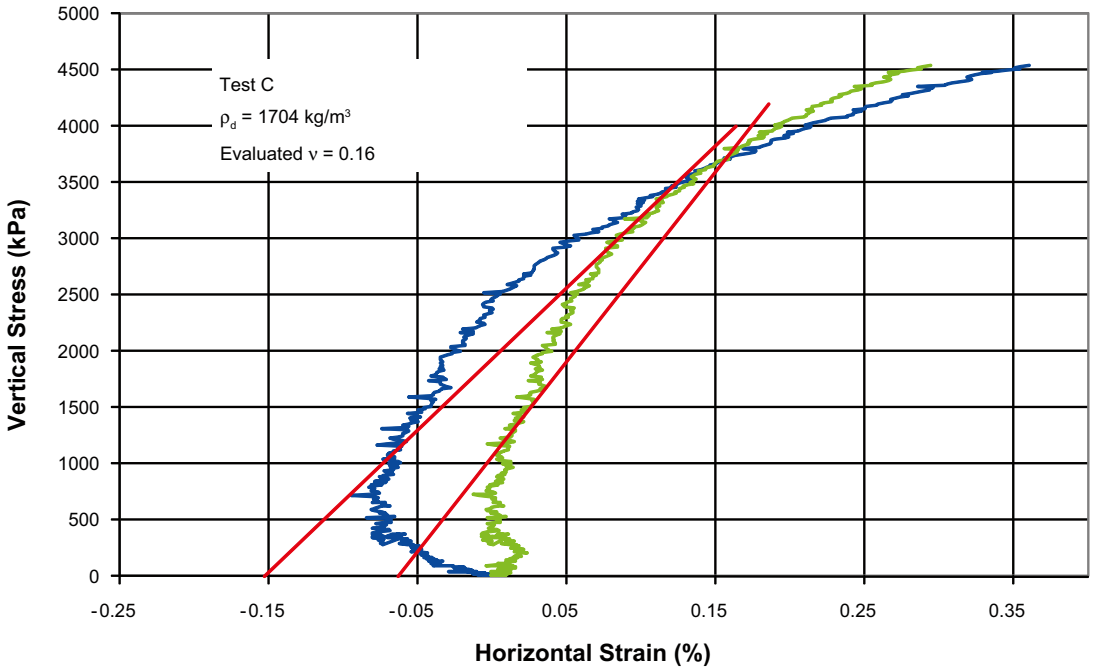
Test C
ρ_d = 1704 kg/m^3
Evaluated ν = 0.16
Vertical Stress (kPa)
Horizontal Strain (%)
5000
4500
4000
3500
3000
2500
2000
1500
1000
500
0
-0.25
-0.15
-0.05
0.05
0.15
0.25
0.35